

①

A STUDY OF THE RELATIONSHIP BETWEEN  
STRUCTURE AND CHEMICAL PROPERTIES OF  
FUNCTIONALIZED MACROCYCLIC POLYAMINES

機能性大環状ポリアミンに関する  
活性構造化学的研究

1989年 12月

岡崎国立共同研究機構分子科学研究所  
錯体化学実験施設錯体合成研究部門

指導教授 木村 栄一

塩谷 光彦

A STUDY OF THE RELATIONSHIP BETWEEN  
STRUCTURE AND CHEMICAL PROPERTIES OF  
FUNCTIONALIZED MACROCYCLIC POLYAMINES

機能性大環状ポリアミンに関する  
活性構造化学的研究

1989年 12月

岡崎国立共同研究機構分子科学研究所  
錯体化学実験施設錯体合成研究部門

指導教授 木村 栄一

塩谷光彦

A STUDY OF THE RELATIONSHIP BETWEEN STRUCTURE AND CHEMICAL  
PROPERTIES OF FUNCTIONALIZED MACROCYCLIC POLYAMINES

- I. NEW MACROCYCLIC TETRAAMINE METAL COMPLEXES APPENDED WITH AN  
INTRAMOLECULAR IMIDAZOLE.
- II. SYNTHESIS OF NOVEL FLUORINATED MACROCYCLIC TETRAAMINES AND  
CHEMICAL PROPERTIES OF THEIR METAL COMPLEXES.

by

Mitsuhiko Shionoya

A thesis submitted to the Graduate  
School of Pharmaceutical Sciences in  
Hiroshima University School of Medicine  
in partial fulfillment of the require-  
ments for the degree of Doctor of  
Philosophy in Pharmaceutical Science.

Hiroshima  
1989. 12

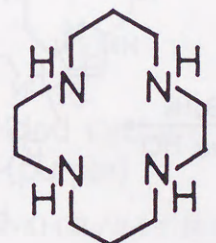
Approved by:

Supervisor

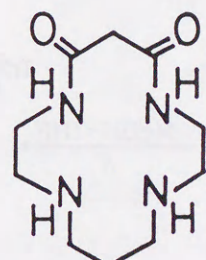
[序]

サイクラム (1,4,8,11-tetraazacyclotetradecane) やジオキソサイクラム (5,7-dioxo-1,4,8,11-tetraazacyclotetradecane) に代表される大環状ポリアミンは、大環状ポリエーテル（クラウンエーテル）と並んで最も注目されている大環状化合物群である。大環状ポリアミンの特徴は、i) 窒素原子の強い塩基性によってコンパクトなポリアンモニウムカチオンを形成し、極性分子やポリアニオンを静電的に捕捉したり、ii) 金属イオン、特に重金属・貴金属・遷移金属イオンを環内に捕捉し、電子やエネルギーの授受体として、或いは基質への伝達媒体として安定性の高い反応場を提供できることである。<sup>1)</sup> これらの諸性質は、生体内分子（ATP, ドバミン等）の選択的捕捉<sup>2)</sup> や膜電位応答を利用したアニオンセンサー、<sup>3)</sup> 或いは金属錯体の酸化還元触媒反応<sup>4)</sup> や放射性金属錯体の核医学的利用等、<sup>5)</sup> 多岐にわたって応用展開されつつある。

本研究は、従来の大環状ポリアミンにいくつかの新しい化学修飾を施し、それらの金属錯体を化学結合や反応性の観点から検討し、さらに生体類似機能や新触媒反応の開発を行なうことを目的とした。



サイクラム



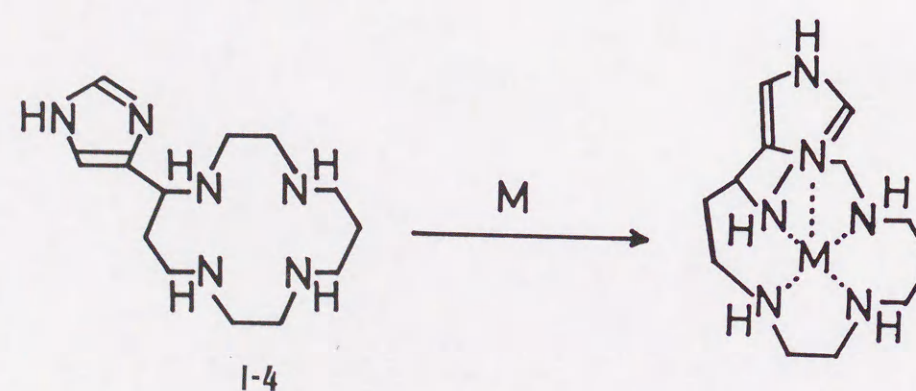
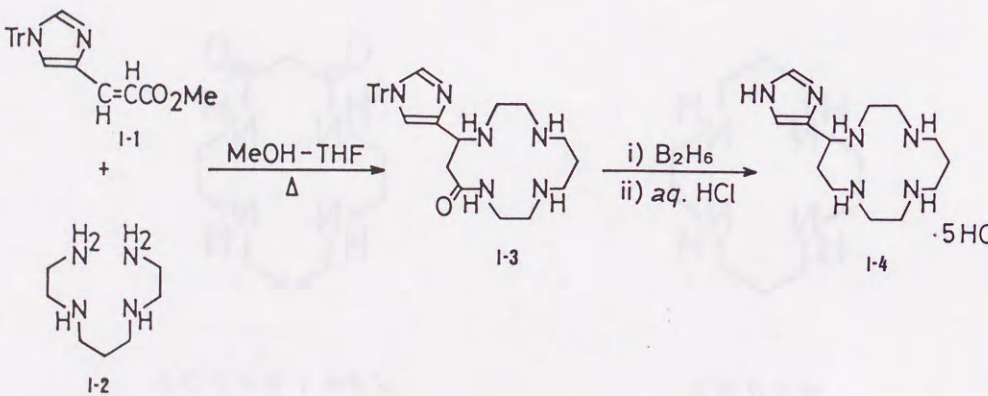
ジオキソサイクラム

[要 約]

[I] 分子内イミダゾール基を有する大環状テトラアミン金属錯体

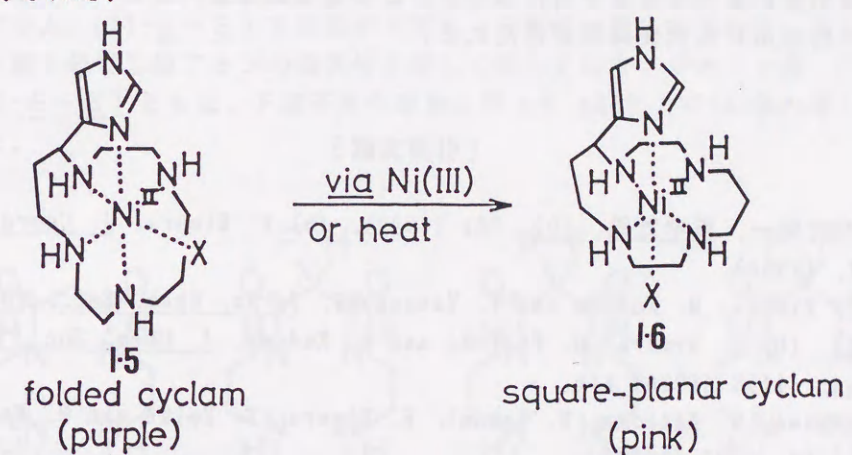
生体内の酸化還元に基づく生化学的機能は、主に金属イオンの酸化還元性の制御という観点から理解されている。例えば、ヘム酵素中の金属ボルフィリン錯体では、近傍のアミノ酸側鎖がアクシャル配位子として中心金属の酸化還元性を巧みにコントロールし、対応する機能( $O_2$ 分子の取込みと活性化、電子移動、有機物質の化学的変換等)を発現している。著者はこの配位様式に深い興味をもち、分子内イミダゾール基をもつ大環状テトラアミン I-4 をデザイン・合成し、イミダゾール基の配位効果を pH滴定法、サイクリックボルタメトリー法、ESR、X線結晶解析および分光学的手法によって検討した。尚、配位子の合成は以下に示すようなルートに従って行なった。<sup>6,7)</sup>

Synthesis



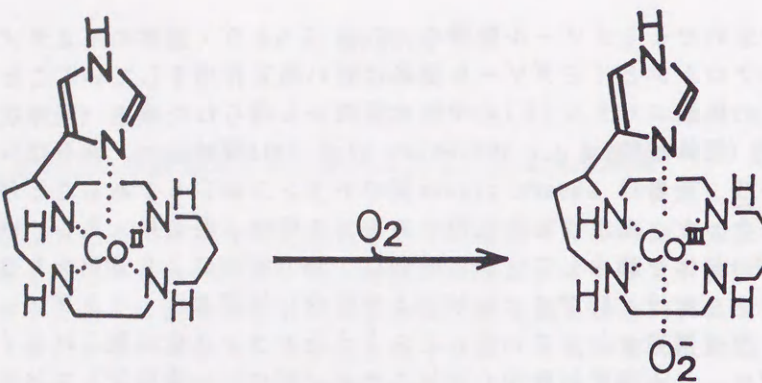
pH滴定法で求めたイミダゾール窒素の  $pK_a$  値 5.6より（通常のイミダゾールは7.1）、環内の二つのプロトンとイミダゾール窒素は強い相互作用をしていることが示唆された。

I-4 と等量の硫酸ニッケル(II)の中性水溶液から得られた紫色（固体状態、 $\lambda_{max}$  522 nm）とピンク色（固体状態、 $\lambda_{max}$  495 nm）の high-spin型結晶は、前者は N4 環の折れ曲ったシス体 I-5、後者は square-planar型のトランス体 I-6 であることが X線結晶解析より明らかになった。速度論的生成物であるシス体は、熱変換、あるいは電気化学的に生成した Ni(III) 錯体を経由して、非可逆的に、熱力学的により安定なトランス体に異性化した。トランス体は、Ni<sup>2+</sup>イオンが N4 平面内に捕捉され、イミダゾール窒素が軸位に位置した 6 配位構造をとっている。このようなトランス体に見られるイミダゾール基の立体的配置は、ヘム酵素活性中心のヒスチジン配位に大変類似しており、 $\pi$  相互作用に基づく、中心金属イオンによる基質の捕捉・活性化や酸化還元の制御に大変好都合であると期待された。



トランス体の Ni(III/II) の酸化還元電位は + 0.54 V vs S.C.E. (saturated calomel electrode) で、無置換のサイクラム (+ 0.50 V) に比べ、酸化されにくくなっている。イミダゾール基の  $\sigma$ -ドナー供与の効果より、 $p\pi-d\pi$  軌道相互作用による最高被占軌道の安定化が大きく効いているためと考えられる。

イミダゾール基のアクシャル配位効果は、Co(II) 錯体の分子状酸素捕捉能にも見られた。アルゴン気流下で調製した I-4 - Co(II) 錯体の水溶液（ピンク色）を酸素に晒すと瞬時に褐色 [ $\lambda_{max}$  319 nm ( $\epsilon$  4300), 446 nm ( $\epsilon$  330)] に変化した。この溶液の ESR スペクトル (77K) は、1 : 1 Co(III)-O<sub>2</sub><sup>-</sup> ( $\leftarrow$  Co(II)-O<sub>2</sub>) 錯体の生成を強く支持した。<sup>8)</sup> この酸素錯体は室温下で褐色固体として単離でき、固体状態の ESR は溶液状態のものとほぼ一致した。以上より I-4 - Co(II) 錯体は、室温下水溶液中で分子状酸素一分子を捕捉・活性化し、安定な 1 : 1 superoxo型錯体を形成する事がわかった。イミダゾール基は環内の Co(II) イオンにアクシャル配位し、酸素分子との結合に有利な電子配置 [(dxz)<sup>2</sup>(dyz)<sup>2</sup>(dxy)<sup>2</sup>(dz<sup>2</sup>)<sup>1</sup>] を与えると考えられる。無置換サイクラム - Co(II) 錯体の場合は、水溶液中では low spin 型  $\mu$ -peroxo Co(III)-O<sub>2</sub><sup>2-</sup>-Co(III) 錯体となることから、これは明らかに分子内イミダゾールのアクシャル配位効果によるものである。



このように I-4 のイミダゾール基は環内の中心金属イオンの酸化状態や第6配位座の反応性に多大な効果をもたらした。この様な配位様式に基づく、新触媒反応ならびに医学的応用にも大変興味が持たれる。

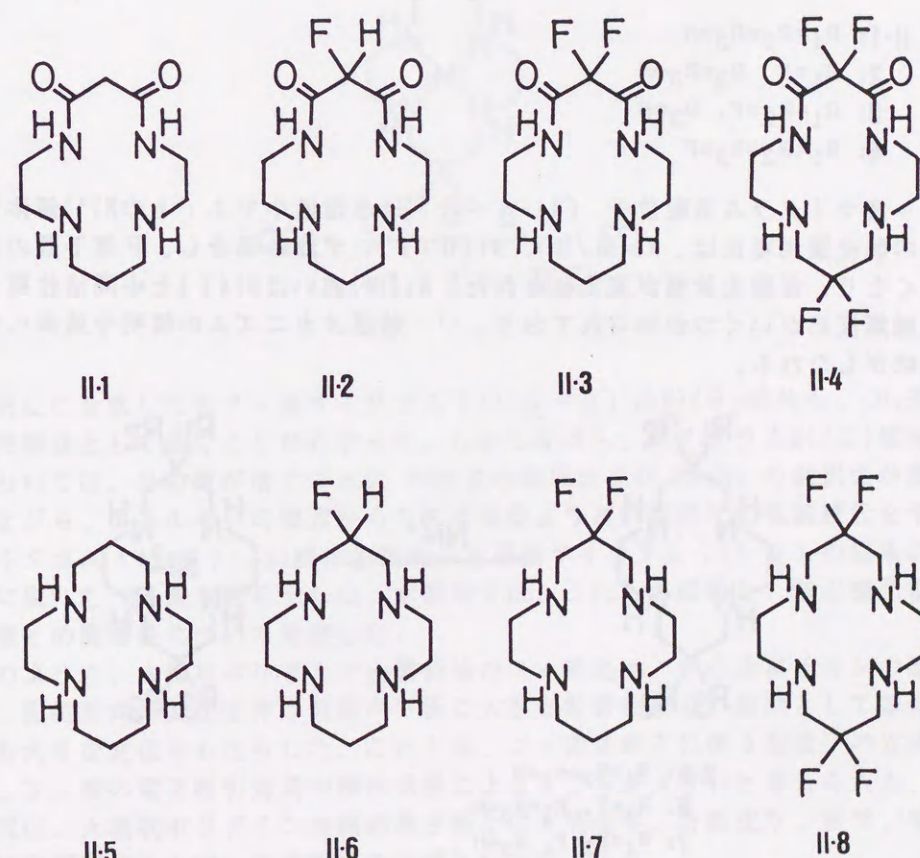
#### [引用文献]

- 1) (a) 木村栄一, 薬学雑誌, 102, 701 (1982). (b) E. Kimura, J. Coord. Chem., 15, 1, (1986).
- 2) (a) E. Kimura, M. Kodama and T. Yatsunami, J. Am. Chem. Soc., 104, 3182 (1982). (b) E. Kimura, H. Fujioka and M. Kodama, J. Chem. Soc., Chem. Commun., 1158 (1986) etc..
- 3) Y. Umezawa, M. Kataoka, W. Takami, E. Kimura, T. Koike and H. Nada, Anal. Chem., 60, 2392 (1988).
- 4) (a) E. Kimura and R. Machida, J. Chem. Soc., Chem. Commun., 499 (1984).  
 (b) M. Beley, J-P. Collin, R. Ruppert and J-P. Sauvage, J. Am. Chem. Soc., 108, 7461 (1986). (c) J. D. Koora and J. K. Kochi, Inorg. Chem., 26, 908 (1987).
- 5) J. R. Morphy, D. Parker, R. Alexander, A. Bains, A. F. Carne, M. A. W. Eaton, A. Harrison, A. Millican, A. Phipps, S. K. Rhind, R. Timas and D. Weatherby, J. Chem. Soc., Chem. Commun., 156 (1988).
- 6) E. Kimura, T. Koike, H. Nada and Y. Iitaka, J. Chem. Soc., Chem. Commun., 1322 (1986).
- 7) E. Kimura, T. Koike and M. Takahashi, J. Chem. Soc., Chem. Commun., 385 (1985).
- 8) (a) E. Kimura, M. Kodama, R. Machida and K. Ishizuka, Inorg. Chem., 21, 595 (1982). (b) Y. Sugiura, J. Am. Chem. Soc., 102, 5216 (1980).

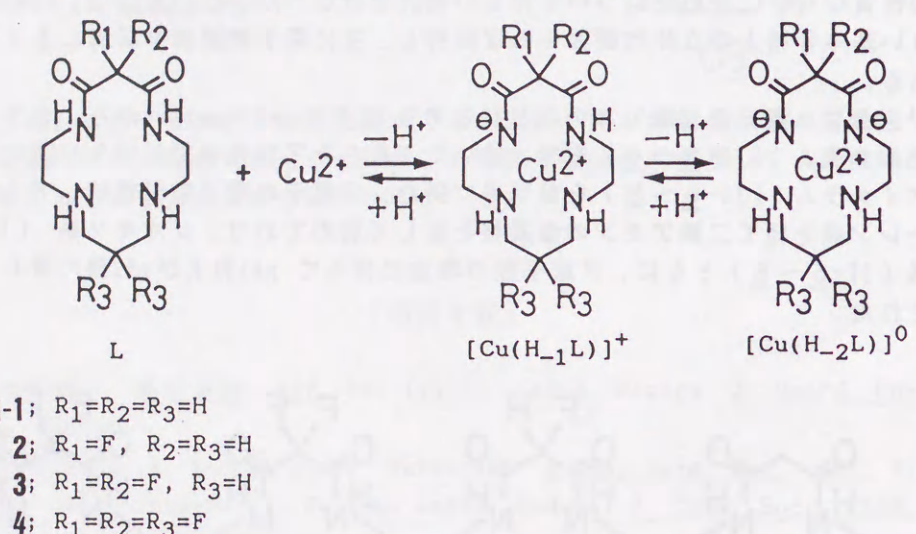
#### [II] 含フッ素大環状ポリアミンの合成とその金属錯体の化学的性質

フッ素 (F) 原子は、本来大変ユニークな性質（大きな電子吸引効果、Hと同じ位の大きさ、耐酸化性、脂溶性、じゅんかつ性等）をもっており、機能性有機化合物の水素原子の”フッ素化”は、これまでに多くの新機能誕生に貢献してきた。本研究では、これらのF原子の特徴を大環状ポリアミンに反映させるべく、種々の含フッ素ジオキソサイクラン (II-2~4) およびサイクラン (II-6~8) を新たに合成し、それらの金属錯体の性質ならびに反応性について詳しい検討を行なった。この変換は、simpleで対称性の良い基本骨格上の立体的要因をほぼ保持し、主に電子的要因を制御しようとするものである。

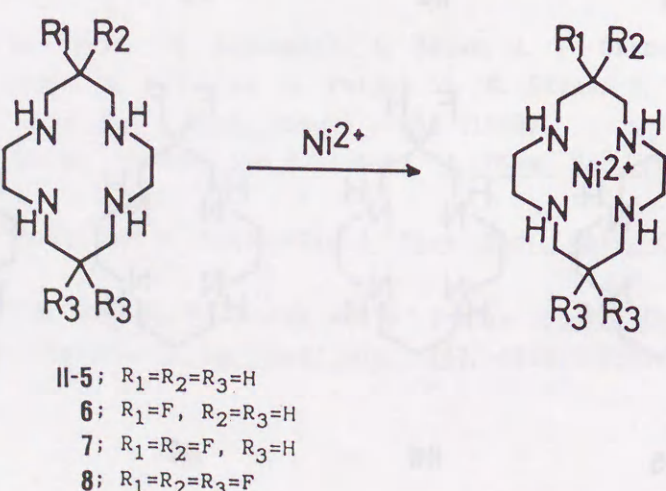
まず、含フッ素マロン酸エステルと対応する 2,3,2-tetraamine から、含フッ素ジオキソサイクラン (II-2~4) を得、続いてこれらを THF 中でジボラン還元し、含フッ素サイクラン (II-6~8) を好収率で得た。F原子の電子吸引性は、アミド基や飽和メチレン鎖を経て二級アミンの塩基性を著しく弱めており、ジオキソ系 (II-2~4) 飽和系 (II-6~8) ともに、F原子数の増加に伴って pK1およびpK2値の著しい低下が観察された。



含フッ素ジオキソ系(II-2～4)配位子は、ジオキソサイクラム(II-1)と同様に水溶液中等量のCu<sup>2+</sup>イオンと反応し、二つのアミド水素を解離したrigidな平面N4型Cu(II)錯体を形成する。この錯体構造は、IR  $\nu_{C=O}$  値の低波数側シフト及びESR因子( $g_L$  2.06,  $g_H$  2.17-2.18,  $A_H$  215-217 G, 77K)から支持された。又、錯生成定数の測定より、アミド間の活性メチレン位のフッ素化は錯生成に対して熱力学的に有利に働くことが示された。これらの錯体は水溶液中で準可逆的なサイクリックボルタムグラムを与える、そのCu(III/II)の酸化還元電位はフッ素化の低酸化状態安定化効果を示した。

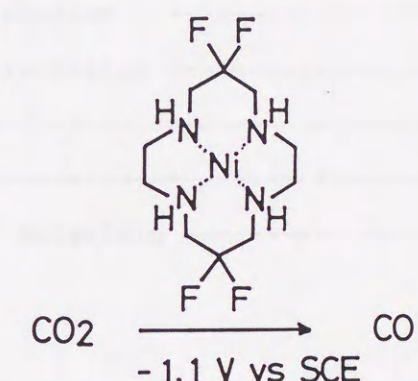


含フッ素サイクラム系配位子(II-6～8)は水溶液中で1:1のNi<sup>2+</sup>錯体を形成した。その酸化還元電位は、Ni(III/II), Ni(II/I)いずれの場合も、F原子数の増加とともに高くなり、低酸化状態が安定化された。Ni(III)或いはNi(I)を中間活性種として利用する触媒反応がいくつか知られており、<sup>1)</sup>触媒メカニズムの解明や効率への影響に大変興味がもたれる。



サイクラム(II-5)-Ni(II)錯体は、水溶液中で6配位high spin型(blue)と4配位low spin型(yellow)の平衡状態[25 °C, I = 0.1 M (NaClO<sub>4</sub>)でそれぞれ29%および71%]にある事が知られているが、<sup>2)</sup>フッ素化とともにhigh spin型の比率が増し、F4サイクラム(II-8)-Ni(II)錯体では、同条件でほぼ100%6配位high spin型[blue,  $\lambda_{max}$  517nm ( $\epsilon$  7)]をとる。いずれの場合も、温度上昇やイオン強度の増大に伴って、4配位low spin型への平衡移動が観察された。又、F4サイクラム(II-8)-Ni(II)·2Cl<sup>-</sup>錯体のX線結晶構造(high spin型)は、対応するサイクラム(II-5)-Ni(II)·2Cl<sup>-</sup>錯体(high spin型)の構造とほとんど変化がなかった。従って、以上観察された諸性質は、主にF原子の電子的吸引効果および疎水効果により説明できる。

ところで、近年、化石燃料の過剰使用により大気中の二酸化炭素濃度が増大し、気象上大きな問題となっている。そのため、二酸化炭素の回収(固定化)や有効利用は最重要課題の一つとなっており、光合成系でのCO<sub>2</sub>固定の機構解明とも関連して数多くのアプローチが行なわれている、その中でもサイクラムNi(II)錯体は電気化学的なCO<sub>2</sub>固定の(還元)触媒の一つとして、CO生成の効率や選択性(vs H<sub>2</sub>)の点で大変注目を集めている。<sup>1b</sup>



今回新たに合成した含フッ素サイクラム(II-6～8)のNi(II)錯体も、CO<sub>2</sub>還元の電気化学的触媒として働くことがわかった。しかしながら、サイクラムNi(II)錯体と同条件下においては、Fの数が増すごとにCO生成の効率およびCO/H<sub>2</sub>の選択性が低下した。しかしながら、エネルギー的観点からみて有利なより高い電位にて電解還元をすると、F4サイクラム(II-8)-Ni錯体は従来の無置換サイクラム(II-5)の錯体にくらべ、はるかに優れたCO<sub>2</sub>還元能を示した。本研究では、これらの機能と、酸化還元電位やスピニ状態との関連性について考察した。

以上のように、大環状ポリアミン金属錯体のフッ素化は、中心金属イオンの酸化還元電位や、配位形式の変化を伴う溶液内平衡に大きな影響を与え、結果として基質との反応性にも大きな変化をもたらした。これらは、フッ素基導入に伴う配位子の立体的要因よりも、フッ素の電子吸引効果や疎水効果によるところが大きいと考えられる。

本研究は、大環状ポリアミン金属錯体を新たに有機化学、分析化学、医学、電気化学等の領域に展開する上で、今後重要な指標となるであろう。

[引用文献]

- 1) (a) E. Kimura and R. Machida, *J. Chem. Soc., Chem. Commun.*, 499 (1984).  
(b) M. Beley, J-P. Collin, R. Ruppert and J-P. Sauvage, *J. Am. Chem. Soc.*, 108, 7461 (1986). (c) J. D. Koora and J. K. Kochi, *Inorg. Chem.*, 26, 908 (1987).  
2) L. Fabbrizzi et al., *J. Chem. Soc., Dalton Trans.*, 1857 (1979).

TABLE OF CONTENTS

	Page
[Abstracts] -----	1

[CHAPTER I]

NEW MACROCYCLIC TETRAAMINE METAL COMPLEXES APPENDED WITH AN INTRAMOLECULAR IMIDAZOLE.

Introduction -----	4
Experimental Section -----	6
Results and Discussion -----	10
Conclusion -----	28
References -----	29
Supplementary Materials -----	31

[CHAPTER II]

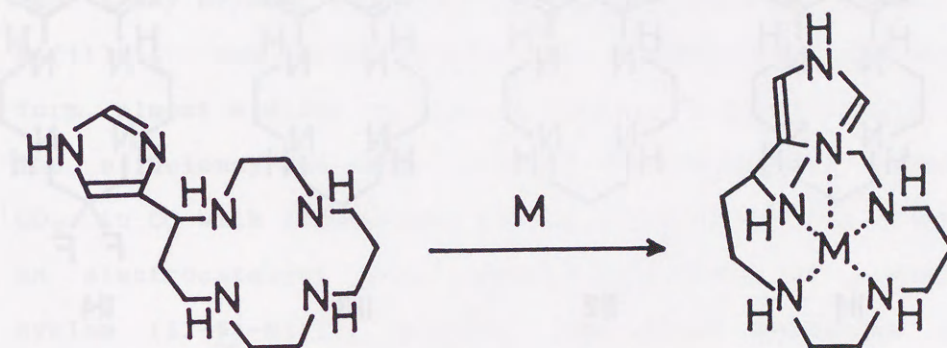
SYNTHESIS OF NOVEL FLUORINATED MACROCYCLIC TETRAAMINES AND CHEMICAL PROPERTIES OF THEIR METAL COMPLEXES.

Introduction -----	39
Experimental Section -----	41
Results and Discussion -----	50
Conclusion -----	81
References -----	83

## [Abstracts]

Chapter I.

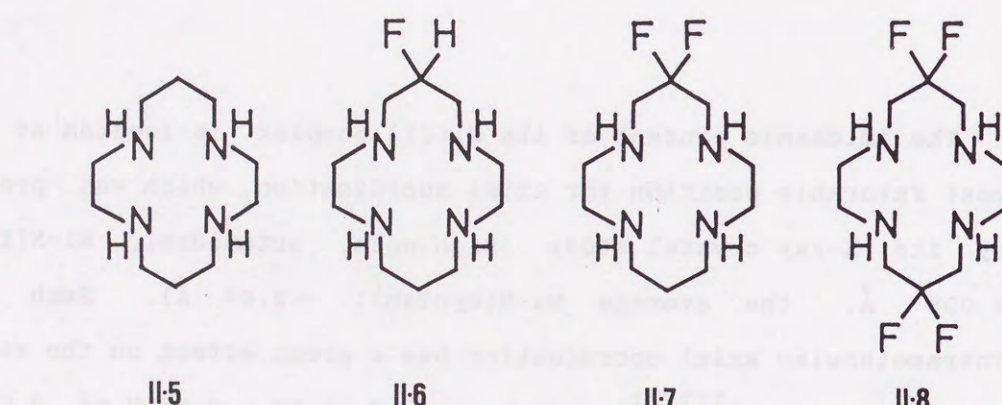
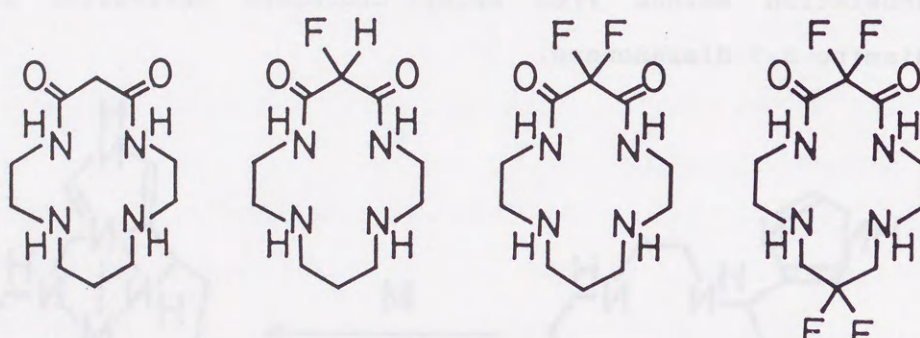
A cyclam ( $1,4,8,11$ -tetraazacyclotetradecane) appended with an intramolecular imidazole pendant was synthesized by an annelation method from methyl urocanate derivative and  $1,9$ -diamino- $3,7$ -diazanonane.



The imidazole pendant of its Ni(II) complex is located at the most favorable position for axial coordination, which was proved by its X-ray crystal study (high-spin, octahedral, Ni-N(Im);  $2.098 \text{ \AA}$ , the average Ni-N(cyclam);  $\sim 2.07 \text{ \AA}$ ). Such an intramolecular axial coordination has a great effect on the redox potential for  $\text{Ni}^{\text{III}}/\text{II}$  complex, raised up to  $+ 0.54 \text{ V vs S.C.E.}$  (saturated calomel electrode). Another remarkable effect of the destined axial imidazole coordination is shown in the formation of the  $1 : 1$  Co(II)-dioxygen complex in aqueous solution at room temperature, which is identified by its low temperature ESR study. The present new ligand may present a simplified model for the study of imidazole coordination effects in biological systems as well as a new redox-related catalysis.

Chapter II.

Novel synthesis and some chemical properties of mono-, di-, and tetrafluorinated dioxocyclams (II-2~4) and cyclams (II-6~8) have been explored.



The effects of successive fluorine substitution on chemical properties of ligands and their metal complexes are demonstrated by: i) the weakened amine basicities of ligands, ii) the increase in solubilities towards organic solvents, iii) the increase in complexation stabilities of  $\text{Cu(II)}\text{H}_2\text{L}$  ( $\text{L} = \text{II-2~4}$ ), iv) a predominance of the octahedral, high spin state of  $\text{Ni(II)}$

complexes at equilibrium in aqueous solution, and v) the destabilization of the higher oxidation states,  $\text{Cu(III)}$  and  $\text{Ni(III)}$ , and the stabilization of the lower oxidation states,  $\text{Ni(I)}$ , in either  $\text{CuH}_2\text{L}^0$  ( $\text{L} = \text{II-2~4}$ ) or  $\text{NiL}^{2+}$  ( $\text{L} = \text{II-6~8}$ ) system. These observations have been explained by the strong electron-withdrawing and hydrophobic effects of fluorine atoms. The X-ray crystal structure of tetrafluorinated cyclam (II-8)- $\text{Ni(II)}\text{Cl}_2$  was established to be in octahedral and high spin form, almost similar to that of cyclam (II-5)- $\text{Ni(II)}\text{Cl}_2$  complex. The efficiency and selectivity of electrochemical reduction of  $\text{CO}_2$  to CO with fluorinated cyclam (II-6~8)- $\text{Ni(II)}$  complexes as an electrocatalyst were compared with those of nonsubstituted cyclam (II-5)- $\text{Ni(II)}$  complex, and their mechanism is also discussed here from a kinetic or thermodynamic point of view. Fluorinated macrocyclic ligands will find great potentials in basic as well as an applied studies.

Among a variety of macrocyclic polyethers, 18-crown-6 (1,4,7,10-tetraazacyclododecane) is one of the most useful crown compounds which have been extensively studied and discussed by the author.<sup>1</sup> The author has also reported the synthesis of various crown compounds, such as dicyanocrown, methacryloylcrown, and so on, and has shown that it is possible to synthesize large numbers of crown compounds by synthetic methods. A new type of macrocyclic polyether, 18-crown-5, has been synthesized and its properties and polymerization behavior have been studied.<sup>2</sup>

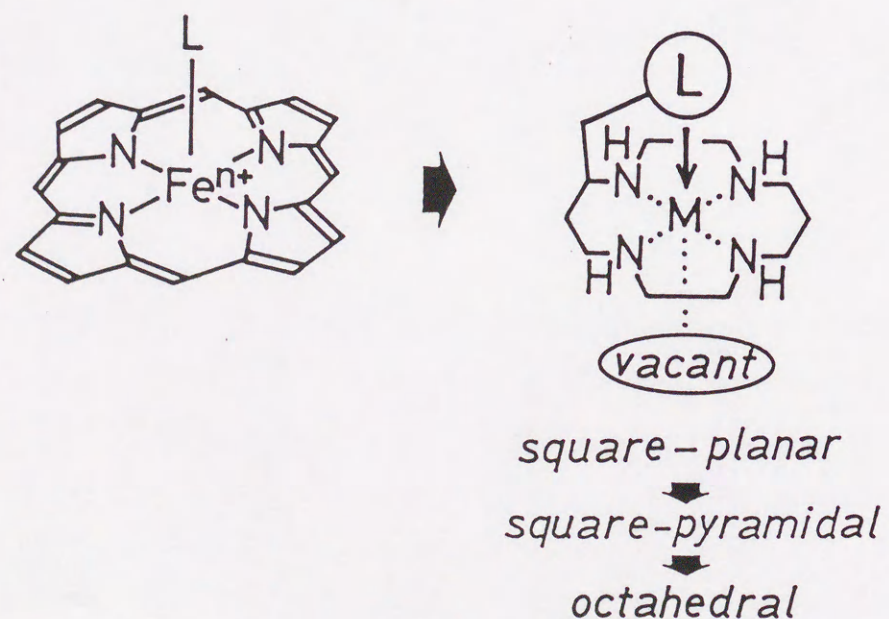
[CHAPTER I]

NEW MACROCYCLIC TETRAAMINE METAL COMPLEXES

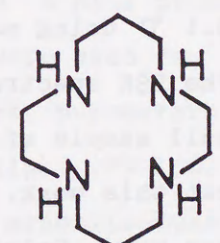
APPENDED WITH AN INTRAMOLECULAR IMIDAZOLE PENDANT

## [Introduction]

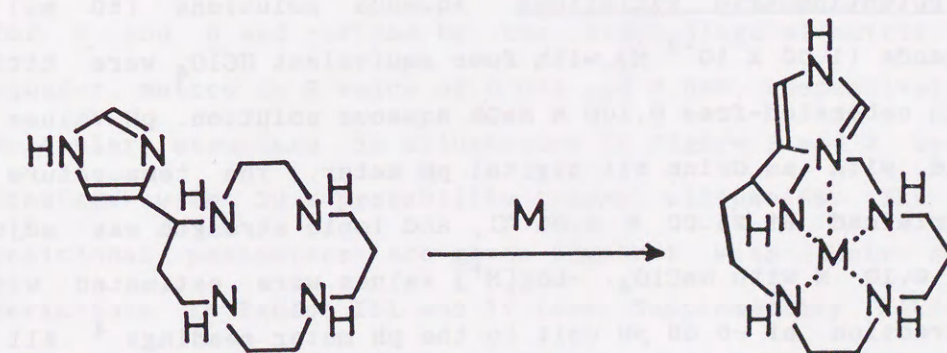
The biologically occurring macrocyclic tetraamine metal complexes are functionalized for their specific activities by having proximate donor ligands at axial position. Many of biochemists and coordination chemists have paid much attention to this interesting coordination fashion. The synthetic tetraaza macrocyclic ligands provide a natural framework (such as heme, chlorophyll and corrinoid) and the four donor nitrogen atoms are more or less rigidly confined to a plane leaving two axial sites available for interaction with substrates or proximate functional groups. Therefore, the incorporation of intramolecular functional groups to macrocyclic framework such that it may easily coordinate to the central metal ion encapsulated in the macrocyclic cavity, should be a good approach to metalloenzyme chemistry.



Among a variety of synthetic tetraaza macrocycles, cyclam (*1,4,8,11-tetraazacyclotetradecane*) is one of the most useful ligands as the models for certain natural occurring metalloproteins and enzymes. Recently, a new and versatile synthetic method for a novel functionalized macrocyclic polyamines bearing an intramolecular pendant donor such as pyridyl<sup>1</sup> and phenol<sup>2,3</sup> groups. This method was applied here for the synthesis of the first cyclam bearing an appended imidazole that would act as an ideal axial donor for an effective  $\pi$ -interaction between imidazole and metal ion in the cyclam cavity. The information derived from such a new complex may substantially help understanding of the apical effects in biological square-planar macrocyclic tetraamine complexes (e.g. porphyrin).



Cyclam



[Experimental Section]

General Methods. All the starting materials for synthesis were obtained commercially and were used without further purification. Aqueous solutions were prepared from analytical grade salts and distilled water. The gases of analytical grade were used without further purification. Melting points were determined by using a Yanako micro melting point apparatus and were uncorrected.  $^1\text{H}$  NMR spectra were obtained on a Hitachi R-40 high-resolution NMR spectrometer (90 MHz, 35 °C, Me<sub>4</sub>Si reference) or a JEOL GX-400 spectrometer (400 MHz, 35 °C, Me<sub>4</sub>Si reference). IR and Mass spectra were obtained on Shimadzu FTIR-4200 and JEOL JMS-01SG-2, respectively. UV-visible spectra were recorded on a Hitachi U-3200 double-beam spectrophotometer or a Shimadzu UV-3100 spectrophotometer at 25.0 ± 0.1 °C using matched quartz cells of 2, 10, or 50 mm path length. The ESR spectra were recorded on a JES-FE1X spectrometer using a small sample of MnO as reference at 77K. For TLC analysis throughout this work, Merck precoated TLC plates (silica gel 60 F<sub>254</sub>) were used. Column chromatography was carried out on silica gel (Wakogel C-300).

Potentiometric Titrations. Aqueous solutions (50 ml) of ligands ( $1.00 \times 10^{-3}$  M) with four equivalent HClO<sub>4</sub> were titrated with carbonated-free 0.100 M NaOH aqueous solution. pH Values were read with an Orion 811 digital pH meter. The temperature was maintained at 25.00 ± 0.05 °C, and ionic strength was adjusted to 0.10 M with NaClO<sub>4</sub>. -Log[H<sup>+</sup>] values were estimated with a correction of -0.08 pH unit to the pH meter readings.<sup>4</sup> All the solutions were carefully protected from air by a stream of humidified argon. The electrode system was calibrated with pH

7.00 and 4.01 buffer solutions and checked by the duplicate theoretical titration curves of  $4.00 \times 10^{-3}$  M HClO<sub>4</sub> with a 0.100 M NaOH solution at 25 °C and  $I = 0.10$  M (NaClO<sub>4</sub>) in high- and low-pH regions.

Electrochemical Measurements. Cyclic voltammetry was performed with a Yanako P-1100 polarographic analyzer system at 25.00 ± 0.05 °C. A three-electrode system was employed: a 3 mm glassy-carbon rod (Tokai Electrode Co. GC-30) or hanging mercury electrode as the working electrode, a Pt wire as the counter electrode, and a saturated calomel electrode (S.C.E.) as the reference electrode. The cyclic voltammograms with scan rates of 100–200 mVs<sup>-1</sup> were evaluated graphically.

Crystallographic Study. A purple prism with dimensions  $0.2 \times 0.2 \times 0.5$  mm<sup>3</sup> of 5 and a pink prism with dimensions  $0.15 \times 0.20 \times 0.30$  mm<sup>3</sup> of 6 were used for data collection at room temperature. The lattice parameters and intensity data were measured on a Philips PW-1100 automatic four-circle diffractometer by using graphite-monochromated Cu K $\alpha$  radiation. Crystal data and data collection parameters are displayed in Table I and II. The structure was solved by the heavy-atom method for 5 and 6 and refined by the block-diagonal-matrix least-squares method to R value of 0.062 and 0.095, respectively. The molecular structure is illustrated in Figure 2 and 3 by ORTEP drawings with 30 % probability thermal ellipsoids. The atomic positional parameters are given together with their standard deviations in Tables III and IV (see Supplementary Materials). Bond distances and angles are presented in Tables V–VIII (see Supplementary Materials). Listing of hydrogen atom positional

parameters and of thermal parameters for 5 and 6 and tables of observed and calculated structure factors for the complexes are omitted.

**Synthesis.** 7-(1-Triphenylmethyylimidazol-4-yl)-1,4,8,11-tetraazacycloazatetradecan-5-one (3) A mixture of N-triphenylmethylated methyl urocanate (1) (1.0 g, 2.5 mmol) and 1,9-diamino-3,7-diazanonane (2) (406 mg, 2.5 mmol) was heated at reflux in 55 ml of MeOH-tetrahydrofuran (THF) (10 : 1) for 18 days. After cooling, the reaction mixture was evaporated to dryness and purified by silica gel chromatography (eluent:  $\text{CH}_2\text{Cl}_2-\text{CH}_3\text{OH}-28\% \text{ aqueous NH}_3 = 5 : 2 : 0.1 \sim 0.15$ ) followed by recrystallization from acetonitrile to give the pure cyclic amide (3) in 8 % yield (107 mg); mp 172.5-173.5 °C; IR (KBr):  $\nu_{\text{C=O}}$  1670  $\text{cm}^{-1}$ ;  $^1\text{H}$  NMR (90 MHz,  $\text{CDCl}_3$ ):  $\delta$  1.4-1.9 (m, 2H), 2.3-3.0 (m, 15H containing three NH protons), 3.2-3.5 (m, 2H), 3.6-4.0 (br, 1H), 6.6 (s, 1H), 7.0-7.4 (m, 16H containing one imidazole proton), 8.9-9.0 (br, 1H  $\text{D}_2\text{O}$  exchangeable).

5-(Imidazol-4-yl)-1,4,8,11-tetraazacyclotetradecane (4) The cyclic amide (3) (1.17 g, 2.2 mmol) was heated at 50~60 °C in freshly distilled diborane-THF solution for 19 h. After cooling, a small amount of crushed ice was cautiously added and the volatile components were taken up in 200 ml of 6 N HCl solution. After the removal of THF by evaporation, the resultant aqueous solution was washed with  $\text{CH}_2\text{Cl}_2$  repeatedly and evaporated to dryness. The residue was neutralized with aqueous  $\text{Na}_2\text{CO}_3$  solution and then evaporated. Inorganic salts, precipitated by the addition of  $\text{CH}_3\text{OH}-\text{CH}_2\text{Cl}_2$ , were filtrated. To methanol solution of the resulting free form of (4) was added 0.5 ml of

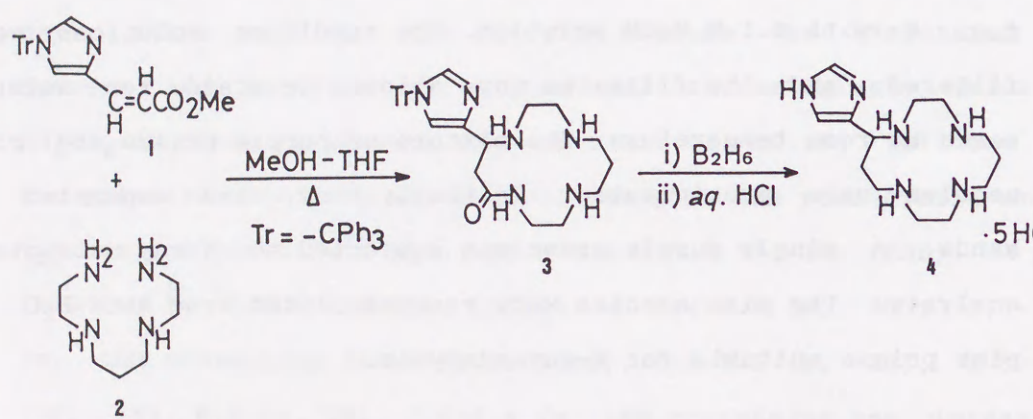
HCl to give the cyclam derivative 4·5HCl as colorless fine needles (771 mg, 77 %); m.p. 228 °C (dec.);  $\text{M}^+$  peak  $m/e$  266 (as free form);  $^1\text{H}$  NMR (90 MHz,  $\text{D}_2\text{O}$ ):  $\delta$  2.1-2.6 (m, 4H), 2.8-3.2 (m, 2H), 3.2-3.8 (m, 12H), 4.3-4.4 (m, 1H), 7.50 (s, 1H), 8.65 (s, 1H).

Preparation of Ni(II) Complexes with 4 Ligand (4) (0.5 mmol) and  $\text{NiSO}_4$  (0.5 mmol) were dissolved in 50 ml of 0.1 M  $\text{NaClO}_4$  aqueous solution at 50 °C, and pH of the mixture was adjusted to c.a. 8 with 0.1 M NaOH solution. The resulting solutions were filtered, and the filtrates were allowed to stand for several weeks at room temperature. The mixture of purple prisms and pink needles were precipitated. Initially they were separated by hands. A single purple prism was subjected to X-ray structure analysis. The pink needles were recrystallized from  $\text{MeCN}-\text{H}_2\text{O}$  to pink prisms suitable for X-ray analysis.

## [Results and Discussion]

Synthesis of Imidazole-pendant Cyclam 4. The new cyclam appended with an imidazole pendant was synthesized by an annelation method previously reported for pyridyl<sup>2</sup> or phenol-appended<sup>3</sup> cyclams as depicted below.

## Synthesis



The acrylate 1 (N-triphenylmethylated methyl urocanate) and equivalent of 1,9-diamino-3,7-diazanonane (2) were refluxed in MeOH-THF (10 : 1) for 3 weeks to give the cyclic amide 3 in 8 % yield. Reduction of the amide with  $B_2H_6$  in THF, followed by HCl treatment yielded crystalline product 4 as pentahydrochloride in 75 % yield. Apparently, the present cyclization step involves the initial Michael-type addition followed by an intramolecular amide formation by the two terminal amines. If this annelation reaction is run with methyl urocanate, the yield is somewhat better. However, the next reduction of amide function was unsuccessful with diborane in tetrahydrofuran.

Properties of Imidazole-pendant Cyclam 4. The stepwise protonation constants ( $pK_a$ ) for the new macrocycle were determined by potentiometric titrations at 25 °C and  $I = 0.1$  M ( $NaClO_4$ ). The pH titration curve of 4 is shown in Figure 1. The amine  $pK_a$  values for 4 are 11.5, 10.2, 5.6 (Imidazole N), < 2 and < 2. The proximity of the imidazole N to the macrocycle in 4 is illustrated by its extremely low  $pK_a$  value of 5.6 (normally 7.1)<sup>5</sup> under the strong influence of the two protons lying in the  $N_4$  ring.<sup>6</sup>

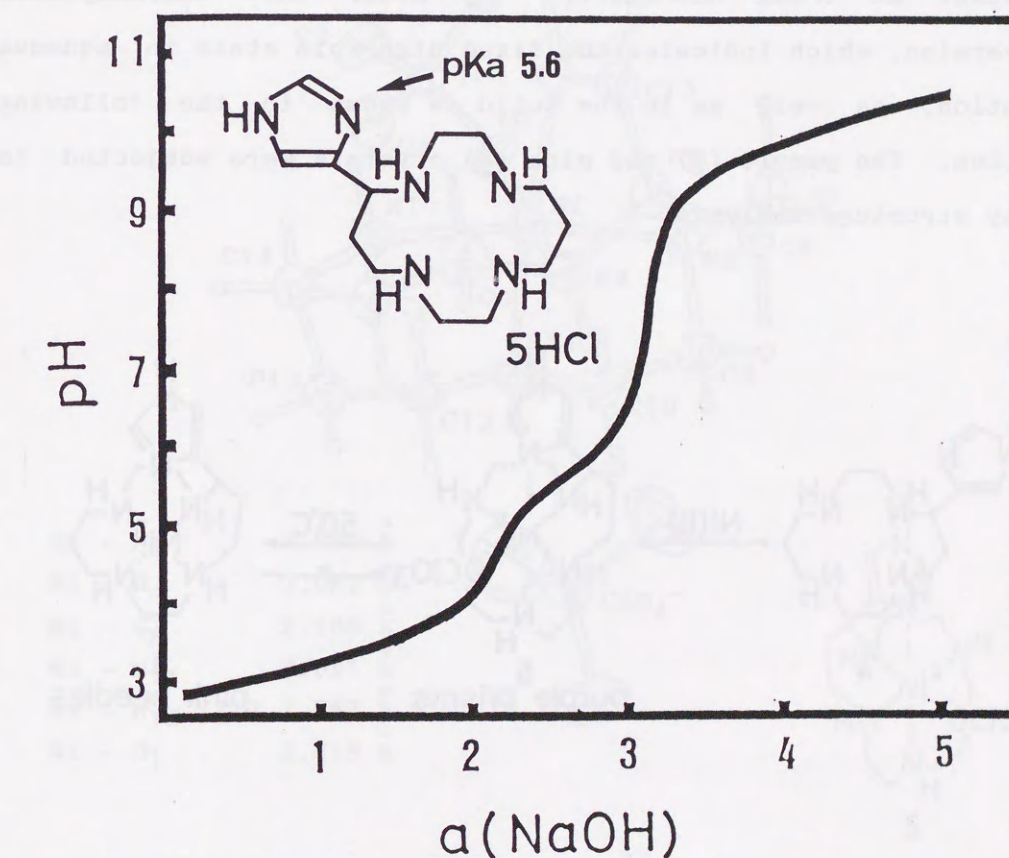
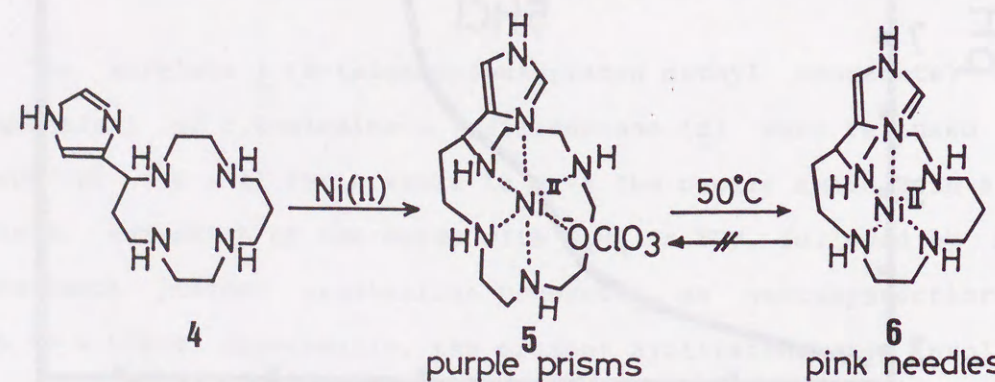


[Figure 1] A titration curve of imidazole-pendant cyclam · 5HCl (4 · 5HCl,  $1 \times 10^{-3}$  M) and  $I = 0.1$  M ( $NaClO_4$ ).

Interaction of Ni(II) with Imidazole-pendant Cyclam 4. Purple and pink crystals were precipitated when equimolar  $\text{NiSO}_4$  and 4 were treated at  $50^\circ\text{C}$  for 10 min in an aqueous solution ( $\text{pH} = 8$ ) in the presence of  $\text{NaClO}_4$ . Initially they were separated by hands. Later, it was found that the purple product [ $\lambda_{\text{max}} 533 \text{ nm}$  ( $\epsilon 8$ ) in  $\text{H}_2\text{O}$  at  $25^\circ\text{C}$ ] is a kinetic one, which by longer treatment in warmer ( $> 70^\circ\text{C}$ ) aq. solution is completely converted to the pink as the ultimate thermodynamic product. The  $\text{d-d}$  absorption maxima (at  $25^\circ\text{C}$  and  $I = 0.1 \text{ M}$  ( $\text{NaClO}_4$ )) is held constant at  $\lambda_{\text{max}} 518 \text{ nm}$  ( $\epsilon 7$ ) after the thermodynamic conversion, which indicates the fixed high-spin state in aqueous solution, as well as in the solid as shown in the following section. The purple (5) and pink (6) crystals were subjected to X-ray structure analysis.



Crystal Structures of Ni(II) Complexes, cis-5 and trans-6. The structure of the axial imidazole-pendant cyclam-Ni(II) complexes, 5 and 6, were established by the present X-ray crystal studies.

The structure of 5 is shown in Figure 2. Crystal data and data collection parameters are displayed in Table I.

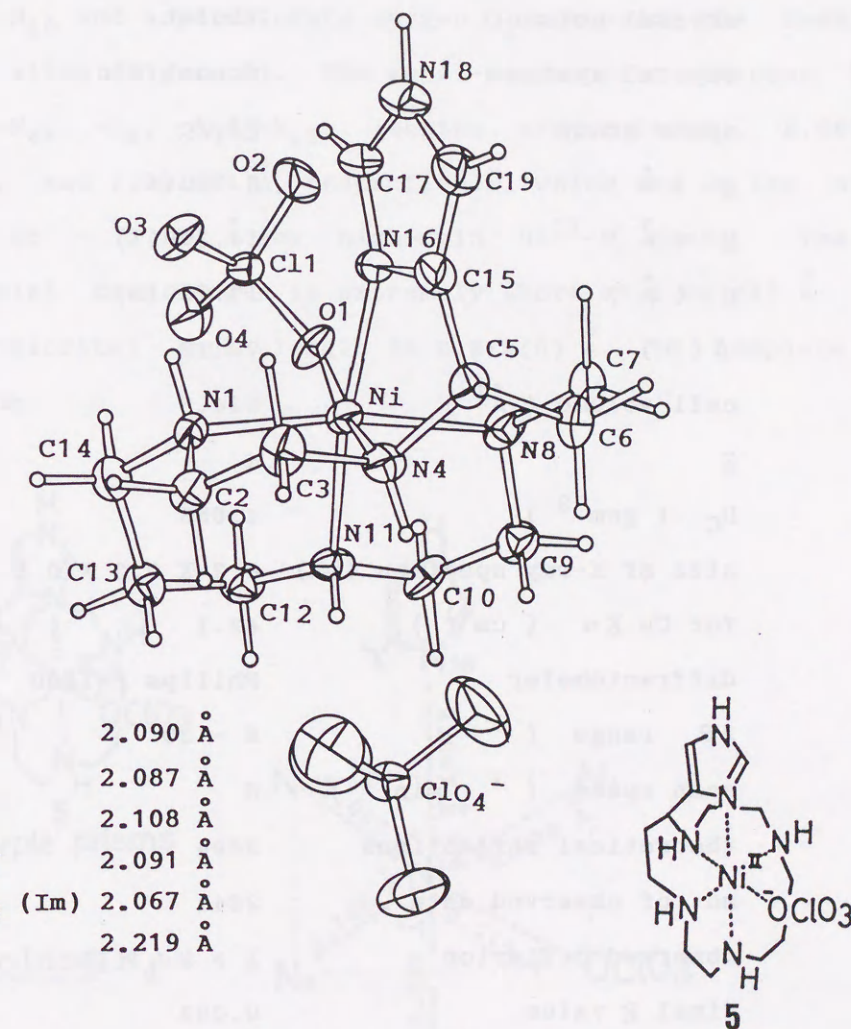
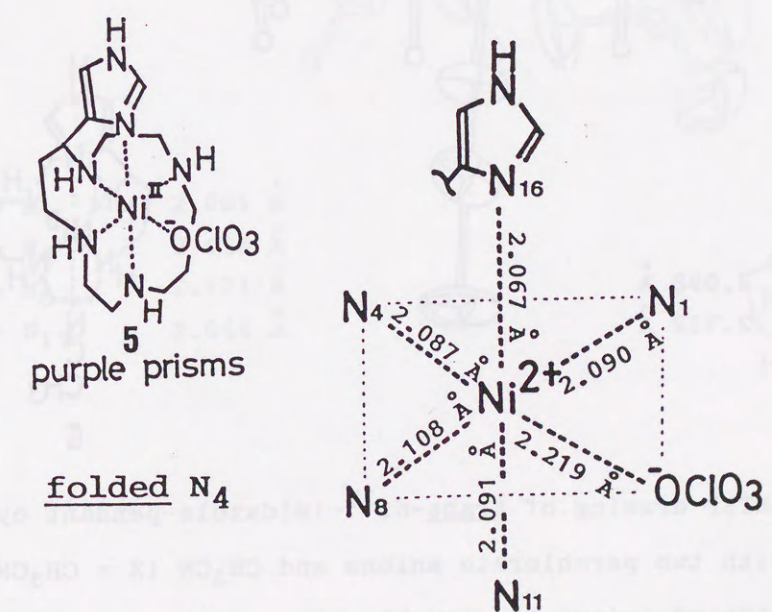


[Figure 2] ORTEP drawing of *cis*- $\text{Ni}^{II}$ -imidazole-pendant cyclam 5 with two perchlorate anions. Atoms are drawn with 30 % probability ellipsoids.

Table I Crystal Data and Data Collection Summary for *cis*-Ni<sup>II</sup>-Imidazole-pendant Cyclam·2ClO<sub>4</sub> (5).

molecular formula	C <sub>13</sub> H <sub>26</sub> N <sub>6</sub> Ni·2ClO <sub>4</sub>
formula weight	523.99
crystal habit	prism
crystal colour	violet
crystal system	monoclinic
space group	P2 <sub>1</sub> /c
a (Å)	8.780(4)
b (Å)	14.309(7)
c (Å)	17.759(9)
β (°)	70.19
cell volume (Å <sup>3</sup> )	524.8
Z	4
D <sub>C</sub> (gcm <sup>-3</sup> )	1.658
size of X-ray specimen (mm)	0.2 X 0.2 X 0.5
for Cu Kα (cm <sup>-1</sup> )	42.1
diffractometer	Philips PW1100
2θ range (°)	6 - 30
scan speed (° min <sup>-1</sup> )	6
theoretical reflections	3694
no. of observed data	2841
observed criterion	I > 2σ (I)
final R value	0.062

The atomic positional parameters for 5 are given together with their standard deviations in Table III (see Supplementary Materials), and selected bond distances and angles are presented in Tables V and VII, respectively (see Supplementary Materials). In six-coordinate 5 (X = OCLO<sub>4</sub><sup>-</sup>, λ max 522 nm in solid), the cyclam moiety is in a folded configuration with the imidazole nitrogen N<sub>16</sub> and a perchlorate oxygen O<sub>1</sub> occupying the remaining two *cis* sites (Figure 2). The metal-macrocyclic nitrogen bonds Ni-N<sub>1</sub>, -N<sub>4</sub>, -N<sub>8</sub>, and -N<sub>11</sub> lengths are 2.090(4), 2.087(5), 2.108(4), and 2.091(5) Å, respectively, which are in the normal range 2.05 - 2.10 Å for high-spin Ni<sup>II</sup>-N bonds. The Ni-N(imidazole) bond length is extremely short at 2.067(5) Å. The Ni-O(perchlorate) bond length is 2.219(5) Å, to complete the octahedron.



The structure of 6 is shown in Figure 3. Crystal data and data collection parameters are displayed in Table II.

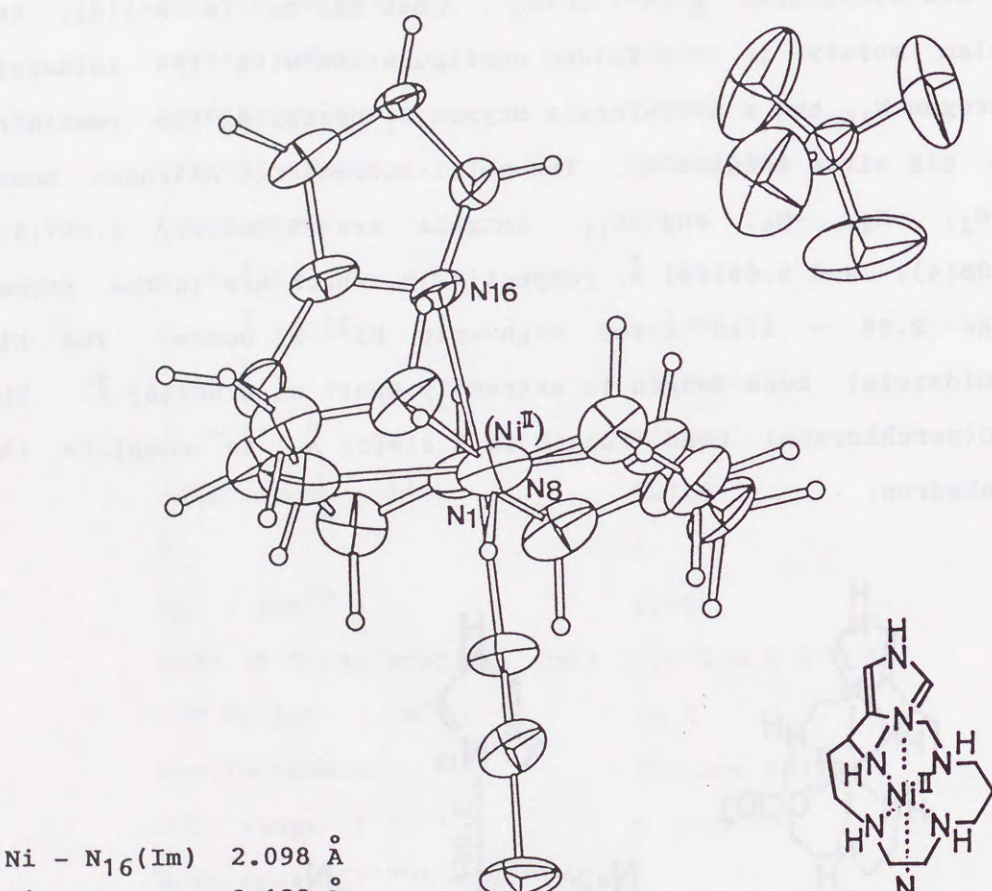
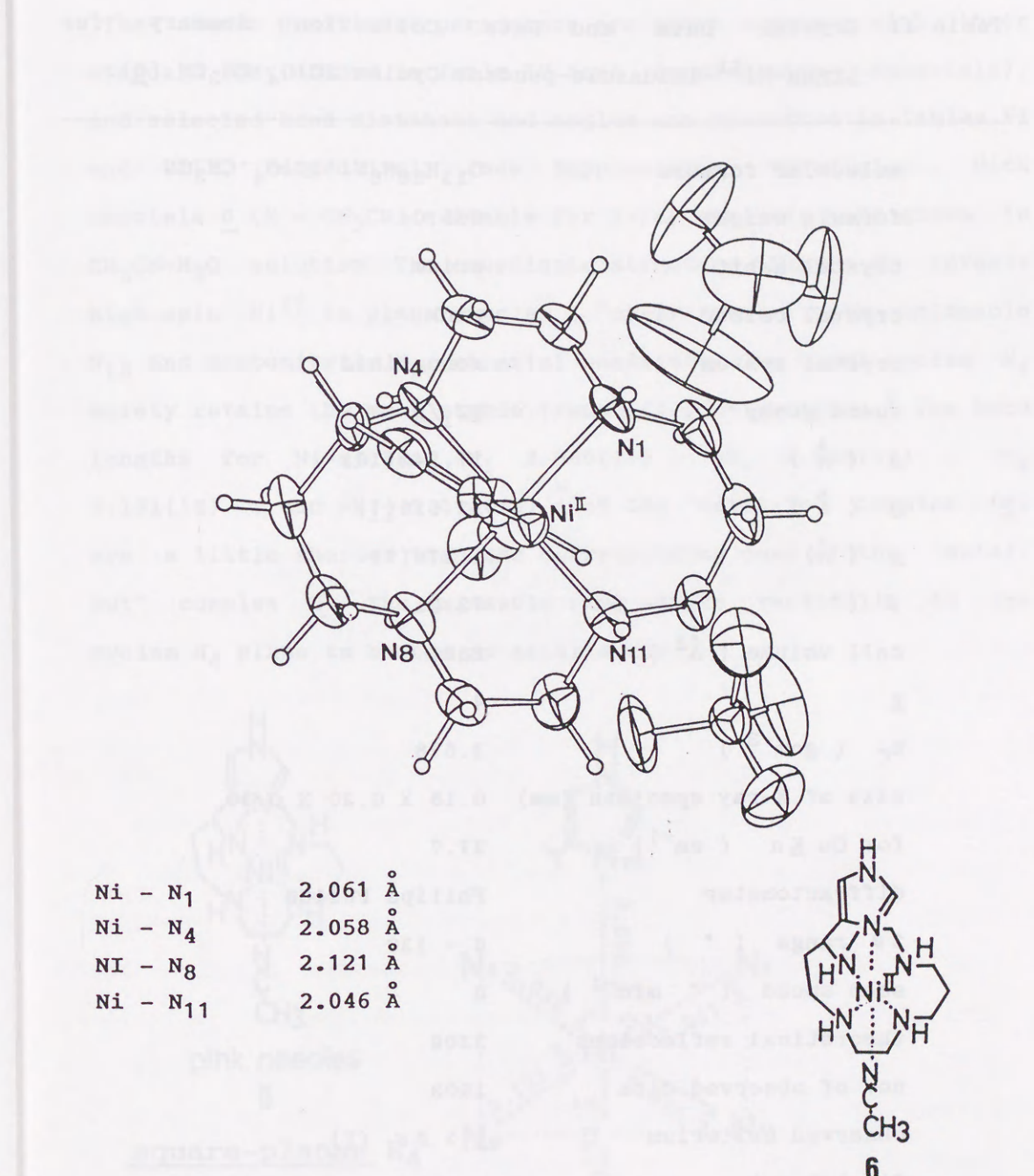


[Figure 3] ORTEP drawing of trans-Ni<sup>II</sup>-imidazole-pendant cyclam 6 with two perchlorate anions and CH<sub>3</sub>CN (X = CH<sub>3</sub>CN); (a) Side-on view (a perchlorate anion is omitted for clarity). Atoms are drawn with 30 % probability ellipsoids.

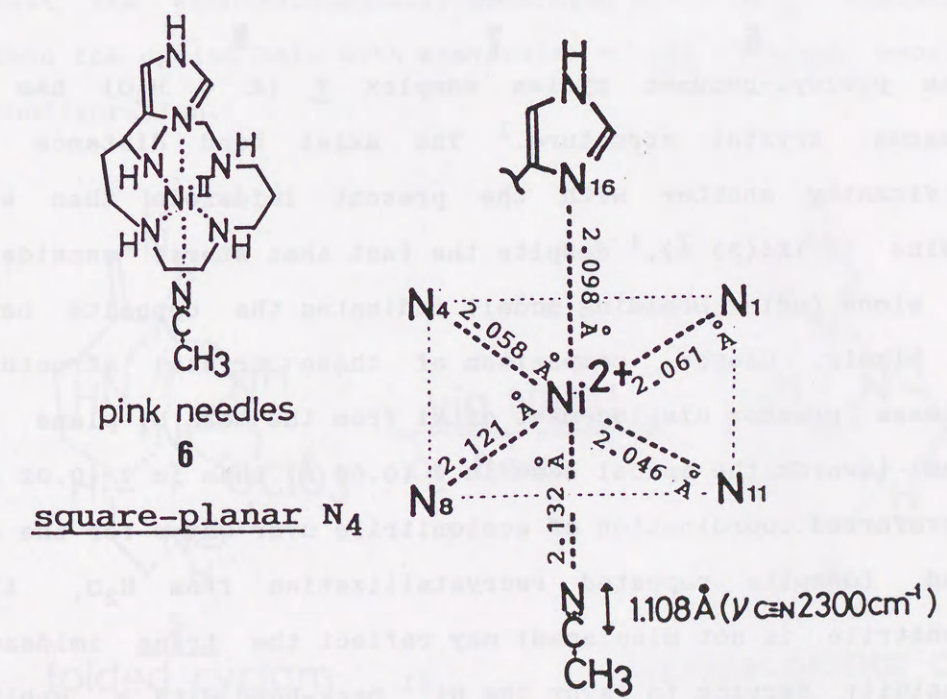


(b) Top view. Atoms are drawn with 30 % probability ellipsoids.

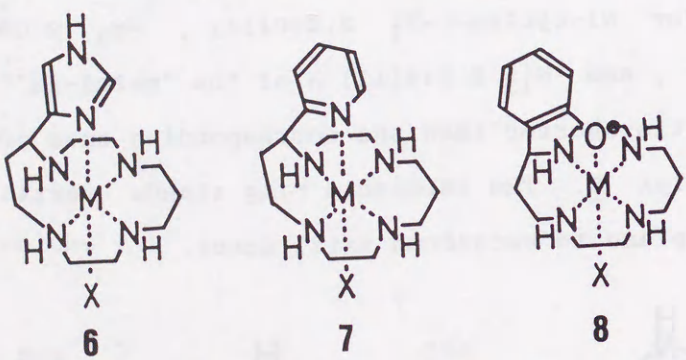
Table II Crystal Data and Data Collection Summary for  
trans-Ni<sup>II</sup>-imidazole-pendant Cyclam·2ClO<sub>4</sub>·CH<sub>3</sub>CN (6).

molecular formula	C <sub>13</sub> H <sub>26</sub> N <sub>6</sub> Ni·2ClO <sub>4</sub> ·CH <sub>3</sub> CN
formula weight	565.04
crystal habit	prism
crystal colour	pink
crystal system	monoclinic
space group	P2 <sub>1</sub> /n
a ( Å )	17.242(10)
b ( Å )	12.515(7)
c ( Å )	11.576(7)
β ( ° )	72.21
cell volume ( Å <sup>3</sup> )	2387
<u>Z</u>	4
D <sub>C</sub> ( gcm <sup>-3</sup> )	1.578
size of X-ray specimen (mm)	0.15 X 0.20 X 0.30
for Cu K $\alpha$ ( cm <sup>-1</sup> )	37.7
diffractometer	Philips PW1100
2θ range ( ° )	6 - 130
scan speed ( ° min <sup>-1</sup> )	6
theoretical reflections	3309
no. of observed data	1903
observed criterion	I > 2σ (I)
final R value	0.095

The atomic positional parameters are given together with their standard deviations in Table IV (see Supplementary Materials), and selected bond distances and angles are presented in Tables VI and VIII, respectively (see Supplementary Materials). Pink crystals 6 (X = CH<sub>3</sub>CN) suitable for X-ray analysis were grown in CH<sub>3</sub>CN-H<sub>2</sub>O solution. The coordinate structure (Figure 3) reveals high-spin Ni<sup>II</sup> in planar cyclam ("chair form") with imidazole N<sub>16</sub> and acetonitrile N<sub>20</sub> at axial positions. The basal cyclam N<sub>4</sub> moiety retains the most stable trans-III configuration.<sup>6</sup> The bond lengths for Ni-cyclam -N<sub>1</sub> 2.060(11), -N<sub>4</sub> 2.058(12), -N<sub>8</sub> 2.121(12), and -N<sub>11</sub> 2.046(12) Å of the "metal-in" complex (6) are a little shorter than the corresponding ones of the "metal-out" complex 5. The imidazole ring stands vertically to the cyclam N<sub>4</sub> plane to become an axial donor.

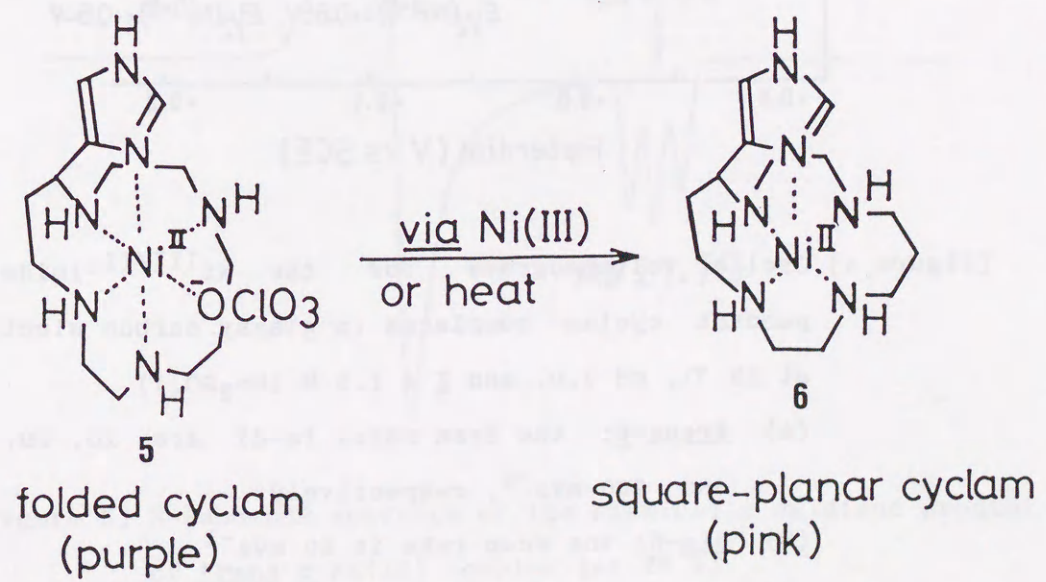


Moreover, the imidazole plane bisects (by 20°) the N<sub>4</sub>(N<sub>1</sub>)-Ni-N<sub>8</sub>(N<sub>11</sub>) angles, which, coupled with short Ni-N<sub>16</sub>(Im) distance of 2.098(9) Å, may facilitate the imidazole → metal π-donation. Similar bond lengths (2.06 - 2.1 Å)<sup>7</sup> and orientations of the imidazole ring of the proximal histidine onto porphyrin plane (20 - 22.5°)<sup>7</sup> are recognized in hemes or their models to serve Im-Fe<sup>II</sup> π-interaction for the trans O<sub>2</sub> binding.<sup>8</sup> The present new cyclam 4 is thus proven to be equipped with an ideal imidazole ligand for axial coordination.



The pyridyl-pendant cyclam complex  $\underline{\lambda}$  ( $X = H_2O$ ) has an analogous crystal structure.<sup>1</sup> The axial bond distance is significantly shorter with the present imidazole than with pyridine ( $2.124(3) \text{ \AA}$ ),<sup>1</sup> despite the fact that steric consideration alone (using Dreiding model) indicates the opposite being more likely. Closer comparison of these crystal structures discloses greater displacement of Ni from the mean  $N_4$  plane (of cyclam) towards the apical base in  $\underline{\lambda}$  ( $0.05 \text{ \AA}$ ) than in  $\underline{\gamma}$  ( $0.02 \text{ \AA}$ ). The preferred coordination of acetonitrile over water for the 6th ligand (despite repeated recrystallization from  $H_2O$ , this acetonitrile is not displaced) may reflect the trans imidazole  $\pi$ -basicity serving to favor the  $Ni^{II}$  back-bond with  $\pi$  orbital of the  $CH_3CN$ .<sup>9</sup>

Electrochemical Behaviors of Ni(II) Complexes: Conversion of cis-5 to trans-6. A unique axial imidazole coordination in 6 affects Ni<sup>III/II</sup> redox potential. Cyclic voltammetry (C.V.) shows a quasi-reversible voltammogram at  $E_{1/2}$  of + 0.54 V vs. saturated calomel electrode (S.C.E.) (0.5 M Na<sub>2</sub>SO<sub>4</sub>, pH = 7.0, 25 °C) with a peak potential separation of ~ 60 mV (Figure 4), which goes between + 0.61 V of the pyridyl coordinate homologue 7 and + 0.35 V of the phenol coordinate 8, but is near to + 0.50 V of the cyclam (without pendant) complex. The cyclic voltammograms have interlinked 5 and 6, where the folded cyclam of 5 is seen to rapidly rearrange to the planar cyclam of 6. An irreversible anodic peak occurring at + 0.69 V in the first scan of 5 gradually diminishes and is replaced by a new growing quasi-reversible wave at + 0.54 V in the subsequent scans (Figure 4). It is interpreted that the electrochemically generated Ni<sup>III</sup> of 5 rapidly goes into the cyclam hole with conversion of cis to trans macrocyclic configuration.



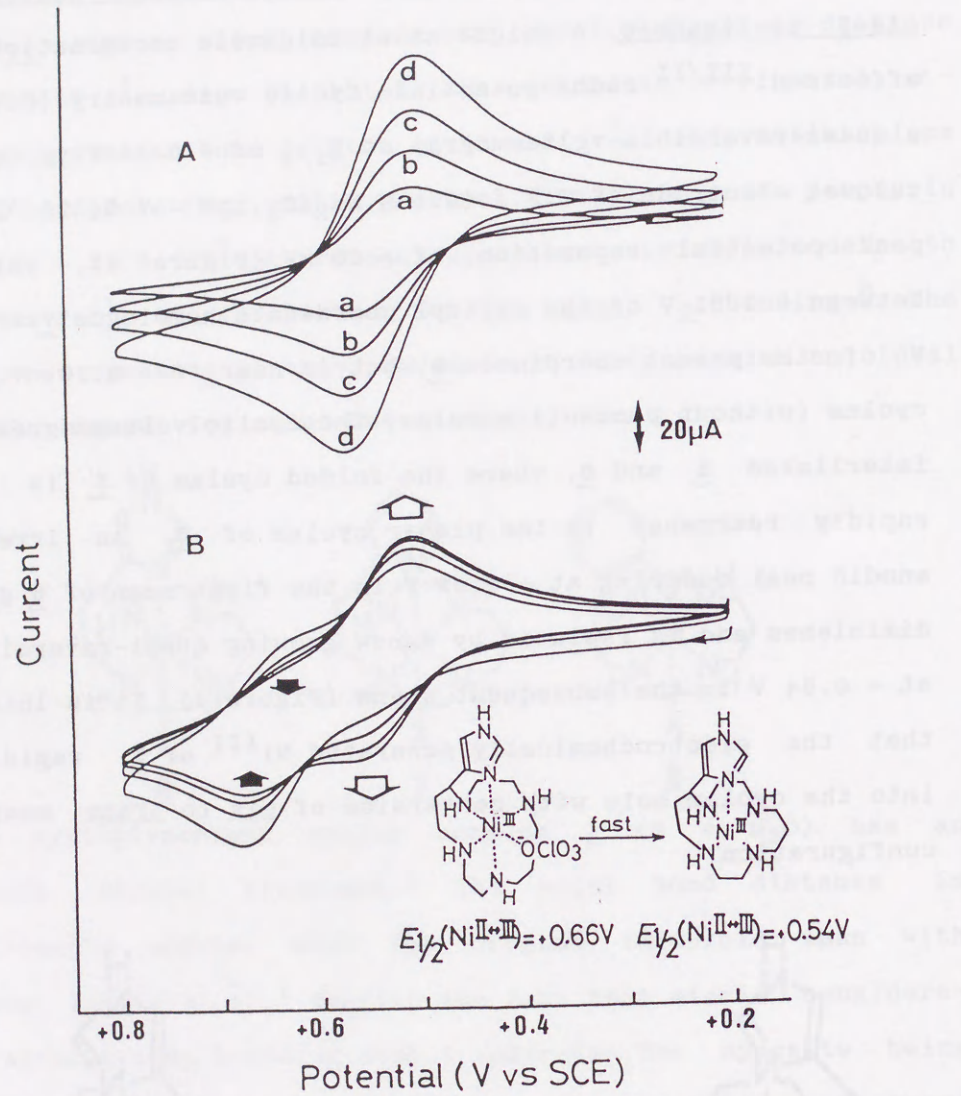


[Figure 4] Cyclic voltammograms for the Ni<sup>III/II</sup>-imidazole-pendant cyclam complexes (a glassy carbon electrode, at 25 °C, pH 7.0, and I = 1.5 M (Na<sub>2</sub>SO<sub>4</sub>)).  
 (A) trans-6; the scan rates (a-d) are 20, 50, 100, and 200 mVs<sup>-1</sup>, respectively.  
 (B) cis-5; the scan rate is 50 mVs<sup>-1</sup>.

The ESR spectrum of the chemically oxidized (e.g. (NH<sub>4</sub>)<sub>2</sub>S<sub>2</sub>O<sub>8</sub> oxidation) product of Ni(II) complex 6 at 77 K (Figure 5) shows axial symmetry, with  $g_{\perp} > g_{\parallel}$ . Further, g is split into three lines. This observation is considered with the existence of a low spin  $\text{q}^7$  Ni(III) complex, where the imidazole N ( $I = 1/2$ ) is axially coordinated.

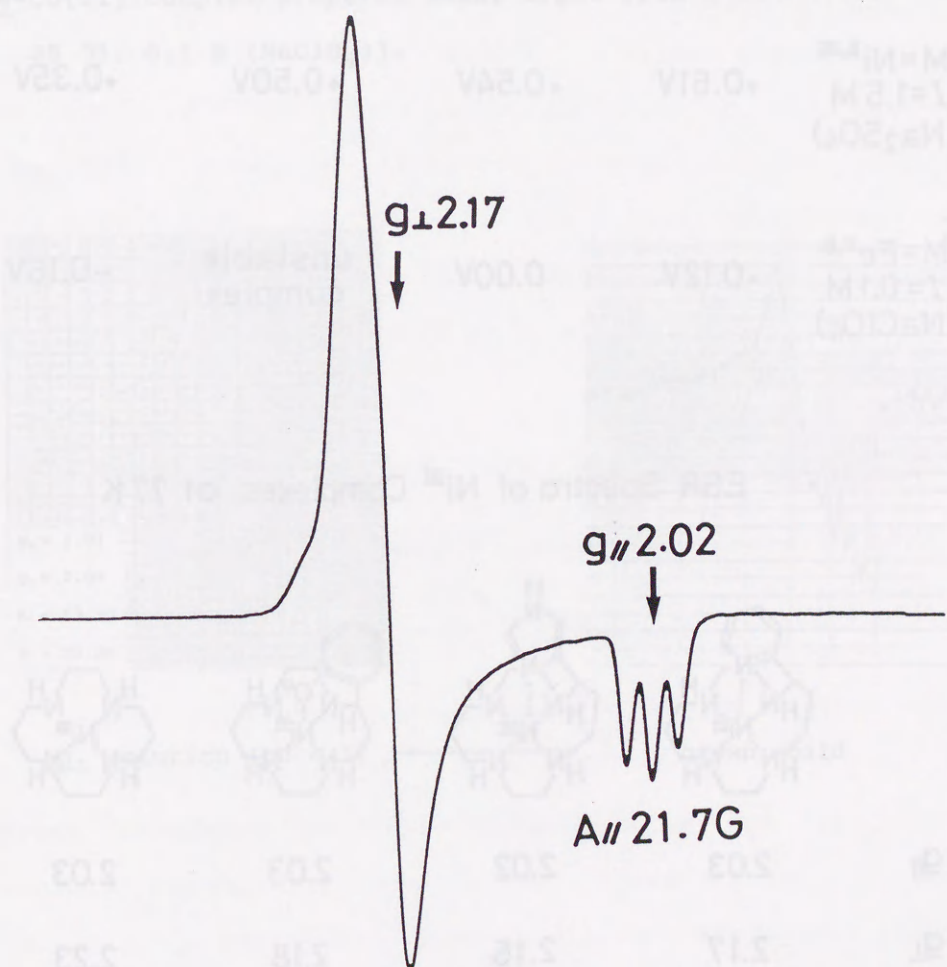


[Figure 5] X-Band ESR spectrum of the chemically oxidized product of trans-6 Ni(II) complex (at 77 K).

Axial Coordination Effects for  $M^{II,III}$ -  
Redox Potentials (V vs. SCE) at 25 °C

<chem>[M]1N2[C@H]3[C@@H]2[C@H]1c4ccccc4[C@H]3N[C@H](C)N</chem>	<chem>[M]1N2[C@H]3[C@@H]2[C@H]1c4ccccc4[C@H]3N[C@H](C)N</chem>	<chem>[M]1N2[C@H]3[C@H]2[C@H]1c4ccccc4[C@H]3N[C@H](C)N</chem>	<chem>[M]1N2[C@H]3[C@H]2[C@H]1c4ccccc4[C@H]3N[C@H](C)N</chem>
M=Ni <sup>II,III</sup> I=1.5 M (Na <sub>2</sub> SO <sub>4</sub> )	+0.61V	+0.54V	+0.50V
M=Fe <sup>II,III</sup> I=0.1 M (NaClO <sub>4</sub> )	+0.12V	0.00V	unstable complex
			-0.16V

ESR Spectra of Ni<sup>III</sup> Complexes at 77 K

<chem>[Ni]1N2[C@H]3[C@@H]2[C@H]1c4ccccc4[C@H]3N[C@H](C)N</chem>	<chem>[Ni]1N2[C@H]3[C@@H]2[C@H]1c4ccccc4[C@H]3N[C@H](C)N</chem>	<chem>[Ni]1N2[C@H]3[C@H]2[C@H]1c4ccccc4[C@H]3N[C@H](C)N</chem>	<chem>[Ni]1N2[C@H]3[C@H]2[C@H]1c4ccccc4[C@H]3N[C@H](C)N</chem>
$g_{  }$	2.03	2.02	2.03
$g_{\perp}$	2.17	2.16	2.18
$A_{  }$	21.2G	21.7G	-

The Formation of Molecular Oxygen Adduct with Co(II)-4 Complex in Aqueous Solution. Another remarkable effect of the destined axial coordination of the imidazole is shown in the O<sub>2</sub> binding of its Co<sup>II</sup> complex in aqueous solution at room temperature.

The oxygen adduct of Co(II) complex with 4 has been confirmed by ESR both in frozen solution and as a solid in low temperature. We prepared 4-Co(II)-O<sub>2</sub> adduct by exposing to oxygen a solution of 4-Co(II) complex prepared under argon with a titration method (at 35 °C, 0.1 M (NaClO<sub>4</sub>)).

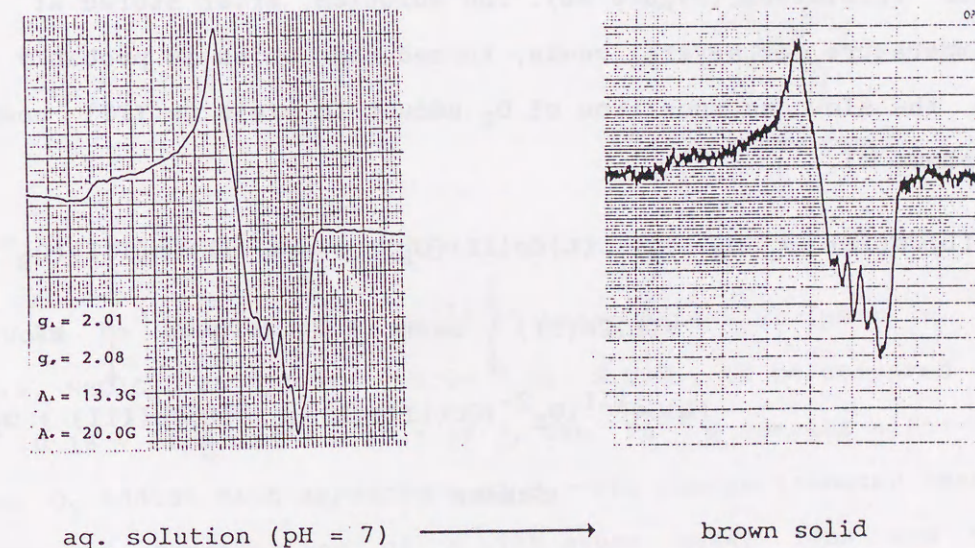
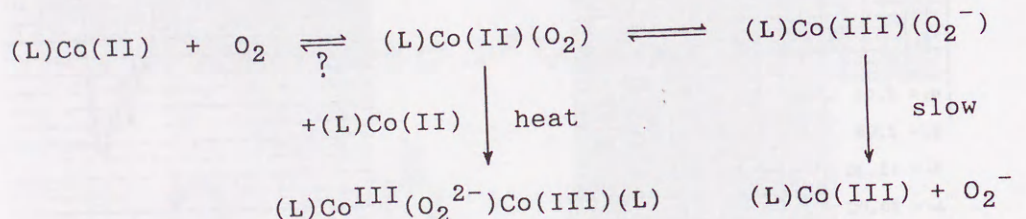


[Figure 6] ESR Spectra of 1 : 1 Co(II)-dioxygen complex with 4:  
(a) in frozen aqueous solution at 12 K  
(b) in solid state at 77 K.

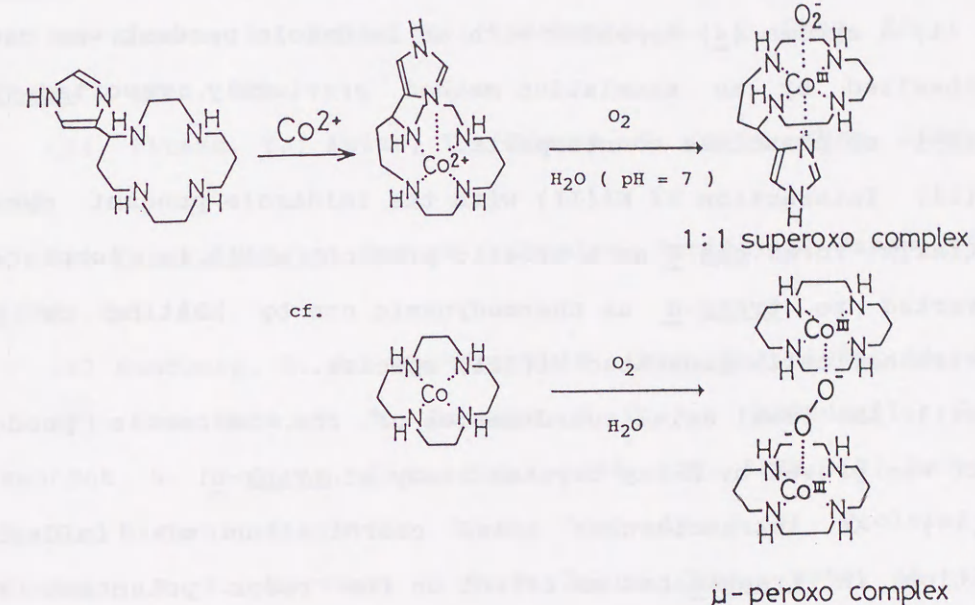
The ESR spectrum was taken from the resulting brown solution [ $\lambda_{\text{max}}$  319 nm ( $\epsilon$  4500), 446 nm ( $\epsilon$  370)] at 12 K. Its ESR parameters are  $g_{\perp} = 2.02$ ,  $g_{\parallel} = 2.07$ ,  $A_{\perp}^{\text{Co}} = 12.2$  G,  $A_{\parallel}^{\text{Co}} = 20.4$  G (Figure 6a). The spectrum exhibits hyperfine lines from a single  $^{59}\text{Co}$  nucleous (the electronic spin of 1/2 is split by the 7/2 nuclear spin of the cobalt center,<sup>10</sup> and is quite similar to those previously reported for 1:1 oxygen adducts of square-planar cobalt(II) complexes.<sup>11-13</sup> From the same solution after several days, a small amount of a dark brown solid precipitated as diperchlorate salts. This solid, cooled to 77 K, gives an ESR spectrum characteristic of 1:1 Co(II)-O<sub>2</sub> adduct, although with poor resolution (Figure 6b). The solution, after stored at room temperature for several weeks, turned red, which is probably due to the slow decomposition of O<sub>2</sub> adduct to yield Co(III) complex (Scheme 1).



### Scheme 1

Most of the water-soluble Co(II)-O<sub>2</sub> complexes previously reported are dinuclear. The Co<sup>II</sup>(cyclam) complex without the pendant imidazole also yields only diamagnetic 2 : 1 O<sub>2</sub> adducts ( $\mu$ -peroxo complex). In view of steric hindrance, it should be possible to form the  $\mu$ -peroxo complex with Co(II)-4. There may be a delicate energy and/or kinetic balance between the formation

of the mononuclear and binuclear oxygen complexes.



In Fe complex of 4, Fe<sup>III/II</sup> redox potential (pH = 7, I = 0.1, NaClO<sub>4</sub>, 25 °C) is + 0.00 V vs. S.C.E., to be compared with - 0.16 V of 8 and + 0.12 V of 7. The Fe<sup>II-4</sup> complex also forms an O<sub>2</sub> adduct with appearance of O<sub>2</sub> → Fe charge transfer band at 344 nm. Complexation of 4 with other metal ions and their interesting applications are anticipated.

## [Conclusion]

The following points are the principal results and conclusions of this investigation.

(i) A cyclam (4) appended with an imidazole pendant was newly synthesized by an annelation method previously reported for pyridyl- or phenolate counterparts.

(ii) Interaction of Ni(II) with the imidazole pendant cyclam initially forms cis-5 as a kinetic product, which is completely converted to trans-6 as thermodynamic one by heating or via electrochemically-generated Ni(III) species.

(iii) An ideal axial coordination of the imidazole pendant donor was proved by X-ray crystal study of trans-6.

(iv) An intramolecular axial coordination of imidazole function in trans-6 has an effect on the redox potential for Ni<sup>III/II</sup> complex (+ 0.54 V vs S.C.E.). The imidazole pendant donor imposes octahedral geometry on the Ni(II) complex formed such that there is no change in coordination number upon the Ni<sup>III/II</sup> redox reaction.

(v) The Co(II) complex of 4 rapidly reacts with molecular dioxygen to form a considerably stable 1 : 1 O<sub>2</sub> adduct in aqueous solution at room temperature, which was confirmed by its ESR study.

These metal complexes are appropriate for models of redox-related metalloenzymes.

## [References and Notes]

- (1) Kimura, E.; Koike, T.; Nada, H.; Iitaka, Y. *J. Chem. Soc. Chem. Comm.*, 1986, 1322.
- (2) Kimura, E.; Koike, T.; Takahashi, M. *J. Chem. Soc. Chem. Comm.*, 1985, 385.
- (3) Iitaka, Y.; Koike, T.; Kimura, E. *Inorg. Chem.* 1986, 25, 402.
- (4) *Kagaku Binran*, 3rd ed.; Chemical Society of Japan: Tokyo, 1984; Vol. II.
- (5) Sundberg, R. J.; Martin, R. B. *Chem. Rev.* 1974, 74, 471.
- (6) (a) Thom, V. J.; Boeyens, J. C. A.; McDougall, G. J.; HancDck, R. D. *J. Am. Chem. Soc.*, 1984, 106, 3198. (b) Barefield, E. K.; Bianchi, A.; Billo, E. J.; Connolly, P. J.; Paoletti, P.; Summers, J. S.; Derveer, D. G. V. *Inorg. Chem.*, 1986, 25, 4197.
- (7) Jameson, G. B.; Molinaro, F. S.; Ibers, J. A.; Collman, J. P.; Brauman, J. I.; Rose, E.; Suslick, K. S. *J. Am. Chem. Soc.*, 1980, 102, 3224.
- (8) James, B. R. "The Porphyrins. Vol. V. Physical Chemistry, Part C" Ed. by D. Dolphin, Academic Press, N.Y., 1978, 238.
- (9) IR.(nujol)  $\nu_{C\equiv N}$  occurs at 2320, 2290  $\text{cm}^{-1}$ ; for comparison,  $\nu_{C\equiv N}$  at 2300, 2270  $\text{cm}^{-1}$  for 7 (X = CH<sub>3</sub>CN) and at 2270  $\text{cm}^{-1}$  for 8 (X = CH<sub>3</sub>CN).
- (10) The ESR spectrum of this solution, in the presence of a small amount of sodium borohydride as a reducing reagent, exhibited that the unpaired electron in an axial orbital of significant dz<sup>2</sup> character, considerable similar to that observed in Co<sup>II</sup>(cyclam)(ClO<sub>4</sub>)<sub>2</sub>. See Endicott, J. F. et al. *J. Am. Chem. Soc.*, 1977, 99, 429.

- (11) Kimura, E.; Kodama, M.; Machida, R.; Ishizu, K. Inorg. Chem., 1982, 21, 595 and references cited therein.  
 (12) Sugiura, Y. J. Am. Chem. Soc., 1980, 102, 5216, and references cited therein.  
 (13) Kumar, K.; Endicott, J. F. Inorg. Chem., 1984, 23, 2447.

## [Supplementary Materials]

Table III Final Fractional Coordinates for cis-(5) Complex with Estimated Standard Deviation in Parenthesis.

atom	x ( $\times 10^5$ )	y ( $\times 10^5$ )	z ( $\times 10^5$ )	$B_{eq}$ , $\text{\AA}^2$
Ni	18450(10)	25583( 4)	38741( 5)	2.58(.01)
atom	x ( $\times 10^4$ )	y ( $\times 10^4$ )	z ( $\times 10^4$ )	$B_{eq}$ , $\text{\AA}^2$
N1	3663( 6)	2925( 4)	4942( 3)	3.3(0.1)
C2	3324( 8)	2419( 5)	5590( 4)	3.9(0.1)
C3	2806( 8)	1427( 5)	5310( 4)	4.4(0.1)
N4	1367( 6)	1476( 3)	4550( 3)	3.3(0.1)
C5	1200( 8)	610( 4)	4071( 4)	4.1(0.1)
C6	-482( 8)	618( 5)	3407( 4)	4.4(0.1)
C7	-605( 8)	1229( 5)	2679( 4)	4.3(0.1)
N8	-237( 6)	2234( 4)	2891( 3)	3.6(0.1)
C9	-1589( 7)	2741( 5)	3004( 4)	3.9(0.1)
C10	-1034( 7)	3709( 5)	3297( 4)	4.0(0.1)
N11	381( 6)	3630( 3)	4048( 3)	3.3(0.1)
C12	1147( 8)	4547( 4)	4301( 4)	4.1(0.1)
C13	2476( 8)	4484( 5)	5122( 4)	4.2(0.1)
C14	3976( 8)	3935( 4)	5144( 4)	3.8(0.1)
C15	2545( 7)	608( 4)	3749( 4)	3.7(0.1)
N16	3072( 6)	1466( 3)	3576( 3)	3.3(0.1)
C17	4202( 8)	1277( 5)	3257( 4)	4.7(0.1)
N18	4400( 8)	351( 4)	3224( 4)	5.6(0.1)
C19	3350( 9)	-89( 5)	3531( 5)	5.0(0.1)
CL1	4032( 2)	3841( 1)	3014( 1)	3.4(0.0)
O1	2501( 5)	3536( 3)	3063( 3)	4.3(0.1)
O2	4167( 7)	3571( 4)	2277( 3)	6.1(0.1)
O3	5329( 5)	3446( 4)	3665( 3)	5.2(0.1)
O4	4094( 6)	4845( 3)	3062( 3)	5.8(0.1)
CL2	-1531( 2)	2305( 1)	5601( 1)	4.0(0.1)
O5	-298( 9)	1828( 6)	6197( 4)	9.5(0.2)
O6	-963(12)	3123( 5)	5412( 6)	12.2(0.3)
O7	-2789( 7)	2446( 6)	5879( 4)	9.3(0.2)
O8	-1929(11)	1739( 6)	4908( 4)	11.0(0.2)

atom	x ( $\times 10^3$ )	y ( $\times 10^3$ )	z ( $\times 10^3$ )	$B_{eq}$ , $\text{\AA}^2$
HN1	461( 7)	265( 4)	488( 3)	4.( 1.)
HC2	231( 7)	275( 4)	571( 3)	4.( 1.)
H'C2	437( 8)	242( 5)	613( 4)	6.( 2.)
HC3	381( 6)	110( 4)	518( 3)	3.( 1.)
H'C3	257(10)	105( 6)	577( 5)	9.( 2.)
HN4	44( 8)	159( 5)	465( 5)	5.( 2.)
HC5	128(10)	0( 6)	444( 5)	9.( 2.)
HC6	-136( 7)	85( 4)	367( 4)	5.( 2.)
H'C6	-77( 8)	-12( 5)	319( 4)	5.( 2.)
HC7	28( 8)	98( 5)	239( 4)	5.( 2.)
H'C7	-182( 9)	119( 5)	222( 4)	7.( 2.)
HN8	-9( 8)	256( 4)	246( 4)	4.( 1.)
HC9	-255( 8)	277( 5)	245( 4)	6.( 2.)
H'C9	-197( 7)	239( 4)	347( 3)	4.( 1.)
HC10	-68( 7)	407( 4)	285( 4)	5.( 1.)
H'C10	-200( 8)	410( 5)	340( 4)	6.( 2.)
HN11	1( 9)	342( 5)	443( 4)	7.( 2.)
HC12	22( 9)	502( 6)	433( 5)	7.( 2.)
H'C12	166( 6)	477( 4)	385( 3)	3.( 1.)
HC13	289( 8)	517( 5)	534( 4)	5.( 2.)
H'C13	201( 9)	418( 5)	553( 4)	7.( 2.)
HC14	448( 8)	422( 5)	472( 4)	5.( 2.)
H'C14	490( 9)	397( 5)	573( 4)	6.( 2.)
HC17	476(12)	172( 7)	307( 6)	12.( 3.)
HN18	517(11)	7( 7)	303( 5)	10.( 3.)
HC19	318( 7)	-73( 4)	356( 4)	5.( 2.)

Table VI Final Fractional Coordinates for trans-(6) Complex with Estimated Standard Deviation in Parenthesis.

atom	x ( $\times 10^5$ )	y ( $\times 10^5$ )	z ( $\times 10^5$ )	$B_{eq}$ , $\text{\AA}^2$
Ni	7770(10)	24723(14)	32730(20)	4.50(.03)

atom	x ( $\times 10^4$ )	y ( $\times 10^4$ )	z ( $\times 10^4$ )	$B_{eq}$ , $\text{\AA}^2$
N1	1802( 5)	1913( 7)	2909(11)	5.7(0.2)
C2	1629( 8)	2056(12)	1602(13)	6.3(0.3)
C3	1274( 8)	3199(12)	1224(14)	6.6(0.3)
N4	557( 6)	3284( 9)	1658(10)	5.8(0.2)
C5	368( 8)	4423(10)	1899(14)	6.1(0.3)
C6	-497( 8)	4477(11)	2058(15)	7.1(0.3)
C7	-533( 8)	4151(11)	3268(16)	7.1(0.3)
N8	-308( 6)	3008( 8)	3589(11)	6.3(0.2)
C9	-185( 8)	2766(11)	4884(15)	7.1(0.3)
C10	232( 8)	1685(11)	5209(16)	7.3(0.3)
N11	1008( 4)	1730( 7)	4918(11)	5.7(0.2)
C12	1404( 9)	639(10)	5022(16)	7.2(0.3)
C13	2182( 8)	674(11)	4664(16)	7.5(0.4)
C14	2059( 8)	828(10)	3353(15)	6.9(0.3)
C15	1015( 7)	4732( 9)	3043(13)	5.4(0.3)
N16	1306( 5)	3947( 7)	3937( 9)	4.6(0.2)
C17	1808( 7)	4277(10)	4860(12)	5.2(0.3)
N18	1854( 6)	5473( 8)	4682(11)	3.9(0.2)
C19	1377( 8)	5678( 9)	3574(15)	6.8(0.3)
N20	76( 6)	1128( 8)	2414(11)	6.3(0.2)
C21	-388( 8)	514(11)	1996(14)	6.6(0.3)
C22	-1036( 8)	-285(12)	1364(16)	8.1(0.3)
CL1	2405( 2)	2816( 2)	8098( 4)	6.2(0.1)
O1	2573(10)	2760(13)	9322(11)	14.0(0.4)
O2	3018( 8)	3332(12)	7764(16)	14.8(0.4)
O3	1653( 7)	3220(12)	7471(15)	14.4(0.4)
O4	2437( 8)	1755(10)	7761(18)	15.7(0.4)
CL2	4001( 2)	3090( 3)	3788( 4)	7.2(0.1)
O5	3759(15)	3143(11)	2594(13)	20.2(0.6)
O6	3424(13)	3209(24)	4194(30)	33.5(1.2)
O7	4517(10)	3844(14)	4424(16)	17.2(0.5)
O8	4257(14)	2142(14)	4060(18)	23.1(0.6)

atom	x (x10 <sup>3</sup> )	y (x10 <sup>3</sup> )	z (x10 <sup>3</sup> )	B <sub>eq</sub> , Å <sup>2</sup>
HN1	223( 7)	238(10)	326(10)	7.( 3.)
HC2	118( 8)	145(11)	111(12)	10.( 4.)
H'C2	215( 7)	195(10)	131(11)	8.( 3.)
HC3	172( 9)	380(12)	167(13)	11.( 4.)
H'C3	112( 9)	331(12)	24(13)	11.( 4.)
HN4	10( 7)	298( 9)	104(10)	7.( 3.)
HC5	40( 5)	494( 7)	113( 8)	4.( 2.)
HC6	-90( 8)	394(11)	136(12)	9.( 4.)
H'C6	-70( 7)	529( 9)	187(10)	7.( 3.)
HC7	-9( 7)	468( 9)	398(10)	7.( 3.)
H'C7	-110( 7)	427(10)	340(10)	8.( 3.)
HN8	-73( 8)	256(12)	309(13)	11.( 4.)
HC9	-76( 7)	276(10)	511(11)	9.( 4.)
H'C9	19(10)	345(14)	550(15)	15.( 6.)
HC10	34( 8)	150(11)	619(12)	9.( 4.)
H'C10	-15( 9)	107(12)	467(13)	11.( 4.)
HN11	136( 6)	222( 9)	555(10)	7.( 3.)
HC12	99( 8)	8(11)	440(11)	9.( 4.)
H'C12	153( 6)	34( 9)	595(10)	6.( 3.)
HC13	254( 9)	131(12)	514(13)	12.( 5.)
H'C13	254( 8)	-4(11)	496(12)	11.( 4.)
HC14	259( 7)	63(10)	312(11)	8.( 4.)
H'C14	159( 7)	25(10)	284(11)	8.( 3.)
HC17	209(18)	407(12)	561(13)	11.( 4.)
HN18	214( 6)	594( 8)	524( 9)	5.( 3.)
HC19	129( 7)	638(10)	312(11)	8.( 3.)

Table V Bond Distances (Å) for cis-(5) Complex with Estimated Standard Deviation in Parenthesis.

Ni - N1	2.090( 4)	N1 - HN1	0.96( 6)
Ni - N4	2.087( 5)	C2 - HC2	1.10( 6)
Ni - N8	2.108( 4)	C2 - H'C2	1.07( 6)
Ni - N11	2.091( 5)	C3 - HC3	1.09( 6)
Ni - N16	2.067( 5)	C3 - H'C3	1.05(10)
Ni - O1	2.219( 5)	N4 - HN4	0.91( 8)
N1 - C2	1.473( 9)	C5 - HC5	1.09( 9)
N1 - C14	1.492( 8)	C6 - HC6	1.08( 7)
C2 - C3	1.522(10)	C6 - H'C6	1.12( 7)
C3 - N4	1.506( 7)	C7 - HC7	1.12( 8)
N4 - C5	1.482( 8)	C7 - H'C7	1.10( 6)
C5 - C6	1.546( 8)	N8 - HN8	0.94( 7)
C5 - C15	1.476(11)	C9 - HC9	1.06( 6)
C6 - C7	1.534(11)	C9 - H'C9	1.11( 7)
C7 - N8	1.494( 9)	C10 - HC10	1.08( 7)
N8 - C9	1.463( 9)	C10 - H'C10	1.08( 8)
C9 - C10	1.500( 9)	N11 - HN11	0.90( 9)
C10 - N11	1.488( 7)	C12 - HC12	1.07( 9)
N11 - C12	1.474( 8)	C12 - H'C12	1.10( 6)
C12 - C13	1.530( 9)	C13 - HC13	1.08( 7)
C13 - C14	1.522(10)	C13 - H'C13	1.04( 9)
C15 - N16	1.382( 8)	C14 - HC14	1.08( 7)
C15 - C19	1.353(11)	C14 - H'C14	1.08( 6)
N16 - C17	1.327(10)	C17 - HC17	0.93(11)
C17 - N18	1.337(10)		
N18 - C19	1.373(12)		
CL1 - O1	1.444( 5)		
CL1 - O2	1.409( 6)		
CL1 - O3	1.435( 5)		
CL1 - O4	1.425( 5)		
CL2 - O5	1.408( 7)		
CL2 - O6	1.359( 9)		
CL2 - O7	1.369( 8)		
CL2 - O8	1.414( 8)		

Table VI Bond Distances ( $\text{\AA}$ ) for trans-(6) Cpmplex with Estimated Standard Deviation in Parenthesis.

Ni - N1	2.060(11)	N1 - HN1	0.94(11)
Ni - N4	2.058(12)	C2 - HC2	1.11(13)
Ni - N8	2.121(12)	C2 - H'C2	1.06(14)
Ni - N11	2.046(12)	C3 - HC3	1.08(14)
Ni - N16	2.098( 9)	C3 - H'C3	1.10(14)
Ni - N20	2.132(10)	N4 - HN4	0.97(10)
N1 - C2	1.461(19)	C5 - HC5	1.12(10)
N1 - C14	1.471(16)	C6 - HC6	1.12(12)
C2 - C3	1.565(20)	C6 - H'C6	1.08(12)
C3 - N4	1.474(20)	C7 - HC7	1.14(11)
N4 - C5	1.506(17)	C7 - H'C7	1.05(13)
C5 - C6	1.560(22)	N8 - HN8	0.96(13)
C5 - C15	1.499(17)	C9 - HC9	1.11(14)
C6 - C7	1.479(25)	C9 - H'C9	1.18(16)
C7 - N8	1.499(17)	C10 - HC10	1.12(13)
N8 - C9	1.480(22)	C10 - H'C10	1.08(14)
C9 - C10	1.524(19)	N11 - HN11	1.00(10)
C10 - N11	1.475(21)	C12 - HC12	1.10(12)
N11 - C12	1.515(16)	C12 - H'C12	1.09(11)
C12 - C13	1.520(24)	C13 - HC13	1.05(14)
C13 - C14	1.480(26)	C13 - H'C13	1.07(14)
C15 - N16	1.403(15)	C14 - HC14	1.06(14)
C15 - C19	1.392(17)	C14 - H'C14	1.11(11)
N16 - C17	1.299(14)	C17 - HC17	0.96(13)
C17 - N18	1.331(16)	N18 - HN18	0.90(10)
N18 - C19	1.320(18)	C19 - HC19	1.01(12)
N20 - C21	1.108(16)		
C21 - C22	1.511(19)		
CL1 - O1	1.360(14)		
CL1 - O2	1.375(17)		
CL1 - O3	1.388(12)		
CL1 - O4	1.388(14)		
CL2 - O5	1.317(15)		
CL2 - O6	1.232(30)		
CL2 - O7	1.352(17)		
CL2 - O8	1.272(18)		

Table VII Bond Angles ( $^{\circ}$ ) for cis-(5) Complex with Estimated Standard Deviation in Parenthesis.

N1 - Ni - N4	84.6( 2)	C10 - C9 - N8	108.8( 5)
N1 - Ni - N8	171.2( 2)	N11 - C10 - C9	108.4( 5)
N1 - Ni - N11	90.0( 2)	C12 - N11 - Ni	117.3( 4)
N1 - Ni - N16	96.8( 2)	C12 - N11 - C10	111.3( 5)
N1 - Ni - O1	98.3( 2)	Ni - N11 - C10	106.9( 4)
N4 - Ni - N8	91.5( 2)	C13 - C12 - N11	111.1( 5)
N4 - Ni - N11	101.9( 2)	C14 - C13 - C12	115.4( 6)
N4 - Ni - N16	79.1( 2)	N16 - C15 - C5	117.1( 6)
N4 - Ni - O1	171.1( 2)	N16 - C15 - C19	110.2( 6)
N8 - Ni - N11	83.1( 2)	C5 - C15 - C19	132.5( 6)
N8 - Ni - N16	90.1( 2)	C17 - N16 - Ni	142.5( 5)
N8 - Ni - O1	86.8( 2)	C17 - N16 - C15	105.6( 5)
N11 - Ni - N16	173.2( 2)	Ni - N16 - C15	111.8( 4)
N11 - Ni - O1	86.6( 2)	N18 - C17 - N16	110.3( 6)
N16 - Ni - O1	92.2( 2)	C19 - N18 - C17	108.8( 7)
C2 - N1 - Ni	106.9( 4)	O1 - CL1 - O2	110.3( 3)
C2 - N1 - C14	111.0( 5)	O1 - CL1 - O3	109.4( 3)
Ni - N1 - C14	118.9( 4)	O1 - CL1 - O4	108.4( 3)
C3 - C2 - N1	108.7( 5)	O2 - CL1 - O3	110.3( 3)
N4 - C3 - C2	108.4( 5)	O2 - CL1 - O4	108.4( 3)
C5 - N4 - Ni	106.9( 4)	O3 - CL1 - O4	110.0( 3)
C5 - N4 - C3	111.4( 5)	O5 - CL2 - O6	110.5( 5)
Ni - N4 - C3	106.2( 4)	O5 - CL2 - O7	107.9( 5)
C6 - C5 - N4	108.4( 5)	O5 - CL2 - O8	106.2( 5)
C6 - C5 - C15	112.8( 6)	O6 - CL2 - O7	111.7( 5)
N4 - C5 - C15	106.7( 5)	O6 - CL2 - O8	106.4( 6)
C7 - C6 - C5	115.0( 6)	O7 - CL2 - O8	114.0( 5)
N8 - C7 - C6	112.9( 6)	Ni - O1 - CL1	133.0( 3)
C9 - N8 - Ni	107.0( 4)	N1 - C14 - C13	114.0( 5)
C9 - N8 - C7	113.3( 5)	C15 - C19 - N18	105.1( 6)
Ni - N8 - C7	118.3( 4)		

Table VIII Bond Angles ( $^{\circ}$ ) for trans-(6) Complex with Estimated Standard Deviation in Parenthesis.

N1 - Ni - N4	85.0( 4)	C10 - C9 - N8	110.0(12)
N1 - Ni - N8	177.6( 4)	N11 - C10 - C9	107.6(12)
N1 - Ni - N11	95.8( 4)	C12 - N11 - Ni	115.9( 8)
N1 - Ni - N16	94.0( 4)	C12 - N11 - C10	111.5(11)
N1 - Ni - N20	92.1( 4)	Ni - N11 - C10	107.3( 8)
N4 - Ni - N8	94.2( 4)	C13 - C12 - N11	111.5(12)
N4 - Ni - N11	177.4( 4)	C14 - C13 - C12	114.9(13)
N4 - Ni - N16	80.6( 4)	N16 - C15 - C5	118.2(11)
N4 - Ni - N20	92.6( 4)	N16 - C15 - C19	105.1(11)
N8 - Ni - N11	85.1( 4)	C5 - C15 - C19	136.2(13)
N8 - Ni - N16	88.1( 4)	C17 - N16 - Ni	144.5( 9)
N8 - Ni - N20	85.8( 4)	C17 - N16 - C15	106.3(10)
N11 - Ni - N16	96.9( 4)	Ni - N16 - C15	109.2( 8)
N11 - Ni - N20	89.8( 4)	N18 - C17 - N16	112.6(11)
N16 - Ni - N20	170.5( 4)	C19 - N18 - C17	107.0(11)
C2 - N1 - Ni	104.7( 8)	C21 - N20 - Ni	168.9(12)
C2 - N1 - C14	114.8(11)	C22 - C21 - N20	176.9(16)
Ni - N1 - C14	115.3( 8)	O1 - CL1 - O2	113.0(10)
C3 - C2 - N1	109.9(11)	O1 - CL1 - O3	114.8(10)
N4 - C3 - C2	105.5(11)	O1 - CL1 - O4	103.3(10)
C5 - N4 - Ni	106.8( 8)	O2 - CL1 - O3	111.0( 9)
C5 - N4 - C3	112.5(11)	O2 - CL1 - O4	106.4(10)
Ni - N4 - C3	109.5( 8)	O3 - CL1 - O4	107.7(10)
C6 - C5 - N4	109.4(11)	O5 - CL2 - O6	111.1(16)
C6 - C5 - C15	111.4(12)	O5 - CL2 - O7	118.8(12)
N4 - C5 - C15	105.2(11)	O5 - CL2 - O8	106.3(13)
C7 - C6 - C5	114.7(12)	O6 - CL2 - O7	100.5(16)
N8 - C7 - C6	114.5(12)	O6 - CL2 - O8	106.1(17)
C9 - N8 - Ni	104.4( 8)	O7 - CL2 - O8	113.4(12)
C9 - N8 - C7	113.1(11)	N1 - C14 - C13	114.3(12)
Ni - N8 - C7	115.8( 9)	C15 - C19 - N18	109.0(12)

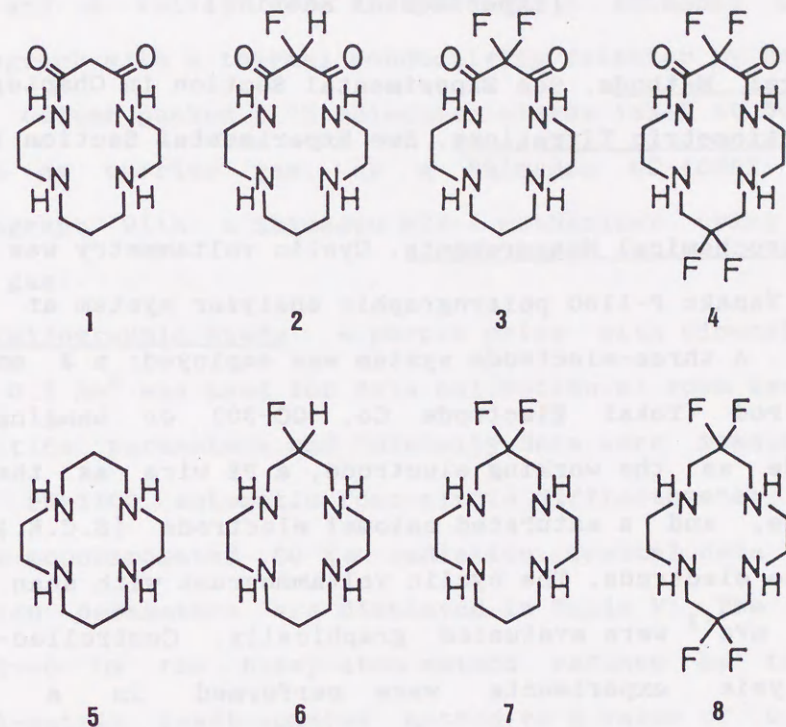
## CHAPTER II

SYNTHESIS OF NOVEL FLUORINATED MACROCYCLIC TETRAAMINES  
AND CHEMICAL PROPERTIES OF THEIR METAL COMPLEXES.

## [Introduction]

Cyclam (1,4,8,11-tetraazacyclotetradecane) (5) has long been a very useful and versatile tetraamine macrocyclic ligand in coordination chemistry, bioinorganic and biomimetic chemistry or catalysis.<sup>1</sup> Recently, renovation of its basic structure by incorporation of carbonyl group(s) adjacent to its amines to monooxocyclam (5-oxo-1,4,8,11-tetraazacyclotetradecane) or dioxocyclam (5,7-dioxo-1,4,8,11-tetraazacyclotetradecane) (1)<sup>2</sup> or by attachment of pendant donors such as phenol,<sup>3,4</sup> catechol,<sup>5</sup> pyridine,<sup>6,7</sup> and imidazole<sup>8</sup> to its carbon skeleton have added new dimensions to the conventional cyclam chemistry.<sup>9</sup>

Much attention has long been focused on the recent advances and trends in the synthesis of useful organofluorine compounds. Historically, fluorine substitution of hydrogens has been a promising method to search for new organic molecules with novel chemical properties, which are widely used for chemical, electrical and mechanical applications. It has been conceived that replacement of the skeletal C-H for C-F in the macrocyclic ligand should affect metal-ligand bond parameters and hence the complex structure, electronic structure (ground and possibly excited states) and oxidation-reduction potentials of the metal ions, the behaviors in solution that are associated with unique solvation effects derived from the highest electronegativity, high lipophilicity or oxidation-resisting nature of fluorine atom.



Here, the novel synthesis of mono-, di- and tetrafluorinated dioxocyclams (2, 3 and 4) and cyclams (6, 7 and 8), and the fluorination effects on the chemical properties and reactivities of the whole series of ligands and their metal complexes,<sup>10</sup> are presented.

[Experimental Section]

General Methods. See Experimental Section in Chapter I.

Potentiometric Titrations. See Experimental Section in Chapter I.

Electrochemical Measurements. Cyclic voltammetry was performed with a Yanako P-1100 polarographic analyzer system at  $25.00 \pm 0.05$  °C. A three-electrode system was employed: a 3 mm glassy-carbon rod (Tokai Electrode Co. GC-30) or hanging mercury electrode as the working electrode, a Pt wire as the counter electrode, and a saturated calomel electrode (S.C.E.) as the reference electrode. The cyclic voltammograms with scan rates of  $100\text{-}200$  mVs $^{-1}$  were evaluated graphically. Controlled-potential electrolysis experiments were performed in a gas-tight electrolysis cell under one atmosphere of CO<sub>2</sub> with a Yanako VE-8 controlled potential electrolyser. The gas-tight cell was a 50 ml three-necked, round-bottomed flask equipped with three side arms. Mercury was used as the working electrode was mercury ( $14$  cm $^2$ ; purity > 99.9 %). The counter electrode (Pt) and the reference electrode (S.C.E.) were separated from the working electrode compartment. The cell volume was 142 ml, of which 108 ml was occupied by gases. The aqueous solution (20 ml) was degassed before electrolysis by bubbling CO<sub>2</sub> through it for 30 min. The internal pressure within the electrolysis cell was kept equal to 1 atm by using syringe techniques. Turnover frequencies were calculated as mol of CO produced per mol of an electrocatalyst in 1 h.

Analytical Methods for CO<sub>2</sub> Reduction. Gas samples (0.5 ml), taken at various intervals with a gas-tight syringe through a

septum and a valve, were analyzed on a Shimadzu GC-8A gas chromatograph with a thermal conductivity detector by using a 3 m x 2.6 φ column packed with molecular sieves 13X-S at 50 °C using nitrogen as carrier gas, or a Shimadzu GC-4CMF FID gas chromatograph with a Shimadzu MTN-1 methanizer using nitrogen carrier gas.

Crystallographic Study. A purple prism with dimensions  $0.05 \times 0.1 \times 0.2$  mm $^3$  was used for data collection at room temperature. The lattice parameters and intensity data were measured on a Philips PW-1100 automatic four-circle diffractometer by using graphite-monochromated Cu K $\alpha$  radiation. Crystal data and data collection parameters are displayed in Table V. The structure was solved by the heavy-atom method refined by the block-diagonal-matrix least-squares method to R value of 0.056. The molecular structure is illustrated in Figure 6 by ORTEP drawings with 50 % probability thermal ellipsoids. The atomic positional parameters are given together with their standard deviations in Table VI. Selected bond distances and angles are presented in Tables VII and VIII, respectively. Listing of hydrogen atom positional parameters and of thermal parameters for the Ni(II) complex 21b and tables of observed and calculated structure factors for the complex are omitted.

Synthesis (Scheme 1a and 1b). 6-Fluoro-5,7-dioxo-1,4,8,11-tetraazacyclotetradecane (2) After ethanol solution (360 ml) of diethyl 2-fluoromalonate<sup>11</sup> (9a) (3.00 g, 16.8 mmol) and 2,3,2-tetraamine (10) (1,9-diamino-3,7-diazanonane, 2.70 g, 16.8 mmol) was heated at reflux for 3 h, the reaction mixture was concentrated under reduced pressure. The residue was column-

chromatographed on 60 g of silica gel with  $\text{CH}_2\text{Cl}_2\text{-CH}_3\text{OH}$ -28 % aqueous  $\text{NH}_3$  (50 : 5 : 1) as an eluent to get 2, which was crystallized from acetonitrile to obtain 1.72 g of the colorless needles (39 %); mp 194.0-194.5 °C; IR (nujol):  $\nu_{\text{C=O}}$  1688  $\text{cm}^{-1}$ ;  $^1\text{H}$  NMR (90 MHz,  $\text{CDCl}_3$ ):  $\delta$  1.5-1.9 (m, 2H), 1.90 (br, 2H), 2.4-3.0 (m, 8H), 3.2-3.8 (m, 4H), 5.23 (d,  $J = 48$  Hz, 1H), 7.45 (br, 2H, amide NH); Anal. Calcd for  $\text{C}_{10}\text{H}_{19}\text{O}_2\text{N}_4\text{F}$ : C, 48.77; H, 7.78; N, 22.75. Found: C, 48.62; H, 7.89; N, 22.70.

6-Fluoro-1,4,8,11-tetraazacyclotetradecane (6) Monofluorinated dioxocyclam (2) (492 mg, 2.0 mmol) was heated at 65 °C in 60 ml of diborane-tetrahydrofuran solution (1.0 M, Aldrich) for 45 h. After cooling, a small amount of crushed ice was cautiously added and the volatile components were removed in vacuo at 70 °C. The residue was dissolved into 200 ml of 6 N HCl solution and evaporated carefully at 70 °C. The resulting crude hydrochloride of 6, after repeatedly dissolution in methanol and evaporation, was passed through column of the strong base anion exchange resin (Amberlite IRA-400) with water to get free form of 6, which was recrystallized from acetonitrile (311 mg, 71 %); mp 170.0-172.0 °C;  $^1\text{H}$  NMR (90 MHz,  $\text{CDCl}_3$ ):  $\delta$  1.5-1.9 (m, 2H), 2.1 (br, 4H), 2.6-2.9 (m, 12H), 2.9-3.2 (m, 4H), 4.70 (dm,  $J = 45$  Hz, 1H); Anal. Calcd for  $\text{C}_{10}\text{H}_{23}\text{N}_4\text{F}$ : C, 55.02; H, 10.62; N, 25.67. Found: C, 54.87; H, 10.61; N, 25.55.

6,6-Difluoro-5,7-dioxo-1,4,8,11-tetraazacyclotetradecane (3) After ethanol solution (140 ml) of diethyl 2,2-difluoromalonate<sup>12</sup> (9b) (1.15 g, 5.9 mmol) and 2,3,2-tetraamine (10) (0.94 g, 5.9 mmol) was heated at reflux for 3 h, the reaction mixture was concentrated under reduced pressure. The residue was

column-chromatographed on silica gel (25 g) with  $\text{CH}_2\text{Cl}_2\text{-CH}_3\text{OH}$ -28 % aqueous  $\text{NH}_3$  (50 : 5 : 1) as an eluent to obtain the desired difluorinated dioxocyclam (3), which was recrystallized from acetonitrile to 556 mg of the colorless needles (36 %); m.p. 179.5-180.0 °C; IR (nujol):  $\nu_{\text{C=O}}$  1705  $\text{cm}^{-1}$ ;  $^1\text{H}$  NMR (90 MHz,  $\text{CDCl}_3$ ):  $\delta$  1.4-1.8 (m, 2H), 1.77 (d,  $J = 24$  Hz, 3H), 2.4-3.0 (m, 10H), 3.0-3.4 (m, 2H), 3.4-3.8 (m, 2H), 7.35 (br, 2H, amide NH); Anal. Calcd for  $\text{C}_{10}\text{H}_{18}\text{O}_2\text{N}_4\text{F}_2\cdot 0.5\text{H}_2\text{O}$ : C, 43.95; H, 7.01; N, 20.50. Found: C, 44.24; H, 7.06; N, 20.69.

6,6-Difluoro-1,4,8,11-tetraazacyclotetradecane (7) Difluorinated dioxocyclam (3) (264 mg, 1.0 mmol) was heated at 65 °C in 30 ml of diborane-tetrahydrofuran solution (1.0 M, Aldrich) for 45 h. After cooling, a small amount of crushed ice was cautiously added and the volatile parts were removed in vacuo. The residue was dissolved in 100 ml of 6 N HCl solution and evaporated slowly at 70 °C. The resulting crude hydrochlorides of 7 were subjected to chromatography on the strong base anion exchange resin (Amberlite IRA-400) with water to free 7, which was recrystallized from acetonitrile (143 mg, 61 %); mp 148.5-149.0 °C;  $^1\text{H}$  NMR (400 MHz,  $\text{D}_2\text{O}$ ):  $\delta$  1.51-1.57 (m, 2H), 2.54-2.67 (m, 12H), 2.87 (t,  $J = 13$  Hz, 4H); Anal. Calcd for  $\text{C}_{10}\text{H}_{22}\text{N}_4\text{F}_2$ : C, 50.83; H, 9.38; N, 23.71. Found: C, 50.98; H, 9.47; N, 23.69.

6,6,13,13-Tetrafluoro-5,7-dioxo-1,4,8,11-tetraazacyclotetradecane (4) and its monohydrochloride (4·HCl) Tetrafluorinated dioxocyclam (4) was synthesized from diethyl difluoromalonate (9a) in three steps and isolated mainly as its monohydrochloride. At first, a mixture of diethyl difluoromalonate (9b) (4.7 g, 24 mmol) and mono-triphenyl-methylated ethylenediamine (11) (14.6 g,

48 mmol) was heated for 3 h at reflux in 250 ml of ethanol under argon. After the solution was cooled, the pure 12 crystallized as colorless needles. These were collected, washed with a small amount of ethanol, dried in vacuo, and recrystallized from acetone to give 11.3 g (66 %) of 12 as colorless prisms; mp 200.0-200.5 °C; IR (nujol):  $\nu_{\text{C=O}}$  1692 cm<sup>-1</sup>; <sup>1</sup>H NMR (400 MHz, CDCl<sub>3</sub>):  $\delta$  1.5-1.8 (br, 2H, amide NH), 2.34 (t, J = 4 Hz, 4H), 3.39 (t, J = 4 Hz, 4H), 7.1-7.3 (m, 18H), 7.3-7.5 (m, 12H).

The amide compound 12 (7.1 g, 10 mmol) was heated at 65 °C in 200 ml of diborane-tetrahydrofuran solution (1.0 M, Aldrich) for 65 h. After cooling, 20 ml of tetrahydrofuran containing 5 % water was carefully added and the volatile components were removed in vacuo. The residue dissolved in 200 ml of 6 N HCl solution was heated at 60 °C for a few minutes to complete removal of the protecting triphenylmethyl group. This aqueous solution was washed with CH<sub>2</sub>Cl<sub>2</sub> repeatedly and evaporated to dryness. The resulting hydrochlorides were dissolved in a small amount of cold water and filtered. The filtrate was added to ethanol dropwise to precipitate white solids, which were collected, washed with ethanol and ether, dried in vacuo to get the desired product, difluoro-2,3,2-tetraamine·4HCl (13·4HCl, 1,9-diamino-3,7-diaza-5,5-difluorononane tetrahydrochlorides) in the yield of 82 % (2.82 g); mp 218-226 °C (dec.); <sup>1</sup>H NMR (400 MHz, D<sub>2</sub>O):  $\delta$  3.38-3.47 (m, 4H), 3.47-3.56 (m, 4H), 3.81 (t, J = 16 Hz, 4H).

Subsequently, difluoro-2,3,2-tetraamine·4HCl (13·4HCl, 1.0 g, 2.9 mmol) was rapidly passed through a column packed with the strong base anion exchange resin (Amberlite IRA-400, 50 cc as wet

volume) using water to yield the monohydrochloride (13·HCl) as a major product and a small proportion of free form of 13. This mixture and diethyl difluoromalonate (9b) (600 mg, 3.1 mmol) in 60 ml of ethanol were stirred under argon at room temperature for 46 h. The reaction mixture was evaporated at low temperature and the resulting residue was recrystallized from acetonitrile-methanol (2 : 1) to give 209 mg (20 %) of colorless prisms (4·HCl); mp 220 ~ 250 °C (dec.); IR (nujol):  $\nu_{\text{C=O}}$  1736(s), 1694(w) cm<sup>-1</sup>; <sup>1</sup>H NMR (400 MHz, D<sub>2</sub>O):  $\delta$  2.93 (t, J = 5 Hz, 4H), 3.24 (t, J = 13 Hz, 4H), 3.41 (t, J = 5 Hz, 4H); Anal. Calcd for C<sub>10</sub>H<sub>17</sub>O<sub>2</sub>N<sub>4</sub>F<sub>4</sub>Cl: C, 35.67; H, 5.09; N, 16.64. Found: C, 35.71; H, 5.18; N, 16.81.

The mother liquid after the recrystallization was evaporated and chromatographed on silica gel (4 g) with CH<sub>2</sub>Cl<sub>2</sub>-CH<sub>3</sub>OH (50 ~ 30 : 1) to obtain free form of tetrafluorinated dioxocyclam (4) (32 mg, 4 %) as colorless needles; mp 214.0-214.5 °C; IR (nujol):  $\nu_{\text{C=O}}$  1705 cm<sup>-1</sup>; m/z 300 (M<sup>+</sup>); <sup>1</sup>H NMR (400 MHz, CD<sub>3</sub>OD):  $\delta$  2.81 (t, J = 5 Hz, 4H), 2.96 (t, J = 13 Hz, 4H), 3.43 (t, J = 5 Hz, 4H); Anal. Calcd for C<sub>10</sub>H<sub>16</sub>O<sub>2</sub>N<sub>4</sub>F<sub>4</sub>: C, 40.00; H, 5.37; N, 18.66. Found: C, 39.91; H, 5.42; N, 18.76.

6,6,13,13-Tetrafluoro-1,4,8,11-tetrazacyclotetradecane (8) To 40 ml of diborane-tetrahydrofuran solution, the monohydrochloride of 4 (337 mg, 1.0 mmol) was added dropwise. The mixture was heated at 70 °C for 67 h. After cooling, a small amount of crushed ice was cautiously added to the reaction mixture to decompose unreacted diborane. The volatile components were removed under reduced pressure and the residue was dissolved in 20 ml of 6 N HCl solution and evaporated. The resulting crude

tetrahydrochlorides, after repeated dissolution in methanol and evaporation, were dissolved in a minimum amount of water and added to ethanol. The white solid precipitated was filtered and subjected to the strong base anion exchange resin (Amberlite IRA-400) with water to obtain 247 mg of colorless solid, which was purified by the recrystallization from 2-propyl alcohol to 200 mg of 8 as colorless needles (73 %); mp 106.5–107.0 °C; <sup>1</sup>H NMR of 4 HCl salts (400 MHz, D<sub>2</sub>O): δ 2.96 (s, 8H), 3.36 (t, J = 12 Hz, 8H); Anal. Calcd for C<sub>10</sub>H<sub>20</sub>N<sub>4</sub>F<sub>4</sub>: C, 44.11; H, 7.40; N, 20.58. Found. C, 44.00; H, 7.51; N, 20.73.

Preparation of the Copper(II) Complexes 14–17 A ligand (0.5 mmol) and CuSO<sub>4</sub>·5H<sub>2</sub>O (125 mg, 0.5 mmol) were dissolved in 50 ml of 0.5 M Na<sub>2</sub>SO<sub>4</sub> aqueous solution at ca. 25 °C, and the mixture was adjusted to pH 8 with 0.1 M NaOH solution. The resulting solution was filtered, and the filtrate was allowed to stand several weeks at room temperature to precipitate crystalline Cu<sup>II</sup>(H<sub>2</sub>L)<sup>0</sup> (where L = 2~4) complexes. The copper(II) complex 14 (L = 1) was prepared as previously described.<sup>13</sup>

15 (blue prisms); Anal. Calcd for C<sub>10</sub>H<sub>17</sub>O<sub>2</sub>N<sub>4</sub>FCu·0.5H<sub>2</sub>O: C, 36.86; H, 5.88; N, 17.20. Found: C, 36.63; H, 5.77; N, 17.13.

16 (blue prisms); Anal. Calcd for C<sub>10</sub>H<sub>16</sub>O<sub>2</sub>N<sub>4</sub>F<sub>2</sub>Cu·1.5H<sub>2</sub>O: C, 34.04; H, 5.43; N, 15.88. Found: C, 34.25; H, 5.16; N, 15.99.

17 (dark red prisms); Anal. Calcd for C<sub>10</sub>H<sub>14</sub>O<sub>4</sub>N<sub>4</sub>F<sub>4</sub>Cu·H<sub>2</sub>O: C, 31.62; H, 4.25; N, 14.75. Found: C, 31.88; H, 4.23; N, 14.58.

Preparation of Ni(II) Complexes with 6, 7, and 8. [Method A] A ligand (0.5 mmol) and NiSO<sub>4</sub> (0.5 mmol) were dissolved in 50 ml of 0.1 M NaClO<sub>4</sub> aqueous solution at 50 °C, and the mixture was adjusted to pH 7 with 0.1 M NaOH solution. The resulting

solutions were filtered, and the filtrates were allowed to stand for several weeks at room temperature. The yellow to orange crystals were obtained.

6-Ni<sup>II</sup>(ClO<sub>4</sub>)<sub>2</sub>·H<sub>2</sub>O (i.e. 19a); Anal. Calcd for C<sub>10</sub>H<sub>23</sub>O<sub>8</sub>N<sub>4</sub>FCl<sub>2</sub>Ni·H<sub>2</sub>O: C, 24.32; H, 5.10; N, 11.34. Found: C, 24.34; H, 4.87; N, 11.52.

7-Ni<sup>II</sup>(ClO<sub>4</sub>)<sub>2</sub>·2H<sub>2</sub>O (i.e. 20a); Anal. Calcd for C<sub>10</sub>H<sub>22</sub>O<sub>8</sub>N<sub>4</sub>F<sub>2</sub>Cl<sub>2</sub>Ni·2H<sub>2</sub>O: C, 22.66; H, 4.95; N, 10.57. Found: C, 22.95; H, 4.68; N, 10.80.

8-Ni<sup>II</sup>(ClO<sub>4</sub>)<sub>2</sub>nH<sub>2</sub>O (i.e. 21a); This yellowish complex obtained from ethanol is hygroscopic and easily turns to pale violet in air.

[Method B] Dichloro(fluorinated cyclam)-nickel(II) complexes were prepared by the method earlier reported.<sup>14</sup> Nickel(II) chloride hexahydrate dissolved in warm ethanol was added to ethanol solution of an equivalent ligand. The resulting light brown solution was warmed on a water bath for a few minutes. After cooled, the resulting mauve precipitate was collected and washed with ether. A single crystal of dichloro(6,6,13,13-tetrafluoro-1,4,8,11-tetraazacyclotetradecane)-nickel(II) suitable for X-ray crystallographic study was obtained by recrystallization from water.

6-Ni<sup>II</sup>Cl<sub>2</sub> (i.e. 19b); Anal. Calcd for C<sub>10</sub>H<sub>23</sub>N<sub>4</sub>FCl<sub>2</sub>Ni: C, 34.52; H, 6.66; N, 16.10. Found: C, 34.04; H, 6.53; N, 15.94.

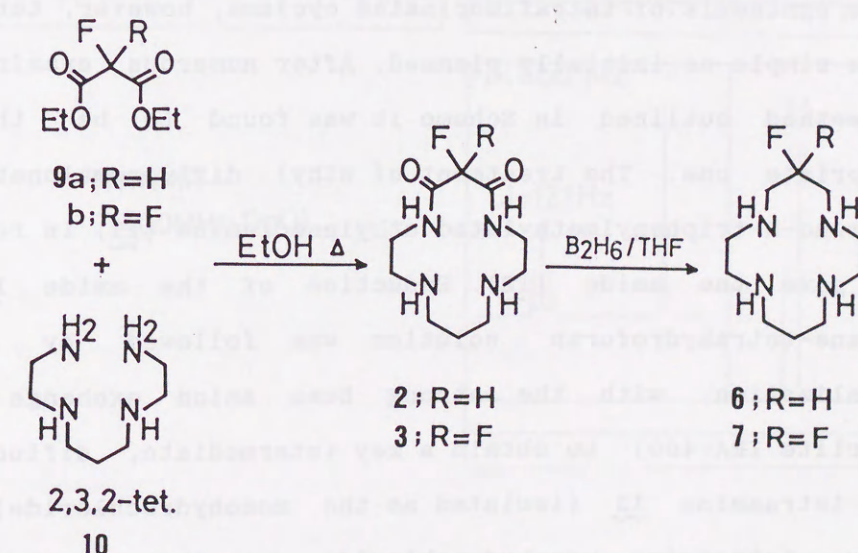
7-Ni<sup>II</sup>Cl<sub>2</sub> (i.e. 20b); Anal. Calcd for C<sub>10</sub>H<sub>22</sub>N<sub>4</sub>F<sub>2</sub>Cl<sub>2</sub>Ni·0.5EtOH: C, 33.97; H, 6.48; N, 14.40. Found: C, 33.65; H, 6.41; N, 14.52.

8-Ni<sup>II</sup>Cl<sub>2</sub> (i.e. 21b); Anal. Calcd for C<sub>10</sub>H<sub>20</sub>N<sub>4</sub>F<sub>4</sub>Cl<sub>2</sub>Ni: C, 29.89; H, 5.02; N, 13.94. Found: C, 29.77; H, 5.09; N, 14.07.

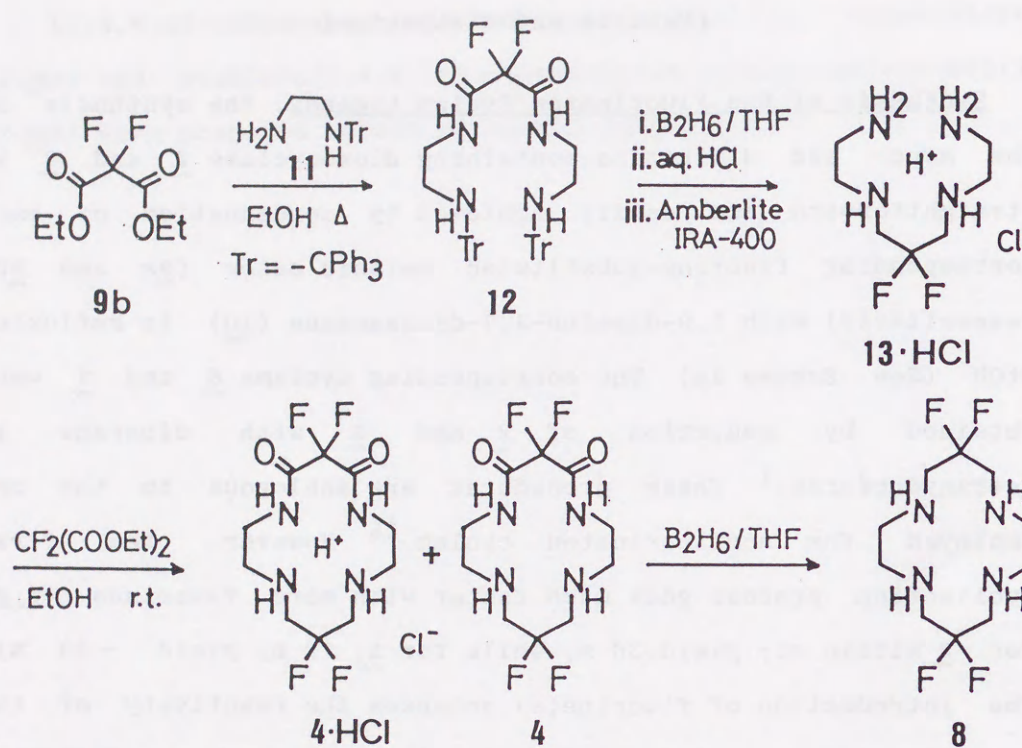
(1,4,8,11-tetraazacyclotetradecane)-nickel(II) diperchlorate (18a) and dichloro(1,4,8,11-tetraazacyclotetradecane)-nickel(II) (18b) were prepared according to the literature.<sup>14</sup>

### [Results and Discussion]

**Synthesis of the Fluorinated Cyclam Ligands.** The synthesis of the mono- and difluorine-containing dioxocyclams 2 and 3 is straightforward and easily achieved by condensation of each corresponding fluorine-substituted malonic ester (9a and 9b, respectively) with 1,9-diamino-3,7-diazanonane (10) in refluxing EtOH (See Scheme 1a). The corresponding cyclams 6 and 7 were obtained by reduction of 2 and 3 with diborane in tetrahydrofuran.<sup>1</sup> These procedures are analogous to the one employed for nonfluorinated cyclam.<sup>15</sup> However, the first cyclization process goes much faster with more fluorines (e.g. for 3 within 3h; yield 36 %, while for 1, 72 h; yield ~30 %). The introduction of fluorine(s) enhances the reactivity of the malonate ester, as indicated by the increasing  $\nu_{C=O}$  frequency (Nujol); 1730 cm<sup>-1</sup> (ethyl malonate), 1745 and 1770 cm<sup>-1</sup> (monofluorinated 9a) and 1780 cm<sup>-1</sup> (difluorinated 9b).



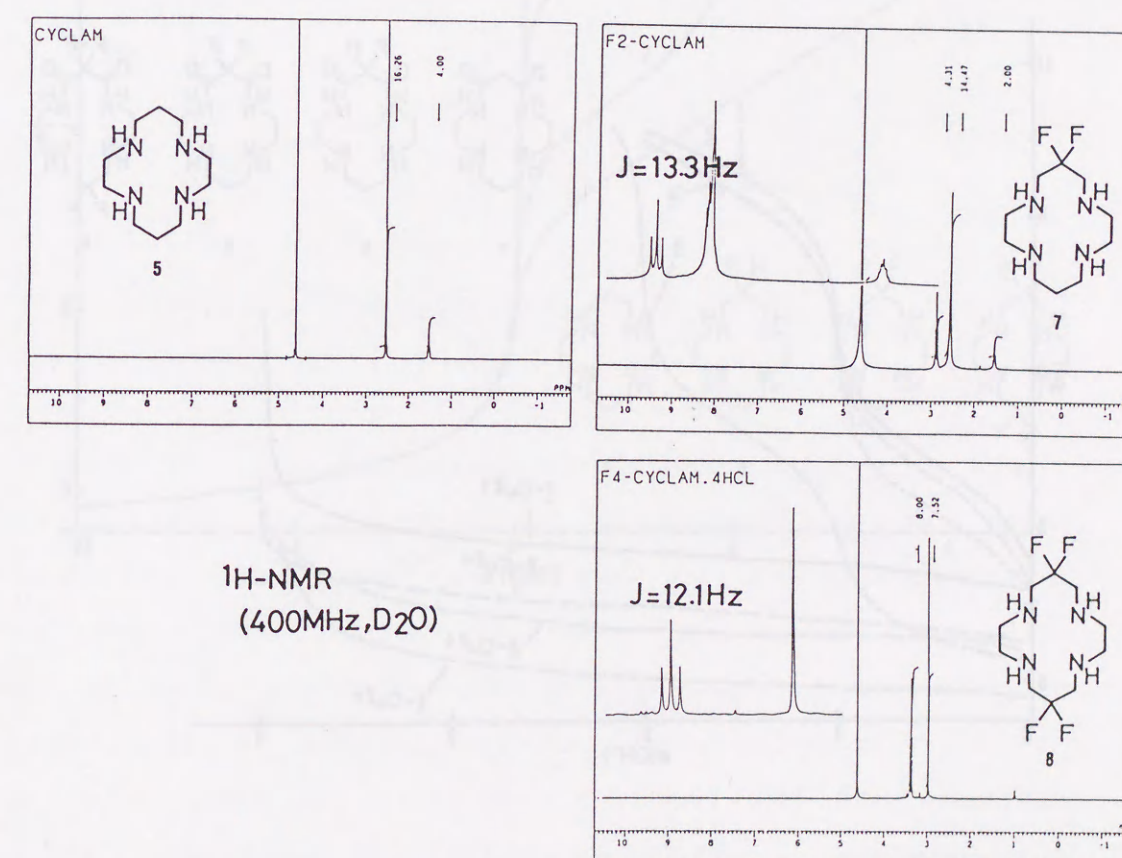
Scheme 1a with hydro cyclams



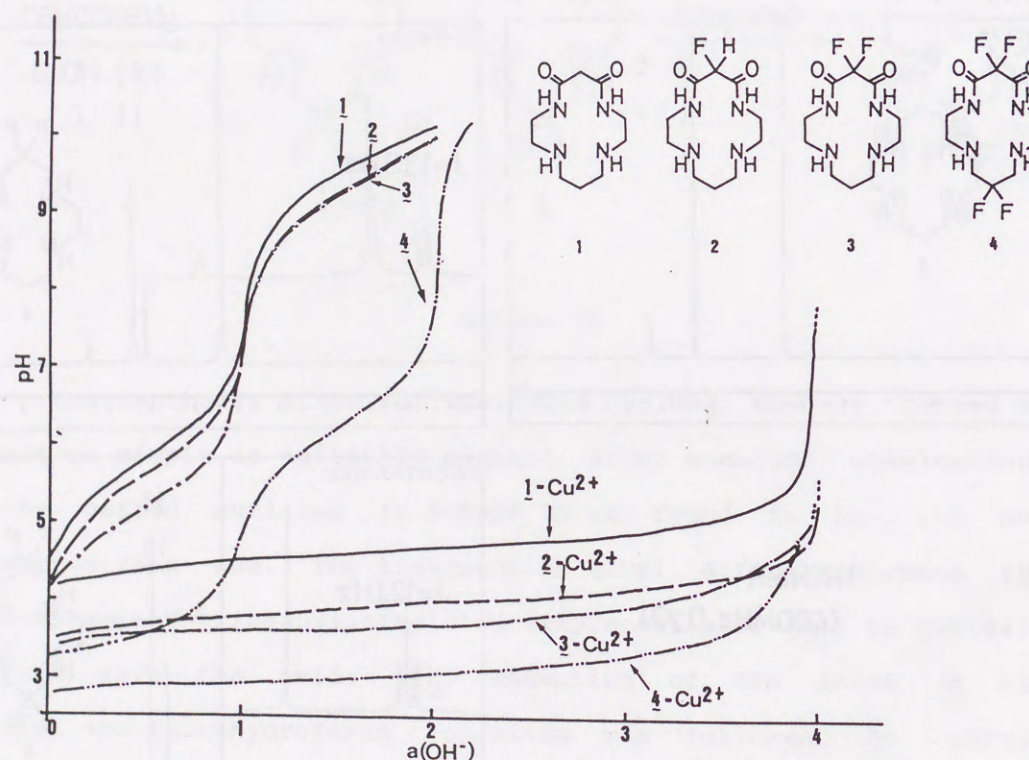
Scheme 1b

The synthesis of tetrafluorinated cyclams, however, turned out not so simple as initially planned. After numerous examinations, the method outlined in Scheme 1b was found to be the most appropriate one. The treatment of ethyl difluoromalonate (9a) with mono-N-triphenylmethylated ethylenediamine (11) in refluxing EtOH gave the amide (12). Reduction of the amide 12 with diborane-tetrahydrofuran solution was followed by partial neutralization with the strong base anion exchange resin (Amberlite IRA-400) to obtain a key intermediate, difluorinated 2,3,2-tetraamine 13 (isolated as the monohydrochloride). This linear tetraamine monohydrochloride was then treated with equivalent ethyl difluoromalonate (9b) in EtOH at room

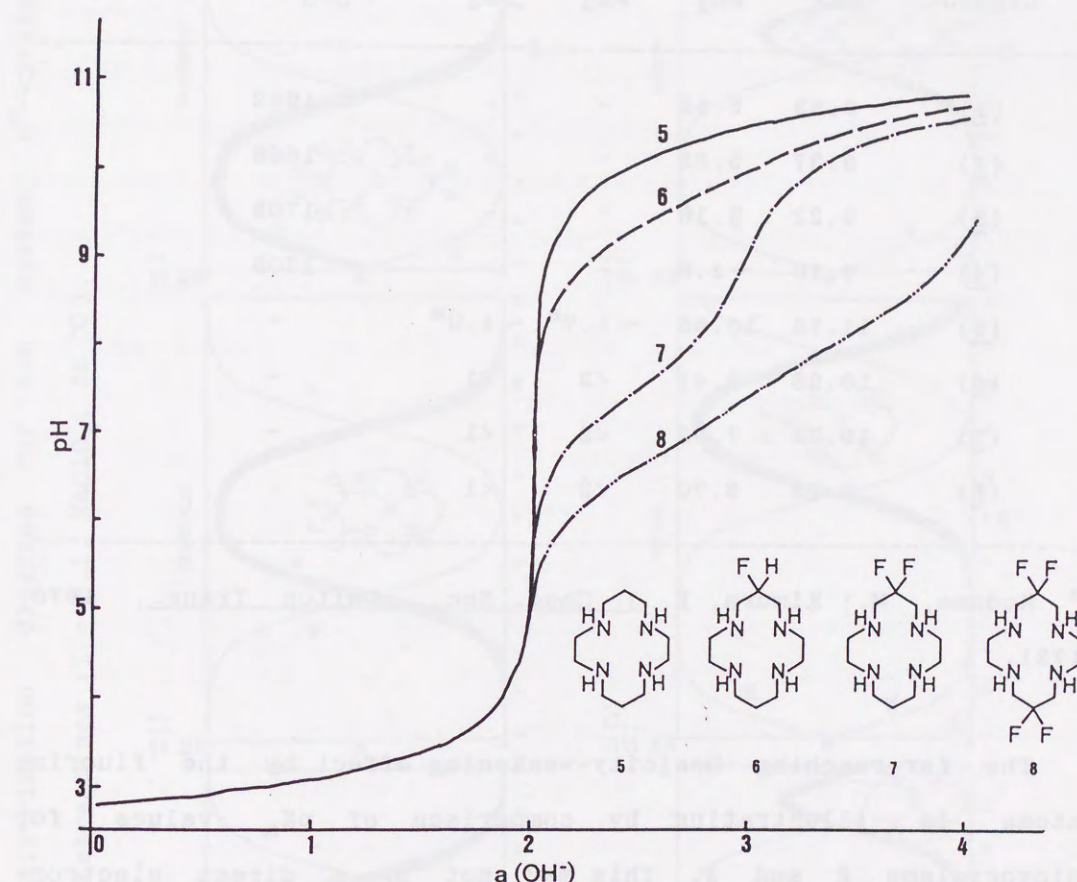
temperature to yield the desired cyclic product, tetrafluorinated dioxocyclam 4 (isolated as the monohydrochloride in yield 20 % and as free form in yield 4 %). If this cyclization is run with free form of 13, the degradation of 13, resulting in poorer yield of 4. Finally, the reduction of the diamide group in 4 took place with diborane in tetrahydrofuran, and the symmetric, tetrafluorinated cyclam 8 was obtained. The Nmr spectra of 7 and 8 are compared with that of 5.



Basicities of the Fluorinated Cyclams. With a series of fluorinated cyclams in hand, systematic investigation of the protonation constants has become possible, which shed light on the effect of fluorination on the amine basicity in cyclams. The stepwise protonation constants ( $pK_a$ ) for the new macrocycles  $\tilde{2}-\tilde{4}$  and  $\tilde{6}-\tilde{8}$  determined by potentiometric titrations at  $25^\circ\text{C}$  and  $I = 0.1 \text{ M} (\text{NaClO}_4)$  (Figures 1 and 2) are listed in Table I.



[Figure 1] pH Titration Curves of Dioxocyclams  $\tilde{1}-\tilde{4}$  in the Absence and the Presence of Equimolar Cu(II) at  $25^\circ\text{C}$  and  $I = 0.1 \text{ M} (\text{NaClO}_4)$ .



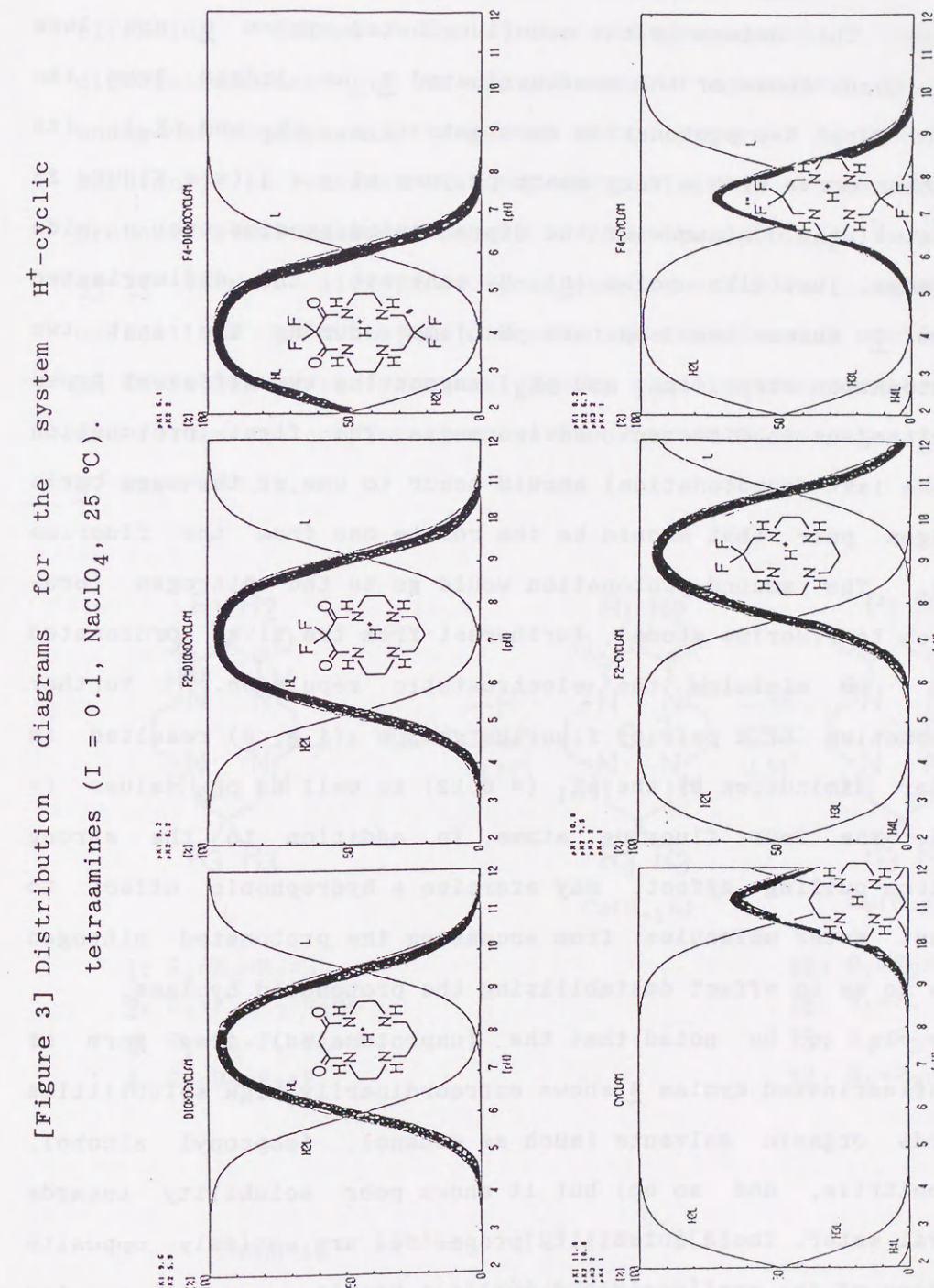
[Figure 2] pH Titration Curves of Cyclams  $\tilde{5}-\tilde{8}$  at  $25^\circ\text{C}$  and  $I = 0.1 \text{ M} (\text{NaClO}_4)$ .

Table I. Protonation Constants at 25 °C and  $I = 0.1$  (NaClO<sub>4</sub>) and Infrared Spectra Data of Free Ligands.

Ligands	pK <sub>1</sub>	pK <sub>2</sub>	pK <sub>3</sub>	pK <sub>4</sub>	$\nu_{C=O}$ cm <sup>-1</sup> (nujol)
(1)	9.63	5.85	-	-	1662
(2)	9.37	5.65	-	-	1688
(3)	9.22	5.18	-	-	1705
(4)	6.10	~1.9	-	-	1705
(5)	11.78	10.55	~1.7 <sup>a</sup>	~1.0 <sup>a</sup>	-
(6)	10.96	9.41	<2	<1	-
(7)	10.78	7.52	<2	<1	-
(8)	8.22	6.70	<2	<1	-

<sup>a</sup> Kodama, M.; Kimura, E. *J. Chem. Soc., Dalton Trans.*, 1976, 1721.

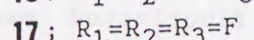
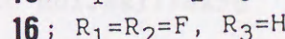
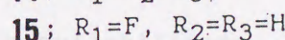
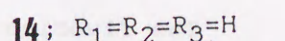
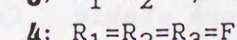
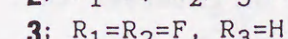
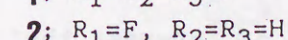
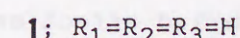
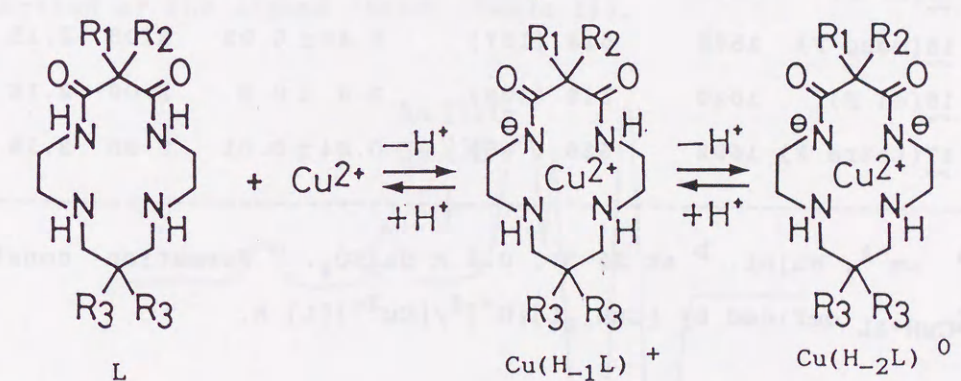
The far-reaching basicity-weakening effect by the fluorine atoms is illustrating by comparison of pK<sub>a</sub> values for dioxocyclams 2 and 3. This may not be a direct electron-withdrawing effect but rather an indirect one through the strengthened hydrogen bonding between acidified (due to the electron-withdrawing effect of fluorine atom) proximal amide hydrogens and the remote N lone pairs. As seen by 4, an additional pair of fluorine atoms weaken their basicity, and no proton is seen in the cavity of 4 above neutral pH (see distribution diagrams in Figure 3).



A similar space effect also seems to work at the fluorinated cyclams. The amines in the monofluorinated cyclam 6 are less basic than those of the nonfluorinated 5, as judged from the smaller first two protonation constants (*i.e.*,  $pK_1$  and  $pK_2$ ). Its titration curve with a very sharp pH jump at  $\alpha = 2$  (see Figure 2) indicates the dominance of the diprotonated species over a wide pH range, just like cyclam (5). By contrast, the difluorinated cyclam 7 shows two separate pH jumps during the last two deprotonation steps, ( $pK_1$  and  $pK_2$ ) suggesting two different types of nitrogens in different environments. The first protonation (or the last deprotonation) should occur to one of the more basic nitrogen pair that should be the remote one from the fluorine atoms. The second protonation would go to the nitrogen (proximate to fluorine atoms), furtherest from the first protonated amine to minimize the electrostatic repulsion.<sup>16</sup> Further introduction of a pair of fluorine groups (*i.e.* 8) resulted in greater diminution of the  $pK_1$  (= 8.22) as well as  $pK_2$  values (= 6.70). The four fluorine atoms, in addition to the strong electron-pulling effect, may exercise a hydrophobic effect to prevent water molecules from accessing the protonated nitrogen atoms so as to effect destabilizing the protonated cyclams.

It is to be noted that the (unprotonated) free form of tetrafluorinated cyclam 8 shows extraordinarily high solubilities towards organic solvents (such as ethanol, isopropyl alcohol, acetonitrile, and so on) but it shows poor solubility towards neutral water. These solubility properties are entirely opposite to those of the nonfluorinated cyclam 5. Similar trends are also seen in their metal complexes, as described later.

Copper(II) Complexes with Dioxocyclams 1-4. In the pH-titration curves for the diprotonated macrocyclic dioxotetraamines 1-4 in the presence of equivalent Cu(II) ion under an atmosphere of argon at 25 °C (Figure 1 in the previous section), it is clear that the neutralization of the two amide protons simultaneously occurs to form the  $Cu^{II}(H_{-2}L)^0$  complexes 14-17 (Figure 1). Those complexes are indeed isolated as crystalline products, as described in Experimental section. The pH titration curves were analyzed by assuming the equilibria (1) and (2) in the complexation for fluorinated macrocycles 2-4 (with 1, see ref 17).



$$K_{CuH-1L} = [Cu(H_{-1}L)][H^+]/[Cu^{II}][L] \quad (1)$$

$$K_{-2H} = [Cu(H_{-2}L)][H^+]/[Cu(H_{-1}L)^+] \quad (2)$$

$$K_{CuH-2L} = [Cu(H_{-2}L)][H^+]^2/[Cu^{II}][L] \quad (3)$$

The complexation constants  $K_{CuH_2L}$ , as expressed by (3), were calculated as before<sup>13</sup> and the final values are summarized in Table II.

Table II IR and Visible Absorption Spectra (at 25 °C, 0.5 M Na<sub>2</sub>SO<sub>4</sub>), Stability Constants, (at 25 °C, 0.1 M NaClO<sub>4</sub>), and ESR Parameters (at 77 K) of Cu(II)-deprotonated Dioxotetraamine Complexes  $\tilde{14-17}$ , Cu(H<sub>2</sub>L)<sup>0</sup>.

Complexes	$\nu_{C=O}^a$	Visible <sup>b</sup> $\lambda_{max}$ , nm( $\epsilon$ )	Log $K_{CuH_2L}(M)^c$	ESR		
				$g_{\perp}$	$g_{\parallel}$	$A_{\parallel}, G$
$\tilde{14}$ (no F)	1580	505 (100)	$0.11 \pm 0.01$	2.06	2.17	215
$\tilde{15}$ (mono F)	1575	518 (137)	$0.49 \pm 0.03$	2.06	2.18	217
$\tilde{16}$ (di F)	1620	515 (108)	$2.5 \pm 0.2$	2.06	2.18	217
$\tilde{17}$ (tetra F)	1652	526 (95)	$0.84 \pm 0.01$	2.06	2.18	212

<sup>a</sup> cm<sup>-1</sup>, Nujol. <sup>b</sup> at 25 °C, 0.5 M Na<sub>2</sub>SO<sub>4</sub>. <sup>c</sup> Formation constants,  $K_{CuH_2L}$  defined by  $[CuH_2L][H^+]^2/[Cu^{2+}][L] M$ .

The fluorine atoms in dioxocyclams have a marked effect on the stabilization of Cu(H<sub>2</sub>L)<sup>0</sup> complexes. It is of interest that the fluorinated macrocycles  $\tilde{2-4}$  generally forms more stable Cu(II) complexes  $\tilde{15-17}$  than the parent nonfluorinated  $\tilde{1}$ . The highest complex stability has been shown with the difluorinated  $\tilde{3}$ . On the other hand, an additional pair of fluorine atoms near the secondary amines (in  $\tilde{4}$ ) lowers the complex stability.

The strong electron-withdrawing from the two proximate imide nitrogens is well reflected in the higher stretching frequencies

of amide carbonyl  $\nu_{C=O}$  of the isolated  $\tilde{15-17}$ , Cu<sup>II</sup>(H<sub>2</sub>L)<sup>0</sup> (see Table II). Furthermore, in contrast to  $\tilde{1-3}$ , the complexation of  $\tilde{4}$  is much slower, each titration requiring more than 60 min for equilibration. This may be due to the fact that the secondary amines in the most hydrophobic tetrafluorinated  $\tilde{4}$  may be least accessible for the hydrated copper(II).

The ESR parameters for paramagnetic Cu(II) complexes are almost similar within a series of CuH<sub>2</sub>L complexes  $\tilde{14-17}$ , indicating more or less the same well-fit macrocyclic square planar N<sub>4</sub> ligand fields (Table II). The typical spectrum with  $\tilde{17}$  is shown in Figure 4. The wave length of maximal d-d absorptions red-shifts upon fluorination, which implies the successive reduction of the ligand fields (Table II).

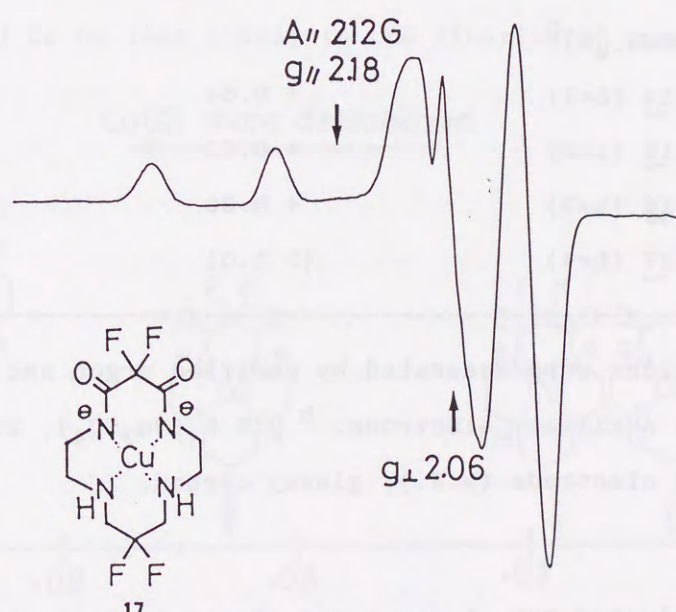


[Figure 4] X-Band ESR Spectrum of the Cu(II) Complex  $\tilde{17}$  in H<sub>2</sub>O at 77 K.

It has been earlier shown that in macrocyclic polyamine complexes the uncommon Cu<sup>3+</sup>, Ni<sup>3+</sup> oxidation states can be kinetically and thermodynamically stabilized by incorporation of amide nitrogen donors. A broad family of macrocyclic polyamine ligands containing amide functions have been developed.<sup>2a</sup> The effects of the cavity size, number of amide functions, type of appended substituents and the number and type of donor atoms on their redox properties have been discussed.<sup>9</sup>

Table III Half-wave Potentials (V vs SCE)<sup>a</sup> for Cu<sup>III/II</sup> Couple in 14-17.

Complex	$E_{1/2}$ (V <u>vs</u> SCE) for Cu <sup>III/II</sup> , <sup>b</sup>
[CuH <sub>2</sub> L] <sup>0</sup>	
<u>14</u> (L=1)	+ 0.64
<u>15</u> (L=2)	+ 0.69
<u>16</u> (L=3)	+ 0.83
<u>17</u> (L=4)	(> 1.0)

<sup>a</sup> All solutions were deaerated by purified argon and a Pt wire was used as auxiliary electrode. <sup>b</sup> 0.5 M (Na<sub>2</sub>SO<sub>4</sub>), 25 °C, pH = 7.0. Working electrode (W.E.); glassy carbon.

The fluorinated CuH<sub>2</sub>L complexes 15 and 16 both showed quasi-reversible cyclic voltammograms for Cu<sup>III/II</sup> in 0.5 M Na<sub>2</sub>SO<sub>4</sub> aqueous solution at 25 °C, as so did 14 (Table III and Figure 5). The redox potential of Cu<sup>III/II</sup> in 17 failed to be seen in the

normal range in water, which should go up to >1.0 vs S.C.E..

On the other hand, the quasi-reversible cyclic voltammogram for tetrafluorinated cyclam-Cu(II) complex 17 could be seen at +0.87 vs S.C.E. in dimethylformamide (0.1 M NaClO<sub>4</sub>, 25 °C). The other Cu(II) complexes (14-16) were insoluble in dimethyl formamide.

Upon fluorination, the imide anions weaken their σ donor properties and hence the higher oxidation state M<sup>3+</sup> successively becomes destabilized with respect to M<sup>2+</sup>. Another factor to affect their redox behaviors may be the hydrophobic effect. In general, the release of the axial water molecules from the coordination sphere would occur upon the electronic configurational change from d<sup>9</sup> to the low-spin d<sup>8</sup> during oxidation process. The stabilization by such desolvation is considered to be less likely in the fluorinated complexes.

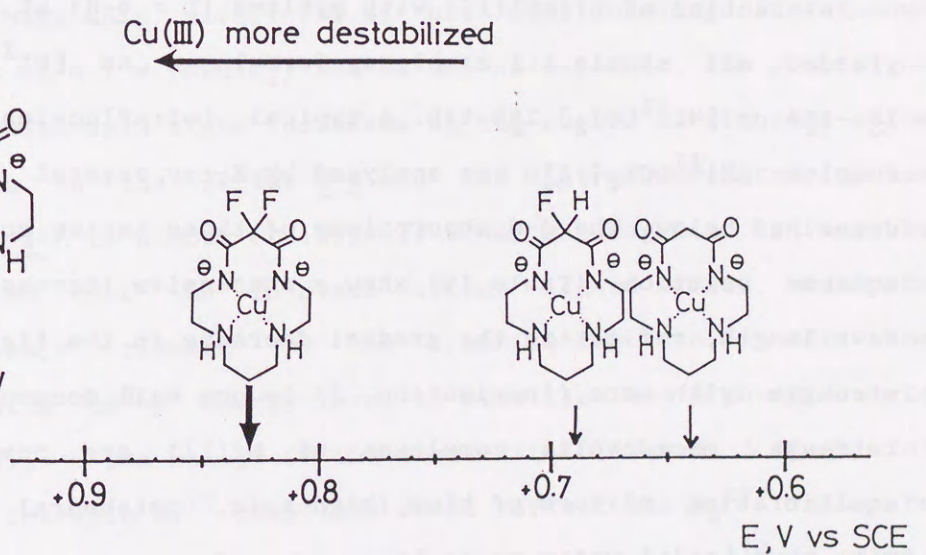
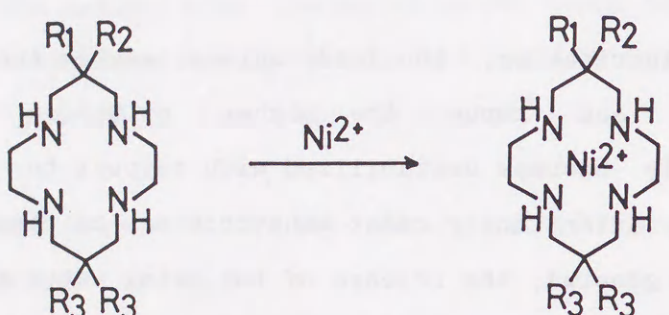


[Figure 5] Fluorination effects on Cu<sup>III/II</sup> redox potentials.(0.5 M Na<sub>2</sub>SO<sub>4</sub>, 25 °C)

Ni(II) Complexes with Fluorinated Cyclams 5-8. The potentiometric determination of the complexation constants with Ni<sup>II</sup> were almost impossible (like the nonfluorinated cyclam 5) due to the extremely slow Ni<sup>II</sup>-macrocyclic ligand interaction rates and also instability of some fluorinated ligands.<sup>18</sup>



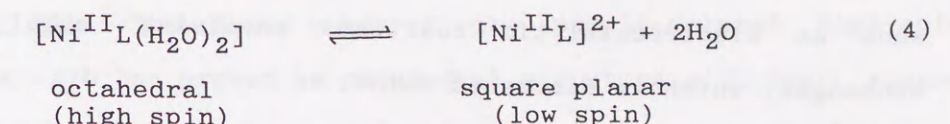
5; R<sub>1</sub>=R<sub>2</sub>=R<sub>3</sub>=H

6; R<sub>1</sub>=F, R<sub>2</sub>=R<sub>3</sub>=H

7; R<sub>1</sub>=R<sub>2</sub>=F, R<sub>3</sub>=H

8; R<sub>1</sub>=R<sub>2</sub>=R<sub>3</sub>=F

Interaction of nickel(II) with cyclams (L = 5-8) at neutral pH yielded all stable 1:1 complexes formulated as [Ni<sup>II</sup>L](ClO<sub>4</sub>)<sub>2</sub> 18a-21a or [Ni<sup>II</sup>LCl<sub>2</sub>] 18b-21b. A typical tetrafluorinated cyclam complex [Ni<sup>II</sup>LCl<sub>2</sub>] 21b was analyzed by X-ray crystal study, as described below. The d-d absorptions of these series complexes in aqueous solution (Table IV) show a successive increase in the wave length, reflecting the gradual decrease in the ligand field strength with more fluorination. It is now well documented that tetraaza macrocyclic complexes of Ni(II) are composed of equilibrating mixture of blue (high spin, octahedral structure with two axial water molecules) and yellow (low spin, square planar), and that the ligand electronic and steric features affect this equilibrium.<sup>19</sup>



The effect of fluorination on the solution behavior of Ni(II) complexes is assessed by measuring the Ni(II) spin states. This is monitored by the spectroscopic method using the low spin-specific absorption bands ( $\lambda_{\text{max}}$  445, 454, 462, and 476 nm for Ni(II) complexes with 5, 6, 7, and 8, respectively). In all the cases, the equilibrium 4 shifts to the right with an increase in temperature and in the ionic strength, ultimately to a leveling 100 % yellow diamagnetic form. We thus estimated the limiting  $\varepsilon$  values for 100 % high-spin complexes 19a, 20a in the presence of  $> 5$  M of NaClO<sub>4</sub> salts and at 25 °C.

With the nonfluorinated cyclam complex 18a, a low-spin (71 %) and a high-spin Ni(II) (29 %) are equilibrating in aqueous solution at 0.1 M (NaClO<sub>4</sub>) and 25 °C. As expected, the proportion of the high-spin state increases as the number of fluorine atom increases in the series 5-8 and the tetrafluorinated cyclam complex 21a is almost exclusively blue, paramagnetic. It may be considered that the in-plane cyclam ligand field might be considerably reduced by the fluorination to lower the antibonding  $d_{x^2-y^2}$  energy level to stabilize the high-spin state of Ni(II). The energy of the single visible band  $\nu$  (d-d) for yellow low-spin Ni<sup>II</sup> complexes would reflect the  $D_q^{xy}$  value to represent the strength of Ni-N in-plane interactions.<sup>17c</sup> In fact,  $\nu$  (d-d) decreases with more fluorine substitution (Table IV).

The increasing proportion of the high spin state of Ni(II)

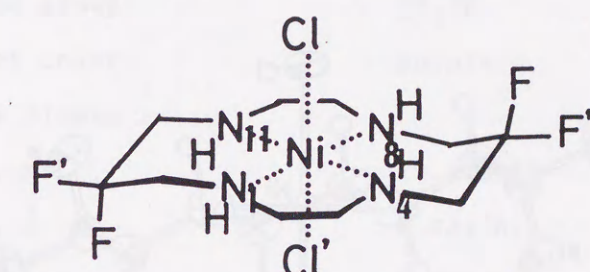
might be important in catalytic behaviors by cyclam complexes, such as electrocatalytic reactions involving axial ligand exchanges, which is discussed below.

Table IV Visible Absorption Maxima and Selectivities towards Metal Spin States of Ni(II) Complexes  $\text{18a-21a}$   
 $([\text{Ni}^{\text{II}}\text{L}]_2(\text{ClO}_4)_2$ , where  $\text{L} = \text{18a-21a}$ ) at Equilibrium in  
 $0.1 \text{ M NaClO}_4$  Aqueous Solution at  $25^\circ\text{C}$ , and Energy of  
the  $d-d$  Absorption band ( $\nu_{d-d}$ ) for 100 % low-spin  
Complexes.

$[\text{Ni}(\text{II})\text{L}]^{2+}$ Complex	$\lambda_{\text{max}}$ nm ( $\epsilon$ , $\text{M}^{-1}\text{cm}^{-1}$ )	high-spin form (%)	low-spin form (%)	$\nu_{d-d}$ <sup>b</sup> $\text{cm}^{-1}$
$\text{18a (L=5)}^{\text{a}}$	445 (46)	29	71	22740
$\text{19a (L=6)}$	451 (28)	38	62	22030
$\text{20a (L=7)}$	504 (6)	86	14	21650
$\text{21a (L=8)}$	517 (7)	>99	<1	$\sim 21000^{\text{c}}$

<sup>a</sup> See; Anichini, A.; Fabbrizzi, L.; Paoletti, P.; Clay R. M. *Inorg. Chim. Acta*, 1977, **24**, L2. <sup>b</sup>Energy values of the  $d-d$  absorption band for 100 % low-spin complexes were determined in  $>5 \text{ M NaClO}_4$  aqueous solution. <sup>c</sup> The limiting  $\epsilon$  value for low-spin species of  $\text{21a}$  could not be determined exactly because the precipitation occurred immediately before reaching its limit.

Crystal Structure of a Ni(II) Complex of the tetrafluorinated cyclam  $\text{21b}$ . The X-ray study of the purple-colored high-spin complex  $\text{21b}$  has proved an octahedral structure with four square planar nitrogens and two axial chlorides (Figure 6). Crystal data and data collection parameters are displayed in Table V. Selected molecular dimensions, bond angles are listed in Table VI, VII, and VIII, respectively.

**21b**

The  $R,R,S,S-$  (or *trans-III*)<sup>20</sup> configuration of the macrocyclic ligand is fundamentally identical to that for the high-spin, octahedral  $\text{Ni}^{\text{II}}(\text{cyclam})\text{Cl}_2$  complex  $\text{18b}$ .<sup>21</sup> The nickel ion stays coplanar with  $\text{N}_4$ . Interestingly, the four equatorial Ni-N bond distances  $2.077(4)$  ( $\text{Ni-N1}, \text{Ni-N8}$ ),  $2.064(4)$  ( $\text{Ni-N4}, \text{Ni-N11}$ ) Å are not as elongated as anticipated and they fall in the typical high-spin  $\text{Ni}^{\text{II}}-\text{N}$  lengths, as found in the nonfluorinated cyclam complex  $\text{18b}$  [ $2.066(8)$  and  $2.050(8)$  Å, respectively].<sup>21</sup> The average axial  $\text{Ni}-\text{Cl}$  bond length [ $2.479(1)$  Å] is a little shorter than that of  $\text{18b}$  [ $2.492(3)$  Å]. From a consideration of these X-ray study, the F substitutions do not significantly affect the structural factors, but only do the electronic effect on the remote nitrogen donors. The tetragonal distortion in the Ni-N

bonding is accompanied by the deviations from 90 °C of N-Ni-Cl bond angles, which may reflect the intramolecular non-bonding interactions between the hydrogens and apical chlorines.<sup>21</sup> The structural changes from nonfluorinated 18b to fluorinated 21b as a whole are surprisingly minor. Two equatorially-attached fluorine groups are in a suitable position for weakening the ligand field through F-C-C-N bondinds.

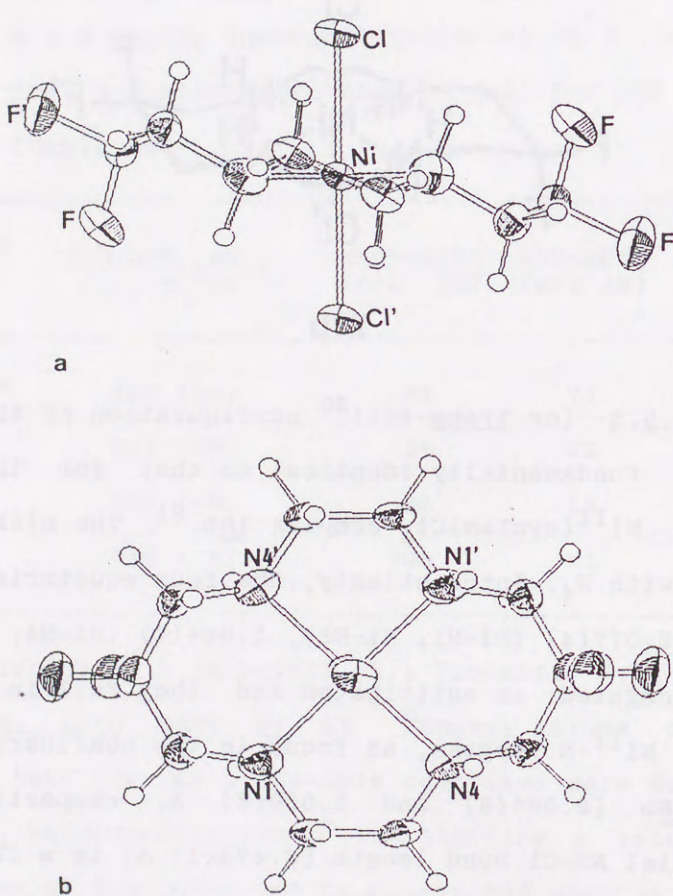


[Figure 6] ORTEP Drawing of 21b: (a) side-on view and (b) top view. Atoms are drawn with 50 % probability ellipsoids.

Table V. Crystal Data and Data Collection Summary.

Ni(II) complex <u>21b</u>	
formula	C <sub>10</sub> H <sub>20</sub> N <sub>4</sub> F <sub>4</sub> Cl <sub>2</sub> Ni
M <sub>r</sub>	401.9
cryst syst	monoclinic
space group	P2 <sub>1</sub> /n
cryst color	purple
cell dimens	
a, Å	14.218(8)
b, Å	8.524(5)
c, Å	6.538(5)
β (°)	98.46(5)
V, Å <sup>3</sup>	783.7
Z	2
calcd density, g cm <sup>-3</sup>	1.703
cryst dimens, mm	0.05 x 0.1 x 0.2
radiation (graphite monochromated)	Cu K $\alpha$
μ, cm <sup>-1</sup>	54.0
2θ range, deg	6 - 156
scan speed, deg min <sup>-1</sup>	6
phasing	heavy-atom method
no. of measd reflns	1572
no. of indep reflns (I > 2σ I)	1550
final R	0.056

Table VI Final Fractional Coordinates ( $x \times 10^4$ ) for  $\tilde{21b}$  with Estimated Standard Deviation in Parenthesis.

atom	x	y	z	$B_{eq}, \text{\AA}^2$
Ni	0( 0)	0( 0)	0( 0)	1.95(.01)
N(1)	-1436( 2)	517( 5)	-146( 6)	3.7 (0.1)
C(2)	-1749( 3)	-345( 6)	1617( 7)	2.8 (0.1)
C(3)	-1303( 3)	-1953( 6)	1755( 7)	2.7 (0.1)
N(4)	-246( 2)	-1752( 5)	2037( 5)	3.4 (0.1)
C(5)	242( 4)	-3253( 6)	1847( 8)	3.0 (0.1)
C(6)	1302( 4)	-3027( 6)	1927( 8)	3.2 (0.1)
C(7)	1700( 3)	-2182( 6)	231( 8)	3.1 (0.1)
F(6)	1654( 2)	-2329( 4)	3799( 5)	4.3 (0.1)
F'(6)	1693( 2)	-4513( 4)	2029( 6)	5.3 (0.1)
Cl(1)	443( 1)	1775( 1)	2991( 2)	2.9 (0.0)

atom	x	y	z	$B_{eq}, \text{\AA}^2$
HN(1)	-182( 5)	3( 8)	-161(10)	6.7 (1.8)
HC(2)	-153( 4)	28( 7)	298( 9)	4.4 (1.4)
H'C(2)	-249( 4)	-44( 7)	141( 9)	4.8 (1.4)
HC(3)	-154( 4)	-260( 7)	37( 9)	4.9 (1.4)
H'C(3)	-152( 4)	-258( 7)	302( 8)	4.1 (1.3)
HN(4)	1( 4)	-133( 8)	363( 9)	5.4 (1.5)
HC(5)	-2( 5)	-378( 7)	41( 9)	4.2 (1.3)
H'C(5)	14( 4)	-402( 7)	308( 9)	4.5 (1.4)
HC(7)	143( 4)	-273( 7)	-123( 9)	5.1 (1.5)
H'C(7)	245( 4)	-231( 7)	47( 8)	4.0 (1.3)

Table VII. Bond Distances ( $\text{\AA}$ ) for  $\tilde{21b}$  with Estimated Standard Deviations in Parenthesis.

N(1) - C(2)	1.489(6)	C(6) - F(6)	1.387(6)
N(1) - C(7)	1.467(7)	C(6) - F'(6)	1.381(6)
C(2) - C(3)	1.507(7)	C(7) - N(1)	1.467(7)
C(3) - N(4)	1.498(6)	Ni - N(1)	2.077(4)
N(4) - C(5)	1.470(6)	Ni - N(4)	2.064(4)
C(5) - C(6)	1.512(7)	Ni - Cl(1)	2.479(1)
C(6) - C(7)	1.501(8)		

Table VIII Bond Angles ( $^\circ$ ) for  $\tilde{21b}$  with Estimated Standard Deviations in Parenthesis.

C(2)-N(1)-C(7)	113.8(4)	C(5)-C(6)-F'(6)	106.1(4)
C(3)-C(2)-N(1)	108.9(4)	F(6)-C(6)-F'(6)	105.1(4)
N(4)-C(3)-C(2)	108.0(4)	N(1)-C(7)-C(6)	111.7(4)
C(5)-N(4)-C(3)	111.5(4)	N(1)-Ni-N(4)	85.69(15)
C(6)-C(5)-N(4)	111.5(4)	N(1)-Ni-Cl	92.34(11)
C(7)-C(6)-C(5)	121.2(4)	N(1)-Ni-N'(4)	94.31(15)
C(7)-C(6)-F(6)	108.6(4)	N(1)-Ni-Cl	87.66(11)
C(7)-C(6)-F'(6)	106.4(4)	N(4)-Ni-Cl	88.86(10)
C(5)-C(6)-F(6)	108.3(4)		

## Redox Properties of Nickel(II)-Fluorinated Cyclam Complexes.

The fluorinated cyclams 6-8 were expected to destabilize the higher oxidation states or stabilize the lower oxidation states of the encapsulated metal ions more than the nonfluorinated cyclam 5 does. The cyclic voltammograms of the present new cyclams (25 °C in 0.5 M Na<sub>2</sub>SO<sub>4</sub> aqueous solution) showed all reversible Ni<sup>III</sup>/Ni<sup>II</sup> redox behaviors with the peak potential separation of 70 mV (scan rate 100 mV/sec) and the peak current ratios of unity (for 8, see Figure 7a). These redox potentials  $E_{1/2}$  values, as anticipated, successively become more positive with the increasing number of incorporated fluorine atoms (Table IX and Figure 8).

Table IX Half-wave Potentials ( $V$  vs SCE)<sup>a</sup> for Ni<sup>III/II</sup> and  
Ni<sup>II/I</sup> Couples in 18a-21a.

Complex	$E_{1/2}$ (v vs SCE)
$\text{Ni}^{\text{III}/\text{II}}, \text{b}$	$\text{Ni}^{\text{II}/\text{I}}, \text{c}$
<hr/>	<hr/>
$[\text{NiL}]^{2+}$	
$\text{18a } (\text{L=5})$	+ 0.50 - 1.56
$\text{19a } (\text{L=6})$	+ 0.52 - 1.52
$\text{20a } (\text{L=7})$	+ 0.63 - 1.46
$\text{21a } (\text{L=8})$	+ 0.81 - 1.42
<hr/>	<hr/>

<sup>a</sup> All solutions were deaerated by purified argon and a Pt wire was used as auxiliary electrode. <sup>b</sup> 0.5 M ( $\text{Na}_2\text{SO}_4$ ), 25 °C, pH = 6-7. W.E.; glassy carbon. <sup>c</sup> 0.1 M ( $\text{NaClO}_4$ ), 25 °C, pH = 7.0. W.E.; hanging-mercury-drop electrode.

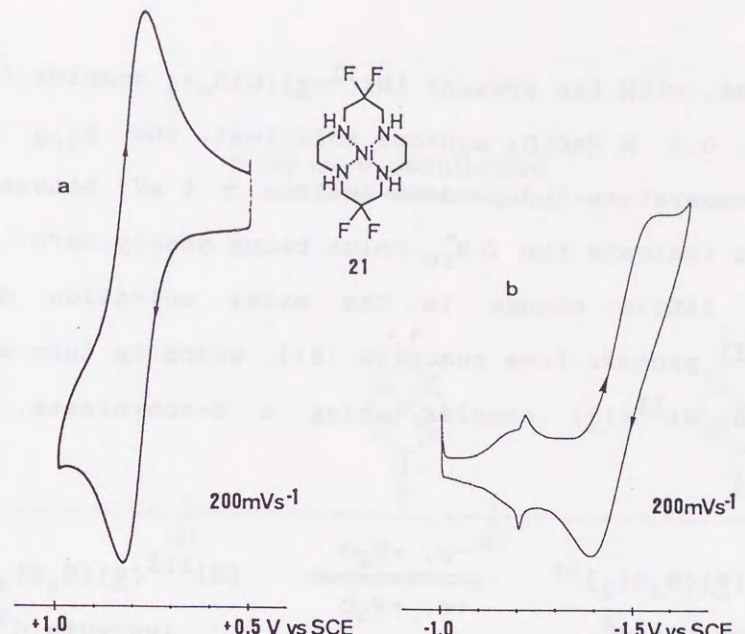
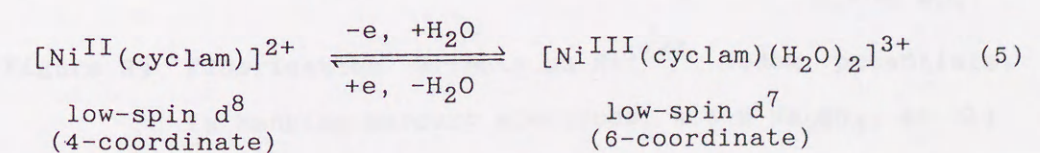
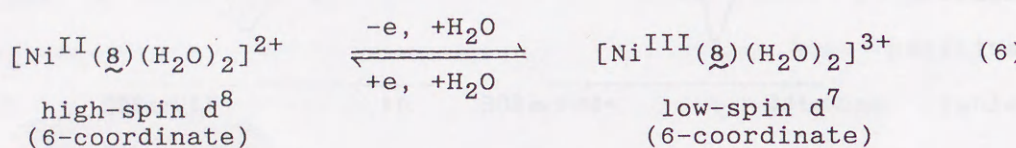


[Figure 7] Cyclic voltammograms of Ni(II)-8 complex 21a: (a) Ni<sup>III/II</sup> redox couple in 0.5 M Na<sub>2</sub>SO<sub>4</sub> at 25 °C using a glassy carbon electrode. (b) Ni<sup>II/I</sup> redox couple in 0.1 M NaClO<sub>4</sub> at 25 °C using a hanging mercury electrode.

The reaction entropies for  $\text{Ni}^{\text{III}}/\text{Ni}^{\text{II}}$  redox couple,  $\Delta S_{\text{rc}}^\circ$ , were estimated from the slope of the straight lines for  $E_{1/2}$  vs T plots.<sup>20</sup> In a previous study for the  $\text{Ni}^{\text{III}}/\text{II}-\text{cyclam}$  complex, a large positive  $\Delta S_{\text{rc}}^\circ$  value of  $34.3 \text{ cal mol}^{-1} \text{ K}^{-1}$  was reported for the 100 % low-spin  $\text{Ni}^{\text{II}}$  complex (attained in 3.5 M  $\text{NaClO}_4$  solution).<sup>21</sup> This fact was interpreted to represent a reaction (5) involving strong hydrations upon oxidation to  $\text{Ni}^{\text{III}}$ .<sup>22</sup> On the



other hand, with the present  $[\text{Ni}^{\text{II}}\text{-8}](\text{ClO}_4)_2$  complex (>99 % high-spin in 0.1 M  $\text{NaClO}_4$  aqueous solution), the  $E_{1/2}$  values are almost temperature-independent (within  $\pm 5$  mV) between 10 °C and 50 °C to indicate the  $\Delta S_{\text{rc}}^{\circ}$  value being nearly zero. This fact reflects little change in the axial solvation during the  $\text{Ni}^{\text{III}}/\text{Ni}^{\text{II}}$  process [see reaction (6)], which in turn supports the high-spin  $\text{Ni}^{\text{II}}\text{-8}$  complex taking a 6-coordinate, octahedral geometry.



The reduction potentials for  $\text{Ni}^{\text{II}}/\text{Ni}^{\text{I}}$  in the series of cyclam complexes in aqueous solution<sup>25</sup> are also determined in argon atmosphere from the reversible cyclic voltammograms (for 8, see Figure 7b) and the results are summarized in Table IX. As the number of fluorine increases,  $E_{1/2}$  become successively less negative values, indicating, as anticipated, the more the fluorine substitution, the more the  $\text{Ni}^{\text{I}}$  complex stabilized (Figure 9).

Ni(III) more destabilized

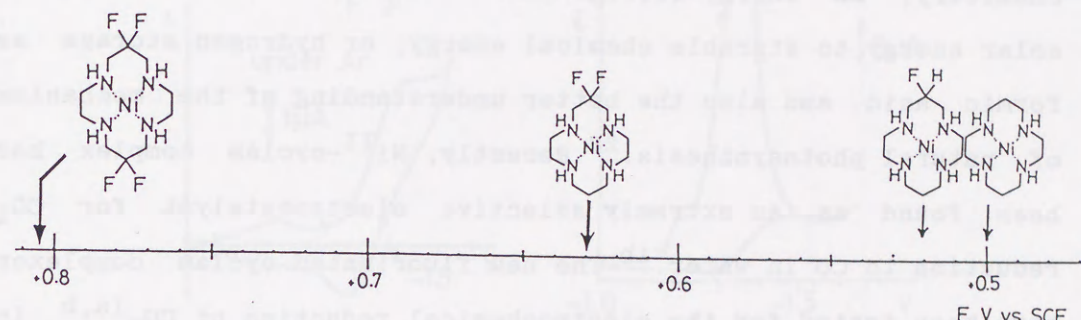


[Figure 8] Fluorination effects on  $\text{Ni}^{\text{III}}/\text{II}$  redox potentials.  
(a glassy carbon, 0.5 M  $\text{Na}_2\text{SO}_4$ , 25 °C)

Ni(II) more destabilized

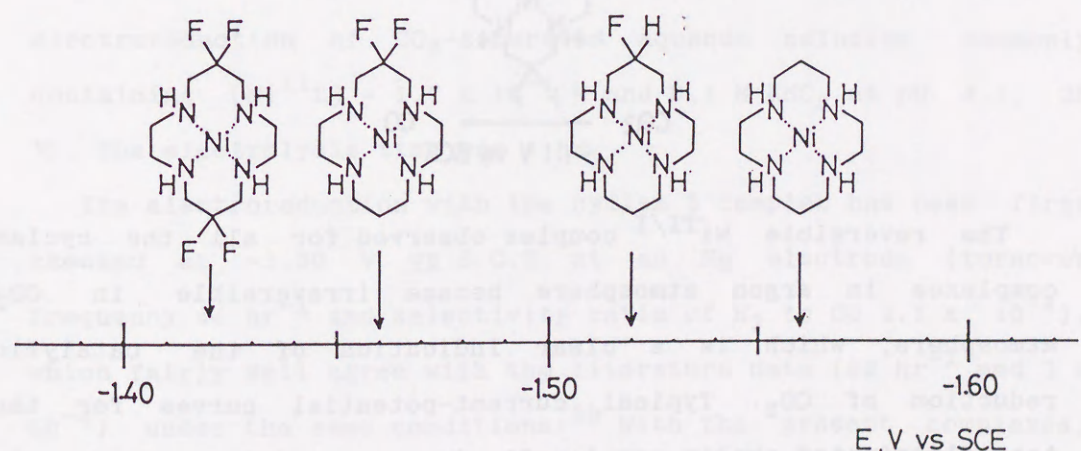
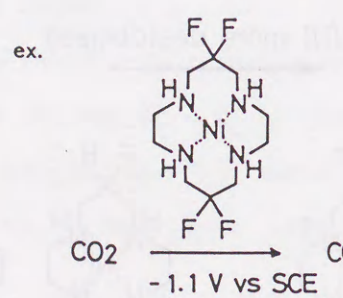


[Figure 9] Fluorination effects on  $\text{Ni}^{\text{II}}/\text{I}$  redox potentials.  
(a hanging mercury electrode, 0.5 M  $\text{Na}_2\text{SO}_4$ , 25 °C)

An Application of the Ni(II) Complexes of Fluorinated Cyclams to Electrocatalytic Reduction of CO<sub>2</sub>. The reduction of CO<sub>2</sub> has been a subject of recent interest, as a key route to C<sub>1</sub> chemistry, an energy storage measurement by the conversion of solar energy to storable chemical energy, or hydrogen storage as formic acid, and also the better understanding of the mechanism of natural photosynthesis.<sup>26</sup> Recently, Ni<sup>II</sup>-cyclam complex has been found as an extremely selective electrocatalyst for CO<sub>2</sub> reduction to CO in water.<sup>1b</sup> The new fluorinated cyclam complexes have been tested for the electrochemical reduction of CO<sub>2</sub><sup>1a,b</sup> in aqueous solution. The present fluorinated cyclams, that more stabilize Ni<sup>I</sup> complex, appeared to have an advantage over the nonfluorinated cyclam  $\tilde{5}$  in the higher reduction potentials to be required in generating Ni<sup>I</sup>.



The reversible Ni<sup>II/I</sup> couples observed for all the cyclam complexes in argon atmosphere became irreversible in CO<sub>2</sub> atmosphere, which is a clear indication of the catalytic reduction of CO<sub>2</sub>. Typical current-potential curves for the tetrafluorinated cyclam complex  $\tilde{21a}$  in argon and CO<sub>2</sub> are shown in Figure 10. The surprising high shift (>100 mV) was observed in the reduction potential of the Ni<sup>II</sup> complex  $\tilde{21a}$  under CO<sub>2</sub>, as seen in that of cyclam complex  $\tilde{18a}$ .

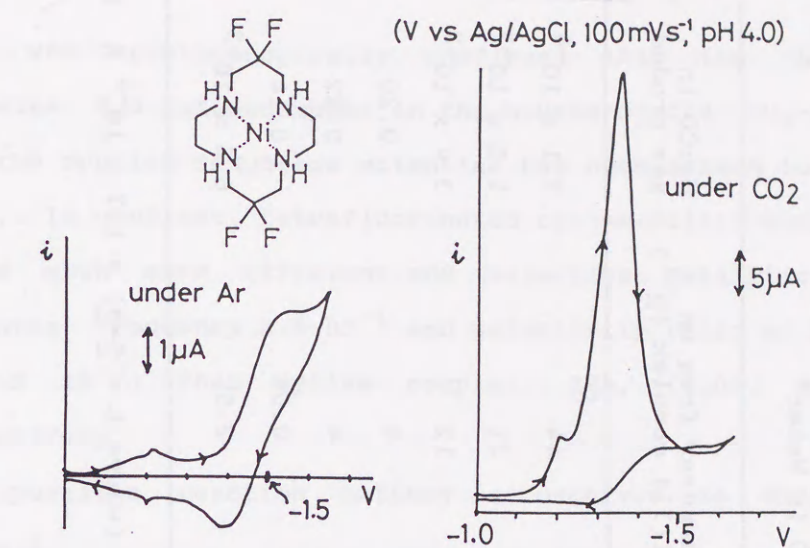


[Figure 10] Current-potential curves for the tetrafluorinated cyclam-Ni<sup>II</sup> complex  $\tilde{21a}$  ( $10^{-3}$  M) in 0.1 M NaClO<sub>4</sub> (pH 4.0) under argon (curve a) or CO<sub>2</sub> (curve b); hanging mercury electrode as working electrode, scan rate 100 mV/sec.

Table X compares the catalytic efficiencies of the electroreduction of CO<sub>2</sub>-saturated aqueous solution commonly containing [Ni<sup>II</sup>L] =  $1.7 \times 10^{-4}$  M and 0.1 M KNO<sub>3</sub> at pH 4.1, 25 °C. The electrolysis time was 4 hr.

The electroreduction with the cyclam  $\tilde{5}$  complex has been first checked at -1.30 V vs S.C.E. at an Hg electrode (turnover frequency  $44 \text{ hr}^{-1}$  and selectivity ratio of H<sub>2</sub> to CO  $2.1 \times 10^{-4}$ ), which fairly well agree with the literature data ( $32 \text{ hr}^{-1}$  and  $3 \times 10^{-4}$ ) under the same conditions.<sup>2b</sup> With the present complexes, the CO production yield decreased as the number of fluorine increases. At the same time, higher ratio of H<sub>2</sub>, a reduction product of H<sub>2</sub>O was produced (Table X).

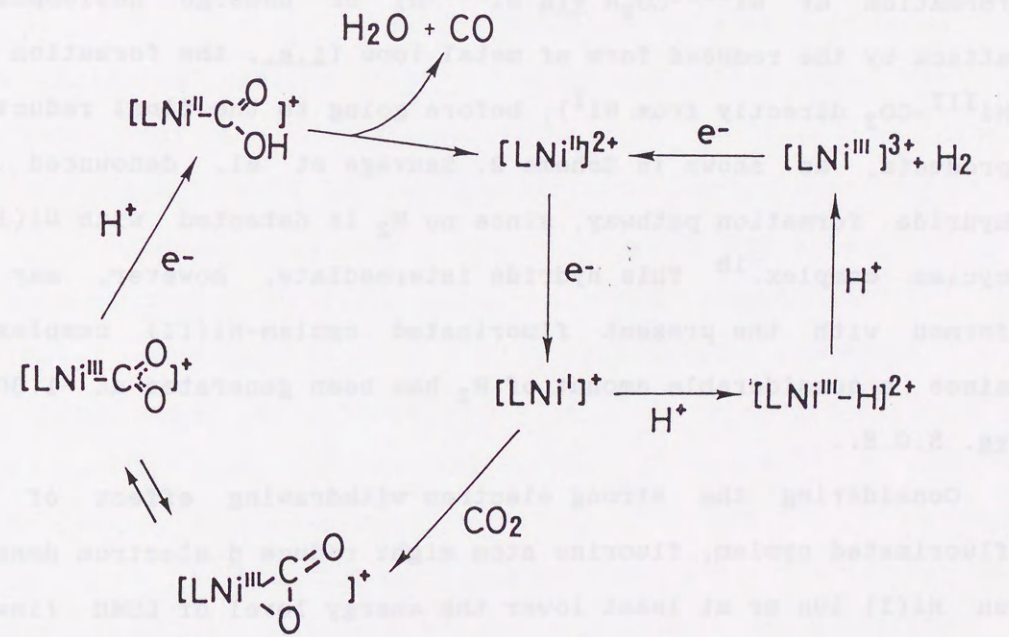
Table X. The Efficiency and Selectivity in the Process of  
Electrochemical Reduction of CO<sub>2</sub> to CO in Water<sup>a</sup>

expt	electrctlyst	applied potential V vs SCE	tot. vol of CO prodcd (mL)	turnover freq on Ni(II) complex (h <sup>-1</sup> )	H <sub>2</sub> :CO in gas prodcd
1	(5)-Ni(II)·Cl <sub>2</sub> (18b)	-1.30	14.7	4.4	2.1 x 10 <sup>-4</sup>
2	(6)-Ni(II)·(ClO <sub>4</sub> ) <sub>2</sub> (19a)	-1.30	10.2	31	1.5 x 10 <sup>-3</sup>
3	(7)-Ni(II)·Cl <sub>2</sub> (20b)	-1.30	4.1	12	3.4 x 10 <sup>-3</sup>
4	(8)-Ni(II)·Cl <sub>2</sub> (21b)	-1.30	2.9	9	0.20
5	(8)-Ni(II)·(ClO <sub>4</sub> ) <sub>2</sub> (21a)	-1.30	1.4	4	0.22
6	(5)-Ni(II)·Cl <sub>2</sub> (18b)	-1.10	0.02	0.06	0.14
7	(8)-Ni(II)·(ClO <sub>4</sub> ) <sub>2</sub> (21a)	-1.10	0.82	2.5	6.6 x 10 <sup>-3</sup>

<sup>a</sup> For experimental conditions, see Experimental Section; [NiL]<sup>2+</sup> (where L = 5-8) = 1.7 x 10<sup>-4</sup> M in 0.1 M KNO<sub>3</sub> (pH 4.1). Electrolysis time: 4 hr.

It was spectroscopically confirmed that the Ni<sup>II</sup>-cyclam complexes did not decompose in the course of the CO<sub>2</sub>-reduction. Then the applied reduction potential has been raised to -1.1 V vs S.C.E.. In contrast, tetrafluorinated cyclam-Ni(II) complex, 21a, showed much more efficient and selective catalytic activity (turnover frequency 2.5 hr<sup>-1</sup> and selectivity ratio of H<sub>2</sub> to CO 6.6 x 10<sup>-3</sup>) than cyclam complex, 18b, (0.06 and 0.14, respectively).

A possible reaction pathway is conceived as displayed in Scheme 2.



Scheme 2

The initial step in the catalytic cycle for the CO<sub>2</sub> reduction should be the generation of Ni<sup>I</sup> species, which would be strongly adsorbed on the electrode surface. Thus generated Ni<sup>I</sup> species would subsequently react either directly with CO<sub>2</sub> to yield Ni<sup>III</sup>-CO<sub>2</sub>, or competitively with a proton to form a Ni<sup>III</sup>-H.

In saturated macrocyclic complexes (such as cyclam), the d electrons tend to localize on the metal. When a substrate molecule such as CO<sub>2</sub> (or H<sub>3</sub>O<sup>+</sup>) interacts with the complexes, they are most likely to be directly reduced on the metal ion, in contrast to unsaturated macrocyclic complexes such as metalloporphyrines. Carbon dioxide might bind with the metal possibly with an oxidative addition mechanism (*i.e.*, the formation of Ni<sup>III</sup>-CO<sub>2</sub>H via Ni<sup>III</sup>-H) or undergo nucleophilic attack by the reduced form of metal ions (*i.e.*, the formation of Ni<sup>III</sup>-CO<sub>2</sub> directly from Ni<sup>I</sup>), before going to the final reduction products, as shown in Scheme 2. Sauvage et al. denounced the hydride formation pathway, since no H<sub>2</sub> is detected with Ni(II)-cyclam complex.<sup>1b</sup> This hydride intermediate, however, may be formed with the present fluorinated cyclam-Ni(II) complexes, since a considerable amount of H<sub>2</sub> has been generated at -1.30 V *vs.* S.C.E..

Considering the strong electron withdrawing effect of the fluorinated cyclam, fluorine atom might reduce d electron density on Ni(I) ion or at least lower the energy level of LUMO (lowest unoccupied molecular orbital) of Ni(II) ion. This may cause a kinetical disadvantage in nucleophilic attack by Ni(I) ion toward CO<sub>2</sub>.

In addition, the Ni(II) complex of tetrafluorinated cyclam 21a

takes almost 100 % of high-spin form (octahedral with two water molecules axially coordinated) in 0.1 M KNO<sub>3</sub> aqueous solution, whereas the Ni(II)-cyclam complex 18b does mainly low-spin form (square-planar), as mentioned before. Accordingly, with the former case, the axial water molecules should be released before the interaction between the intermediate Ni<sup>I</sup> species and CO<sub>2</sub>, this step possibly being kinetically disadvantageous.

These results will provide a promising outlook toward an electrochemical fixation of CO<sub>2</sub> even at energetically advantageous, higher potentials.

[Conclusion]

The following points are the principal results and conclusions of this investigation.

(i) The novel synthesis of the mono-, di-, and tetrafluorinated dioxocyclams (2-4) and cyclams (6-8) was achieved.

(ii) An electron-withdrawing effect of fluorine atoms on ligand properties is demonstrated by the weakened amine basicities with successive fluorine substitutions.

(iii) The fluorinated macrocycles 2-4, as a whole, exhibit higher stability constants for the formation of Cu(II) complexes. This is due to the electron-withdrawing effect of fluorine atoms at carbon between amide carbonyl groups.

(iv) With Ni(II) complexes of 5-8 in aqueous solution, the ratio of octahedral, high spin state increases as the number of fluorine atoms increases in the series. Tetrafluorinated cyclam-Ni(II) complex 21a takes almost 100 % high spin state.

(v) The effect of the fluorine substitution is most evident in electrochemical properties of Cu and Ni complexes. In either  $\text{CuH}_{-2}\text{L}^0$  ( $\text{L} = \underline{\underline{2-4}}$ ) or  $\text{NiL}^{2+}$  ( $\text{L} = \underline{\underline{6-8}}$ ) system, the higher oxidation states,  $\text{Cu}^{\text{III}}$  and  $\text{Ni}^{\text{III}}$ , become successively destabilized with respect to  $\text{Cu}^{\text{II}}$  and  $\text{Ni}^{\text{II}}$ , while the lower oxidation states,  $\text{Ni}^{\text{I}}$ , become successively stabilized with respect to  $\text{Ni}^{\text{II}}$ .

(vi) The X-ray structure of tetrafluorinated cyclam-Ni(II) $\text{Cl}_2$ , 21b, showed its octahedral, high spin form. The structural changes from nonfluorinated 18b to tetrafluorinated 21b as a whole are surprising minor.

(vii) The Ni(II) complexes with 6-8 all act as an

electrocatalyst for electrochemical  $\text{CO}_2$  reduction. The amount of CO produced decreases and the  $\text{H}_2$  ratio becomes higher with more fluorines at  $-1.30$  vs S.C.E.. In contrast, at the raised applied potential of  $-1.1$  V vs S.C.E., tetrafluorinated cyclam-Ni<sup>II</sup> complex 21a works as a much more efficient and selective electrocatalysis compared with cyclam complex 18b. This will provide a promising outlook toward an electrochemical fixation of  $\text{CO}_2$  at energetically advantageous, higher potentials. A possible reaction pathway involving  $\text{Ni}^{\text{III}}$ -hydride intermediate is proposed.

Thus, a series of fluorinated macrocyclic ligands in this study will find great potentials in progress in coordination chemistry of macrocyclic polyamines.

## [References and Notes]

- (1) For recent articles: (a) Beley, M.; Collin, J.-P.; Ruppert, R; Sauvage, J.-P. *J. Chem. Soc., Chem. Commun.* 1984, 1315. (b) Idem, *J. Am. Chem. Soc.* 1986, 108, 7461 and refs cited therein. (c) Grant, J.L.; Goswami, K.; Spreer, L.O.; Otvos, J.W.; Calvin, M.; *J. Chem. Soc., Dalton Trans.* 1987, 2105. (d) Tsukube, H. *J. Chem. Soc., Perkin Trans. I* 1985, 615. (e) Taniguchi, I.; Nakashima, N.; Yasukouchi, K. *J. Chem. Soc., Chem. Commun.* 1986, 1814. (f) Loncin, M.F.; Desreux, J.F.; Merciny, E. *Inorg. Chem.* 1986, 25, 2646. (g) Kunitake, T.; Ishikawa, Y.; Shimoumura, M. *J. Am. Chem. Soc.* 1986, 108, 327. (h) Ram, M.S.; Espenson, J.M.; Bakac, A. *Inorg. Chem.* 1986, 25, 4115. (i) Blake, A.J.; Gould, R.O.; Hyde, T.I.; Schrder, M. *J. Chem. Soc., Chem. Commun.* 1987, 431. (j) Bond, A.M.; Khalita, M.A. *Inorg. Chem.* 1987, 26, 413. (k) Koora, J.D.; Kochi, J.K. *Inorg. Chem.* 1987, 26, 908. (l) Takiguchi, T.; Nonaka, T. *Chem. Lett.* 1987, 1217. (m) Collin, J.-P.; Sauvage, J.-P. *J. Chem. Soc., Chem. Commun.* 1987, 1075. (n) Wagler, T. R.; Burrows, C. J. *J. Chem. Soc., Chem. Commun.*, 1987, 277. (o) Kinneary, J. F.; Wagler, T. R.; Burrows, C. J. *Tetrahedron Lett.*, 1988, 29, 877. (p) Wagler, J. F.; Burrows, C. J. *Tetrahedron Lett.*, 1988, 29, 5091. (q) Wagler, T. R.; Fang, Y.; Burrows, J. C. *J. Org. Chem.*, 1989, 54, 1584.
- (2) (a) For review; Kimura, E.; *J. Coord. Chem.* 1986, 15, 1. (b) Ishizu, I.; Hirai, J.; Kodama, M.; Kimura, E. *Chem. Lett.* 1979, 1045. (c) Hay, R.W.; Pujari, M.P.; McLaren, F. *Inorg. Chem.* 1984, 23, 3033. (d) Kimura, E.; Sakonaka, A.; Machida, R. *J. Am. Chem. Soc.*, 1982, 104, 4255. (e) Kimura, E.; Koike, T.; Machida, R.; Nagai, R.; Kodama, M. *Inorg. Chem.* 1984, 23, 4181.

- (f) Kimura, E.; Dalimunte, C.A.; Yamashita, A.; Machida, R. *J. Chem. Soc., Chem. Commun.* 1985, 1041. (g) Fabbrizzi, L.; Kaden, T.A.; Perotti, A.; Seghi, B.; Siegfried, L. *Inorg. Chem.* 1986, 25, 321. (h) Kimura, E.; Lin, Y.; Machida, R.; Zenda, H. *J. Chem. Soc., Chem. Commun.* 1986, 1020. (i) Kobayashi, N.; Zao, X.; Osa, T.; Kato, K.; Hanabusa, K.; Imoto, T.; Shirai, H. *J. Chem. Soc., Dalton Trans.* 1987, 1801.
- (3) Kimura, E.; Koike, T.; Takahashi, M. *J. Chem. Soc., Chem. Commun.*, 1985, 385.
- (4) Kimura, E.; Koike, T.; Uenishi, K.; Hediger, M.; Kuramoto, M.; Joko, S.; Arai, Y.; Kodama, M.; Iitaka, Y. *Inorg. Chem.* 1987, 26, 2975.
- (5) Kimura, E.; Joko, S.; Koike, T.; Kodama, M. *J. Am. Chem. Soc.* 1987, 109, 5528.
- (6) Kimura, E.; Koike, T.; Nada, H.; Iitaka, Y. *J. Chem. Soc., Chem. Commun.*, 1986, 1322.
- (7) Kimura, E.; Koike, T.; Nada, H.; Iitaka, Y. *Inorg. Chem.*, 1988, 27, 1036.
- (8) Kimura, E.; Shionoya, M.; Mita, T.; Iitaka, Y. *J. Chem. Soc. Chem. Commun.* 1987, 1712.
- (9) Kimura, E. *Pure & Appl. Chem.*, 1989, 61, 823.
- (10) Kimura, E.; Shionoya, M.; Okamoto, M.; Nada, H. *J. Am. Chem. Soc.*, 1988, 110, 3679.
- (11) Bergmann, E. D.; Cohen, S.; Shakak, I. *J. Chem. Soc.*, 1959, 3286.
- (12) This compound was synthesized from diethyl 2-fluoromalonate by using fluorinating reagent, N-fluoro-2,4,6-trimethylpyridinium triflate, newly developed by Umemoto and co-

- workers. See: Umemoto, T.; Kawada, K.; Tomita, K. *Tetrahedron Lett.*, 1986, 4465.
- (13) Kodama, M.; Kimura, E. *J. Chem. Soc., Dalton Trans.*, 1981, 694.
- (14) Bosnich, B.; Tobe, M. L.; Webb, G. A. *Inorg. Chem.*, 1965, 4, 1109.
- (15) Tabushi, I.; Taniguchi, Y.; Kato, H. *Tetrahedron Lett.* 1977, 1049.
- (16) Nave, C.; Truter, M. R. *J. Chem. Soc.*, 1974, 2351.
- (17) Kodama, M.; Kimura, E. *J. Chem. Soc., Dalton Trans.*, 1979, 325.
- (18) Hinz, F.P.; Margerum, D.W. *Inorg. Chem.* 1974, 13, 2941.
- (19) For dioxo tetramines; (a) Kimura, E.; Koike, T.; Machida, R.; Nagai, R.; Kodama, M. *Inorg. Chem.*, 1984, 23, 4181 and refs 2(a) and 16. For dioxo-free tetraamines; (b) Anichini, A.; Fabbrizzi, L.; Paoletti, P. *Inorg. Chim. Acta*, 1977, 24, L21. (c) Fabbrizzi, L. *Inorg. Chem.*, 1977, 16, 2667. (d) Fabbrizzi, L. *J. Chem. Soc., Dalton Trans.*, 1979, 1857. (e) Sabatini, L.; Fabbrizzi, L. *Inorg. Chem.*, 1979, 18, 438. (f) Fabbrizzi, L.; Micheloni, M.; Paoletti, P. *Inorg. Chem.*, 1980, 19, 535.
- (20) (a) Thom, V. J.; Boeyens, J. C. A.; McDougall, G. J.; Hancock, R. D. *J. Am. Chem. Soc.*, 1984, 106, 3198. (b) Barefield, E. K.; Bianchi, A.; Billo, E. J.; Connolly, P. J.; Paoletti, P.; Summers, J. S.; Van Derveer, D. G. *Inorg. Chem.*, 1986, 25, 4197.
- (21) Bosnich, B.; Mason, R.; Pauling, P. J.; Robertson, G. B.; Tobe, M. L. *Chem. Commun.*, 1965, 97.
- (22) (a) Yee, E. L.; Cave, R. J.; Guyer, K. L.; Tyma, P. D.; Weaver, M. J. *J. Am. Chem. Soc.*, 1979, 101, 1131. (b) Hupp, J.;

- (f) Kimura, E.; Dalimunte, C.A.; Yamashita, A.; Machida, R. *J. Chem. Soc., Chem. Commun.* 1985, 1041. (g) Fabbrizzi, L.; Kaden, T.A.; Perotti, A.; Seghi, B.; Siegfried, L. *Inorg. Chem.* 1986, 25, 321. (h) Kimura, E.; Lin, Y.; Machida, R.; Zenda, H. *J. Chem. Soc., Chem. Commun.* 1986, 1020. (i) Kobayashi, N.; Zao, X.; Osa, T.; Kato, K.; Hanabusa, K.; Imoto, T.; Shirai, H. *J. Chem. Soc., Dalton Trans.* 1987, 1801.
- (3) Kimura, E.; Koike, T.; Takahashi, M. *J. Chem. Soc., Chem. Commun.*, 1985, 385.
- (4) Kimura, E.; Koike, T.; Uenishi, K.; Hediger, M.; Kuramoto, M.; Joko, S.; Arai, Y.; Kodama, M.; Iitaka, Y. *Inorg. Chem.* 1987, 26, 2975.
- (5) Kimura, E.; Joko, S.; Koike, T.; Kodama, M. *J. Am. Chem. Soc.* 1987, 109, 5528.
- (6) Kimura, E.; Koike, T.; Nada, H.; Iitaka, Y. *J. Chem. Soc., Chem. Commun.*, 1986, 1322.
- (7) Kimura, E.; Koike, T.; Nada, H.; Iitaka, Y. *Inorg. Chem.*, 1988, 27, 1036.
- (8) Kimura, E.; Shionoya, M.; Mita, T.; Iitaka, Y. *J. Chem. Soc. Chem. Commun.* 1987, 1712.
- (9) Kimura, E. *Pure & Appl. Chem.*, 1989, 61, 823.
- (10) Kimura, E.; Shionoya, M.; Okamoto, M.; Nada, H. *J. Am. Chem. Soc.*, 1988, 110, 3679.
- (11) Bergmann, E. D.; Cohen, S.; Shakak, I. *J. Chem. Soc.*, 1959, 3286.
- (12) This compound was synthesized from diethyl 2-fluoromalonate by using fluorinating reagent, N-fluoro-2,4,6-trimethylpyridinium triflate, newly developed by Umemoto and co-

workers. See: Umemoto, T.; Kawada, K.; Tomita, K. *Tetrahedron Lett.*, 1986, 4465.

(13) Kodama, M.; Kimura, E. *J. Chem. Soc., Dalton Trans.*, 1981, 694.

(14) Bosnich, B.; Tobe, M. L.; Webb, G. A. *Inorg. Chem.*, 1965, 4, 1109.

(15) Tabushi, I.; Taniguchi, Y.; Kato, H. *Tetrahedron Lett.* 1977, 1049.

(16) Nave, C.; Truter, M. R. *J. Chem. Soc.*, 1974, 2351.

(17) Kodama, M.; Kimura, E. *J. Chem. Soc., Dalton Trans.*, 1979, 325.

(18) Hinz, F.P.; Margerum, D.W. *Inorg. Chem.* 1974, 13, 2941.

(19) For dioxo tetramines; (a) Kimura, E.; Koike, T.; Machida, R.; Nagai, R.; Kodama, M. *Inorg. Chem.*, 1984, 23, 4181 and refs 2(a) and 16. For dioxo-free tetraamines; (b) Anichini, A.; Fabbrizzi, L.; Paoletti, P. *Inorg. Chim. Acta*, 1977, 24, L21.

(c) Fabbrizzi, L. *Inorg. Chem.*, 1977, 16, 2667. (d) Fabbrizzi, L. *J. Chem. Soc., Dalton Trans.*, 1979, 1857. (e) Sabatini, L.; Fabbrizzi, L. *Inorg. Chem.*, 1979, 18, 438. (f) Fabbrizzi, L.; Micheloni, M.; Paoletti, P. *Inorg. Chem.*, 1980, 19, 535.

(20) (a) Thom, V. J.; Boeyens, J. C. A.; McDougall, G. J.; Hancock, R. D. *J. Am. Chem. Soc.*, 1984, 106, 3198. (b) Barefield, E. K.; Bianchi, A.; Billo, E. J.; Connolly, P. J.; Paoletti, P.; Summers, J. S.; Van Derveer, D. G. *Inorg. Chem.*, 1986, 25, 4197.

(21) Bosnich, B.; Mason, R.; Pauling, P. J.; Robertson, G. B.; Tobe, M. L. *Chem. Commun.*, 1965, 97.

(22) (a) Yee, E. L.; Cave, R. J.; Guyer, K. L.; Tyma, P. D.; Weaver, M. J. *J. Am. Chem. Soc.*, 1979, 101, 1131. (b) Hupp, J.;

Weaver, M. J. *Inorg. Chem.*, 1984, 23, 3639 and references therein.

(23) Fabbrizzi, L.; Paoletti, A.; Profumo, A.; Soldi, T. *Inorg. Chem.*, 1986, 25, 4256.

(24) (a) LoVecchio, F. V.; Gore, E. S.; Busch, D. H. *J. Am. Chem. Soc.*, 1974, 96, 3109. (b) Sabatini, L.; Fabbrizzi, L. *Inorg. Chem.*, 1979, 18, 438.

(25) (a) Zeigerson, E.; Ginzburg, G.; Schwartz, N.; Luz, Z.; Meyerstein, D. *J. Chem. Soc., Chem. Commun.* 1979, 241. (b) Jubran, N.; Ginzburg, G.; Cohen, H.; Meyerstein, D. *J. Chem. Soc., Chem. Commun.* 1982, 517. (c) Jubran, N.; Ginzburg, G.; Cohen, H.; Koresh, Y.; Meyerstein, D. *Inorg. Chem.* 1985, 24, 251.

(26) For recent reviews: (a) Collin, J. P.; Sauvage J. P. *Coord. Chem. Rev.*, 1989, 93, 245. (b) Taniguchi I. "Modern Aspects of Electrochemistry", Ed. by Bockris, J. O'M.; White, R. E.; Conway, B. E., 1989, Plenum Publishing Co..

## [論文目録]

### I. 学位論文の基礎となる論文

- 1) "A New Cyclam with an Appended Imidazole. The First Biomimetic Ligation of Imidazole for Axial  $\pi$ -interaction with Metal Ions"  
E. Kimura, M. Shionoya, T. Mita, and Y. Iitaka, *J. Chem. Soc., Chem. Commun.*, 1712-1714 (1987).
- 2) "The First Fluorinated Cyclams"  
E. Kimura, M. Shionoya, M. Okamoto, H. Nada, *J. Am. Chem. Soc.*, 110, 3679-3680 (1988).

### II. 参考論文

- 1) "Functionalized Crown Ethers as an Approach to the Enzyme Model for the Synthesis of Peptides"  
S. Sasaki, M. Shionoya, and K. Koga, *Heterocycles*, 20, 124-125 (1983).
- 2) "Functionalized Crown Ethers as an Approach to the Enzyme Model for the Synthesis of Peptides"  
S. Sasaki, M. Shionoya, and K. Koga, *J. Am. Chem. Soc.*, 107, 3371-3372 (1985).
- 3) "Functionalized Crown Ethers as an Approach to the Enzyme Model for the Synthesis of Peptides"  
S. Sasaki, M. Shionoya, H. Chaki, and K. Koga, *Ann. New York Acad. Sci.*, 471, 316-317 (1986).
- 4) "A New  $Mg^{2+}$  Ion Receptor. Macroyclic Polyamines Bearing an Intraannular Phenolic Group"  
E. Kimura, Y. Kimura, T. Yatsunami, M. Shionoya, and T. Koike, *J. Am. Chem. Soc.*, 109, 6212-6213 (1987).
- 5) "The First X-Ray Crystal Structures of the Platinum(II)-in and -out Complexes with Dioxocyclams"  
E. Kimura, S. Korenari, M. Shionoya, and M. Shiro, *J. Chem. Soc., Chem. Commun.*, 1166-1168 (1988).
- 6) "A New Tetradentate ( $N^+$ )<sub>2</sub>S<sub>2</sub> Macroyclic Ligand which is Highly Selective for Platinum(II) and Palladium(II)"  
E. Kimura, Y. Kurogi, S. Wada, and M. Shionoya, *J. Chem. Soc., Chem. Commun.*, 781-783 (1989).
- 7) "Isolation and Unusual Stability of a New Macroyclic Polyamine Containing a Phthalimidine"

E. Kimura, Y. Yoshiyama, M. Shionoya, and M. Shiro, *J. Org. Chem.*, (1990) in press.

8) "A Novel Cyclam Appended with an Ambident Donor Ligand, 3-Hydroxypyridine"

E. Kimura, Y. Kotake, T. Koike, M. Shionoya, and M. Shiro, *J. Chem. Soc., Chem. Commun.*, to be submitted.

9) "A Novel Cyclam Appended with 3-Hydroxypyridine, An Ambident Donor Ligand Comprising of A Pyridyl N and A Phenolate O<sup>-</sup> Donors"

E. Kimura, Y. Kotake, T. Koike, M. Shionoya, and M. Shiro, *Inorg. Chem.*, to be submitted.

### III. 総説

1) "ホストゲスト相互作用" 塩谷光彦, 古賀憲司, 化学総説, 47, 156-165 (1985).

2) "酵素活性と金属イオン" 木村栄一, 塩谷光彦, 化学と教育, 37, 370-373 (1989).

[謝 辞]

本研究を行なうにあたり、終始御指導、御助言ならびに多大な御尽力をいただきました、岡崎国立共同研究機構分子科学研究所教授 木村栄一先生（広島大学医学部教授併任）に心より謹んで感謝の意を表します。

学生時代に多大の御指導をいただき、現在に至るまで数々の貴重な御助言を賜わりました、恩師 東京大学薬学部教授 古賀憲司先生ならびに薬品製造化学教室の皆々様に深謝いたします。

X線結晶解析を行なっていただきました、帝京大学薬学部教授 飯高洋一先生に厚く御礼申上げます。

数々の御指導、御鞭撻を賜わりました、弘前大学教養部教授 児玉睦夫先生に深謝いたします。

研究のみならず公私ともにお世話になりました、広島大学医学部 小池 透先生、高橋利和先生、窪田教子様、木村博子様、高橋啓子様、各研究室の諸先生方、ならびに木村研究室の皆様、卒業生の皆様に心より御礼申上げます。

懇切な御指導、御助言を下さいました、岡崎国立共同研究機構分子科学研究所の諸先生方に深く感謝いたします。

本研究が多くの方々の御尽力によって成し遂げられた事をここに銘記し、直接的、間接的にお世話になりましたすべての皆様に心より感謝いたします。

平成元年 12月

岡崎国立共同研究機構分子科学研究所  
錯体化学実験施設錯体合成研究部門

塩谷光彦

參 考 論 文